STRESS-ACTIVATED MIG6 COMPROMISES HEPATIC METABOLISM DURING DIET-INDUCED OBESITY

Andrew J. Lutkewitte

Submitted to the faculty of the University Graduate School
in partial fulfillment of the requirements
for the degree
Doctor of Philosophy
in the Department of Cellular and Integrative Physiology,
Indiana University

September 2016

Accepted by the Graduate Faculty, Indiana University, in partial fulfilment of the requirements for the degree of Doctor of Philosophy

Doctoral Thesis Committee

Patrick T. Fueger, Ph.D., Chair

Robert Considine, Ph.D.

July 25, 2016

Carmella Evans-Molina, M.D., Ph.D.

Johnathan Tune, Ph.D.

Jeffrey Elmendorf, Ph.D.

ACKNOWLEDGEMENTS

First and foremost, I would like to acknowledge my family for their constant support over the last five years. Specifically, I would like to thank my Father and Mother, who persuaded me to enter graduate school. I hope one day to have the same dedication towards my own children. They have put their children's lives before their own and through those sacrifices raised four very successful children. Secondly, I would like to thank my sister for giving me the skills and confidence to complete my degree.

I would also like to thank the faculty, staff, and students at Indiana University School of Medicine. I can honestly say I have had long conversations with every member of the research group and many of the members of the Physiology Department. I have enjoyed the various perspectives I have gained throughout the years. I will heed the advice of senior scientists and postdocs in the group for years to come. In addition, I would specifically like to thank my committee members, who have been nothing but supportive. They have ensured my future success as a scientist through successful recommendation letters and detailed scientific discussions. I have always felt welcome and never intimidated in their presence, and I think that has given me the confidence so vital to this field.

Lastly, I would like to thank my mentor, Dr. Patrick Fueger. Patrick took a chance giving me a rotation in his laboratory, and I cannot thank him enough for the opportunity he has given me. I know that our relationship is just beginning, and I look forward to see him at Embassy Suite's happy hours at future meetings.

Patrick has always put his students first, and I hope to prove as successful in mentoring as he.

Andrew J. Lutkewitte

STRESS-ACTIVATED MIG6 COMPROMISES HEPATIC METABOLISM DURING DIET-INDUCED OBESITY

Obesity-induced hepatic fat accumulation or nonalcoholic fatty liver disease (NAFLD) is the leading cause of liver disease in the United States. Unfortunately, NALFD patients are at higher risk of cardiovascular disease and mortality. The development of hepatic steatosis is multi-factorial and leads to a variety of pathologies. Yet, the molecular mechanisms behind liver disease during hepatic fat accumulation remain unclear. Here, we describe novel mechanisms of impaired liver function in the context of obesity-induced hepatic stress. Using chemical- and fatty acid-induced endoplasmic reticulum (ER) stress, we discovered ER stress decreases the activation of the pro-growth, pro-survival, receptor tyrosine kinase, epidermal growth factor receptor (EGFR) *in vitro.* Importantly, EGFR was inhibited during these stress conditions by the induction and stabilization of mitogen inducible gene 6 (Mig6). Furthermore, Mig6 knockdown *in vitro* enhanced EGFR signaling and promoted survival.

We demonstrated that mice fed a high fat diet have decreased EGFR activation and increased Mig6 protein expression, likely due to obesity-induced ER stress. To determine the functional consequences of increased Mig6 expression, we generated Mig6 liver-specific knockout mice (Mig6 LKO) and subjected them to high fat feeding. During diet-induced obesity, Mig6 LKO mice had improved hepatic glucose tolerance despite no improvements in whole-body insulin sensitivity or insulin secretion. Hepatic insulin signaling, measured by AKT

activation, was similar between Mig6 LKO and littermate controls. However, several insulin-sensitive genes involved in gluconeogenesis were altered in Mig6 LKO mice compared to controls. In addition, Mig6 LKO mice had higher plasma high density lipoproteins and triglycerides despite similar liver lipid content. Using RNA sequencing we discovered Mig6 regulates several metabolic pathways in liver. These findings indicated Mig6 not only controls hepatic growth and survival but also regulates metabolism. This work will help us to better understand how augmented growth factor signaling impacts metabolic regulation during pathological obesity.

Patrick T. Fueger, Ph.D., Chair

TABLE OF CONTENTS

LIST OF TABLES x

LIST OF FIGURES xi

ABBREVIATIONS xiv

CHAPTER 1: INTRODUCTION 1

Preview 1

NAFLD and hepatic pathologies 8

Mechanisms of hepatic repair 16

AIMS 26

CHAPTER 2: MATERIALS AND METHODS 27

Animal studies 27

Hepatic assessment 29

Cell culture 36

CHAPTER 3: RESULTS 41

Mig6 decreases hepatic EGFR activation and survival during saturated fatty acid-induced endoplasmic reticulum stress 41

Synopsis 41

Introduction 42

Results 44

Discussion 57

CHAPTER 4: RESULTS 62

EGFR activation is decreased and mig6 protein expression is Increased during obesity in mice 62

Synopsis 62

Introduction 62
Results 65
Discussion 81
CHAPTER 5: RESULTS 84
Liver-specific mig6 ablation improves glucose tolerance in HFD fed mice 84
Synopsis 84
Introduction 84
Results 85
Discussion 104
CHAPTER 6: DISSCUSSION AND FUTURE STUDIES 108
Mig6 decreases hepatic EGFR activation and survival during saturated fatty acid-induced endoplasmic reticulum stress 108
Summary and perspectives 108
Future studies 109
EGFR activation is decreased and Mig6 protein expression is increased during obesity in mice 112
Summary and perspectives 112
Future studies 113
Liver-specific Mig6 ablation improves glucose tolerance in high fat fed mice 114
Summary and perspectives 114
Future studies 114

REFERENCES 119

CURRICULUM VITAE

LIST OF TABLES

Table 1: Histological scoring parameters of H&E liver sections 30

Table 2: List of Taqman Probes for qPCR 34

Table 3: List of primers for SYBR green qPCR 35

Table 4: List of antibodies used 38

LIST OF FIGURES

Figure 1: Proposed model for Mig6 activation and EGFR inhibition during obesity-induced stress 25

Figure 2: Palmitate decreases EGFR activation in primary hepatocytes and activates caspase 3/7. 46

Figure 3: Palmitate-induced ER stress increases Mig6 expression in H4IIE cells. 47

Figure 4: ER stress induces Mig6 in rat H4IIE cells. 48

Figure 5: ER stress induces Mig6 in HepG2 cells. 49

Figure 6: ER stress does not activate EGFR inhibitors in cell lines. 50

Figure 7: Mig6 overexpression reduces EGF-stimulated EGFR and ERK phosphorylation. 52

Figure 8: Thapsigargin decreases EGFR activation, induces caspase 3 activation, and stabilizes Mig6 protein expression. 53

Figure 9: Mig6 ablation rescues EGFR activation during ER stress. 55

Figure 10: Mig6 knockdown during palmitate-induced ER stress decreases caspase 3/7 activity in HepG2 cells. 56

Figure 11: Mig6 is increased in diet-induced obesity and prediabetes. 66

Figure 12: Mig6 and EGFR expression and activation are decreased in leptin deficient mice 68

Figure 13: IP EGF injection activates EGFR in C57Bl/6 mice. 70

Figure 14: Male C57Bl/6 mice are obese and hyperglycemic following HFD challenge. 71

Figure 15: EGF mediated ERK activation is decreased in C57Bl/6 mice fed a HFD. 72
Figure 16: Mig6 LKO mice have reduced Mig6 mRNA and protein expression in liver. 74
Figure 17: Mig6 LKO mice have hepatomegaly. 76
Figure 18: Mig6 LKO mice have normal metabolism. 77
Figure 19: Mig6 LKO livers have normal insulin sensitivity with increased total glycogen content. 78
Figure 20: Mig6 LKO mice have improved glucose tolerance on a HFD. 80
Figure 21: Mig6 LKO mice have improved glucose tolerance with similar fasting glucose and body weights. 86
Figure 22: HFD fed Mig6 LKO have similar insulin and pyruvate tolerance compared to controls. 87
Figure 23: Mig6 LKO mice have similar plasma insulin and beta cell area compared to littermate controls. 89
Figure 24: Mig6 LKO mice have hepatomegaly independently of proliferation. .. 92
Figure 25: Mig6 LKO mice have higher total triglycerides on HFD. 94
Figure 26: Mig6 LKO mice have increased plasma triglycerides and HDL cholesterol. 95
Figure 27: Mig6 ablation prevents elevated hepatic ballooning in HFD fed mice. 98
Figure 28: Plasma ALT and Albumin and elevated in Mig6 LKO mice. 99
Figure 29: Mig6 LKO livers have normal insulin sensitivity following HFD. 101

Figure 30: Mig6 LKO mice have increased glucokinase and reduced g6pase gene expression on HFD compared to littermate controls. 103
Figure 31: Oxidative stress induces Mig6 expression in HepG2 cells. 111
Figure 32: Fasting induces Mig6 and g6pase in male C57Bl/6 mice. 117
Figure 33: MDS plot showing separation among treatment groups. 118

ABBREVIATIONS

ATF6	Activating transcription factor 6
cAMP	Cyclic adenosine monophosphate
CD36	Cluster of differentiation 36
CHOP	C/EBP-homologous protein
CPT	Carnitine palmitoyl transferase
CVD	Cardiovascular disease
eif2α	Eukaryotic initiation factor 2 alpha
ER	Endoplasmic reticulum
FATP	Fatty acid transport proteins
FOXO1	Forkhead transcription factor 1
G6P	Glucose-6-phosphate
G6Pase	Glucose-6-phosphatase
GIP	Glucose-dependent insulinotropic polypeptide
GLP-1	Glucagon like peptide-1
GLUT	Glucose Transporter
GTT	Glucose tolerance test
H&E	Hematoxylin and eosin
HDL	High-density lipoprotein
HGP	Hepatic glucose production
HGP	Hepatic glucose production
IL-6	Interleukin 6
IRE1/α	Inositol-requiring enzyme 1 alpha

ITT	Insulin tolerance test
LDL	Low-density lipoprotein
LIRKO	Liver insulin receptor knockout mice
NAFLD	Nonalcoholic fatty liver disease
NASH	Nonalcoholic steatohepatitis
NEFAs	Non-esterified fatty acids
OCT	Optimal cutting temperature resin
PEPCK	Phosphoenolpyruvate carboxykinase
PERK	Protein kinaes RNA –like endoplasmic reticulum kinase
PFA	Paraformaldehyde
PGC-1α	Peroxisome proliferative activated receptor-γ co activator 1
PTT	Pyruvate tolerance test
ROS	Reactive oxygen species
RTK	Receptor Tyrosine Kinase
RTK	Receptor tyrosine kinase
T2DM	Type 2 Diabetes Mellitus
TCA	Tricarboxcylic acid
TG	Triglyceride
TNF-α	Tumor necrosis factor alpha
UPR	Unfolded Protein Response
VLDL	Very low-density lipoprotein

CHAPTER 1: INTRODUCTION

Preview

Obesity-induced liver disease: The global obesity epidemic is associated with increased morbidity and mortality, and despite the consequences, over 35% of the United States population remains obese (Flegal KM et al., 2012; Isomaa et al., 2001; Mokdad AH et al., 2003). Several theories naming obesogenic causes exist, including but not limited to: sedimentary life styles, genetic predisposition, environment, gestational environment, food additives and sweeteners, and even vaccines (Boney et al., 2005; England, 2012; Hales and Barker, 1992; Jebb and Moore, 1999; Lim et al., 2010). Though most explanations are backed by extensive research, the culprit is likely multifactorial. So why does the obesity epidemic matter? Because as the waistline grows, so do the pathological consequences of obesity. In fact, waist circumference is significantly associated with increased risk of cardiovascular disease (CVD) (Koning et al., 2007).

Obesity arises when substrate ingestion and absorption outpace the body's metabolic capacity to utilize substrate as energy. Most excess substrates (monosaccharides, amino acids, and fat droplets) are absorbed in the intestines and stored in muscle, adipose, and liver. Because fats have the lowest thermogenic cost (i.e., the amount of energy needed to absorb, metabolize, and store), they are the preferred storage substrate in the postprandial state (Jéquier, 2002; Coppack et al., 1990). In healthy individuals, a majority of dietary fats are stored in the adipose tissue (Coppack et al., 1990). However, as obesity

increases and adipose tissue reaches its maximum storage capacity, fats are displaced to alternate storage depots, mainly the liver. In this context, the liver gains >5% of its weight in fat and may develop fatty liver disease, which, in the absence of alcohol use, is known as non-alcoholic fatty liver disease (NAFLD). Patients susceptible to NAFLD are at higher risk for CVD, and the severity of CVD increases with severity of NAFLD (Volzke et al., 2005; Targher et al., 2006). Moreover, patients with NAFLD are at an increased risk for postoperative complications following hepatectomy or resection surgeries (McCormack et al., 2007).

Although not all NAFLD is due to obesity, obese individuals have a higher prevalence of NAFLD. NAFLD ranges from simple steatosis (defined as hepatic fat content >5%) to nonalcoholic steatohepatitis (NASH) and cirrhosis (Kleiner et al., 2005). This excess hepatic fat creates insulin resistance, oxidative and endoplasmic reticulum (ER) stress, and inflammation. Fortunately, the liver has several intrinsic mechanisms to repair damage caused by these stressors. However, during obesity, many of these pathways become compromised and ultimately affect physiology, and in susceptible populations, may lead to liver failure. Therefore, the following sections will explore the regulation of hepatic metabolism under physiological conditions, the hepatic pathological consequences associated with obesity, and the endogenous repair mechanisms that restore hepatic function following insults.

Metabolic regulation

Insulin action in extra hepatic tissue: Dietary ingestion of carbohydrates, hepatic glucose production (HGP), and elevations in free fatty acids cause insulin release by the pancreatic β-cell. This process is enhanced by incretin hormones, most notably GLP-1 and GIP, and inhibited by the counterregulatory system, most notably glucagon and the catecholamines epinephrine and norepinephrine (Vilsbøll and Holst, 2004). Insulin lowers plasma glucose both indirectly through brain circuitry and directly through its anabolic action on several tissues. Insulin consists of two polypeptide chains and is released as a hexamer held together by a zinc ion from highly regulated granular exocytosis (Smith et al., 1984). Insulin lowers blood glucose through three main metabolically active tissues skeletal muscle, adipose, and liver. In most tissues, insulin binds to the insulin receptor, a receptor tyrosine kinase (RTK), at the cellular membrane, activates dimerization, and through subsequent conformational changes transactivates the intracellular kinase domains resulting in tyrosine phosphorylation. Activated insulin receptors elicit a majority of metabolic responses through the binding of IRS1/2 PH domain containing adaptor proteins. The active receptor may also bind SHC, GAB1, GAB2, and SH2B, among other adaptor proteins. Once bound, IRS1/2 is phosphorylated and binds PI3K, which converts membrane bound $PI(4,5)P_2$ into $PI(3,4,5)P_3$. $PI(4,5)P_2$ conversion represents a key regulatory step in insulin signaling, as PTEN dephosphorylates $PI(3,4,5)P_3$ back into $PI(4,5)P_2$ thereby terminating signaling. The resultant membrane bound signaling intermediates recruit AKT1/2

for phosphorylation on Thr^{308} and Ser^{473} via PDK1 (White, 2003). AKT1/2 activation is a key regulator of both metabolism and growth. AKT1/2's importance in growth and development is evident by embryonic lethality of whole body knockout animals (Dummler et al., 2006), and dual liver-specific ablation of both AKT1 and AKT2 reveals AKT1/2 as a master regulator of metabolism through phosphorylation of several key metabolic intermediates (Lu et al., 2012). Indeed, AKT1/2 exerts most of its metabolic response by phosphorylation of FOXO1, GSK3β, and mTORC1. Both the regulation and actions of AKT1/2 are tissue and context specific.

Insulin also stimulates the storage of glucose as glycogen through AKT1/2-mediated phosphorylation of GSK3β and subsequent activation of glycogen synthase in both skeletal muscle and liver. In fact, one third of dietary glucose is stored in skeletal muscle (M J Pagliassotti and Cherrington, 1992), where insulin promotes its uptake through AKT1/2 phosphorylation of AS160 and GLUT4 glucose transporter translocation to the membrane. In addition to its direct effects on peripheral tissues, insulin activates vascular delivery of glucose, a process that becomes diminished during insulin resistance and in type 2 diabetes mellitus (T2DM).

In the post-prandial state, insulin action on adipose tissue also stimulates GLUT4 translocation to the membrane; though its main effect is through suppression of lipolysis and uptake of fatty acids for storage as triglycerides. Activation of the insulin receptor in adipose tissue inhibits PKA activation and decreases hormone sensitive lipase activity (lowers lipolysis) while activating

acetyl-coA carboxylase and fatty acid synthase for fatty acid synthesis (Giorgino et al., 2005). Thus insulin creates an anabolic environment in adipose tissue depots.

Control of metabolism through substrates and hormones in liver: Substrate concentration plays a critical role in the regulation of acute metabolic shifting from the fed to the fasting state in the liver. The ability of substrates to control metabolism, however, are mediated by the environment in which they are created. For example, hepatic glucose uptake and production are regulated by acute metabolic intermediates as well as hormonal control of enzymatic gene transcription. The two main hormones in hepatic metabolism are insulin and glucagon. Hepatic insulin action has a multitude of responses. First, insulin signaling transitions the liver from a catabolic to an anabolic state by activating glycolytic and suppressing gluconeogenic gene expression. Second, insulin activates glycogen synthesis and thus stores glucose. Last, insulin signaling initiates *de novo* lipogenesis and promotes β-oxidation. In contrast, the main counterregulatory hormone glucagon opposes these effects through cAMP activated PKA.

Glucose regulation in liver: The liver constitutively expresses the GLUT2 transporter which has a high K_M allowing maximum glucose entry into the hepatocyte. Because GLUT2 can transport glucose bilaterally, the liver must "trap" glucose by phosphorylation into glucose-6-phosphate (G6P) by glucokinase. Despite the presence of an enzymatic system to reverse this trapping step, phosphorylation of glucose represents a critical step in hepatic

glucose uptake and is highly regulated. Glucokinase is indirectly regulated by the binding of glucose to glucokinase regulatory subunit, thereby freeing glucokinase and allowing its translocation from the nucleus to the cytosol. Both glucokinase transcription and activity are increased by insulin, and its expression and activity are decreased in insulin resistant states (Katz et al., 1979).

Following “glucose trapping” the fate of G6P is dependent on fasting vs. fed states. Postprandial G6P is converted to glycogen, enters glycolysis, and in small quantities converted to fatty acids. In contrast, in the fasted state, G6P is hydrolyzed by glucose-6-phosphatse (G6Pase) into glucose for release into the blood stream. G6Pase is transcriptionally activated by cAMP signaling (from glucagon and other counterregulatory hormones) and repressed by insulin (Argaud et al., 1996; Nordlie and Snoke, 1967). Another important switching point in HGP is mediated by phosphoenolpyruvate carboxykinase’s (PEPCK) conversion of the tricarboxylic acid (TCA) cycle intermediate oxaloacetate into phosphoenol pyruvate for use in gluconeogenesis. PEPCK is transcriptionally activated by glucagon and glucocorticoids, yet inhibited by glucose and insulin (Scott et al., 1998).

Hormone-mediated transcriptional control of gluconeogenesis is regulated through forkhead transcription factor 1 (FOXO1) and peroxisome proliferative activated receptor-γ co activator 1 (PGC-1α). As previously stated, FOXO1 is deactivated by insulin mediated activation of AKT1/2 and subsequent phosphorylation and nuclear exclusion. Activated FOXO1 is a transcription factor for gluconeogenic genes such as PEPCK, G6Pase, and fructose-1,6-

biphosphatase (Gross et al., 2008). PGC-1α is also a transcription factor for gluconeogenic genes like PEPCK and PGC-1α and is activated through cAMP signaling (Puigserver et al., 2003).

Lipid regulation in liver: Like glucose metabolism, hepatic lipid metabolism is also regulated by both substrate and hormonal cues. Foremost, the liver secretes bile acids which aid in dietary absorption of lipids through formation of mixed micelles. Following lymphatic uptake, substrate availability is facilitated in fenestrated hepatic capillary beds and hepatic sinusoidal spaces allowing hepatocellular surface lipases unrestricted access to lipid trafficking particles. Once removed, free fatty acids (FFAs) are transported across the membrane through several types of transporters, including the fatty acid transport proteins FATP and CD36. The remaining source of hepatic lipids comes from dietary fat absorption through remnant ApoE bound chylomicrons and hepatic *de novo* lipogenesis, where carbons from glucose are converted into fatty acid chains (Donnelly et al., 2005).

Upon crossing the hepatic membrane, non-esterified fatty acids (NEFAs) are rapidly converted to acyl-CoAs by the FATP and fatty acyl-CoA synthases (Kawano and Cohen, 2013). The fate of cytosolic acyl-CoAs varies depending on the metabolic state of the liver. Acyl-CoAs themselves may act as signaling intermediates directly affecting hepatic metabolism by inhibiting glucokinase and pyruvate dehydrogenase, among many others metabolic enzymes (Faergeman and Knudsen, 1997). Acyl-CoAs are also transported into the mitochondria via conversion to acyl-carnitine by carnitine palmitoyl transferase (CPT) proteins for

TCA cycle utilization or conversion to ketone bodies. In insulin-sensitive hepatocytes, acyl-CoAs are converted into triglycerides (TG) and packaged for secretion in VLDL; however, insulin resistance causes increased storage in the form of TG droplets within the hepatocyte.

Insulin signaling activates *de novo* lipogenesis through coordinated and comprehensive changes in gene transcription. As mentioned previously, insulin signaling activates PI3K which controls lipogenesis through two main pathways. First, AKT2 phosphorylates and inhibits FOXO1 and PGC-1α, thus removing transcriptional restraint on lipogenic genes (Perry et al., 2014). AKT1/2 also activates SREBP-1c processing and subsequent nuclear localization for lipogenic gene expression (Yecies et al., 2011). AKT1/2-mediated FOXO1 activity also regulates several lipogenic genes including ACC, and FAS (Zhang et al., 2006). Together these transcriptional changes promote the conversion of carbons from glucose into lipids for presumably long-term storage.

NAFLD and hepatic pathologies

NAFLD: NAFLD and its spectrum of diseases afflicts one in every three adults in the U.S. and 25% of the global population (Browning et al., 2004; Younossi et al., 2016). NAFLD begins with inappropriate hydrocarbon storage of fat (mainly TG) in hepatocytes. These hydrocarbons originate from both hepatic and extra-hepatic sources. A majority of the carbons utilized in hepatic TG synthesis originate form insulin-resistant adipose tissue (Donnelly et al., 2005). Insulin resistance causes inappropriate lipolysis and transfer of NEFAs to the serum pool (bound to albumin) or converted into TGs for transport in lipoproteins.

As previously mentioned, a large portion of the population has the ability to store lipids in the liver without pathological consequences (benign steatosis). However, estimates as high as 25% of NALFD patients progress to NASH, and fewer still, proceed to fibrosis with cirrhosis and eventual liver failure (Dixon et al., 2001). Although only a small percentage of NAFLD patients fully progress towards liver related death, the sheer number of NALFD patients globally will translate to over 20,000,000 liver related deaths among current NAFLD patients (Rinella and Charlton, 2016). The transition towards NASH often requires a second “hit” as proposed by Day and James in 1998. Whether the secondary hit is required or not, several stressors occur in the context of NAFLD. These stressors arise from lipotoxins and included insulin resistance, oxidative and endoplasmic reticulum (ER) stress, and inflammation (Day and James, 1998; Neuschwander-Tetri, 2010).

Insulin resistance: An early pathology of obesity is whole-body insulin resistance. Insulin resistant diabetes (T2DM) was first noted by Falta and Boller in 1931 and later confirmed by Himsworth in 1936. Each group noted different responses in plasma glucose when patients were given a mixture of glucose and insulin. The patients either exhibited lowered plasma glucose and ketosis, or elevated plasma glucose regardless of an insulin co-infusion (Falta and Boller, 1931; Himsworth, 1936). Since the early studies over the last century, the mechanisms of insulin resistance have been broadly defined.

Calorie intake per capita has increased by 20% over the past three decades (Guyenet and Schwartz, 2012). Chronic increases in caloric intake

cause increased insulin secretion and resistance to insulin in multiple tissues. In the hypothalamus, reduced insulin receptor expression leads to hyperphagia and fat mass gain in rats (Obici et al., 2002a). More importantly, several diet-induced obesity models display inflammatory-mediated hypothalamic insulin resistance (De Souza et al., 2005; Obici et al., 2002b; Posey et al., 2009). Perhaps more studied than insulin in hypothalamic signaling is the functions of adipose-derived leptin. Leptin limits food intake and adiposity and affects multiple tissues. Leptin release correlates with adiposity levels in mice and humans suggesting systemic leptin resistance (Maffei et al., 1995).

In addition to leptin, adipose tissue secretes a large array of metabolic hormones – the so-called adipokines. Adipose expansion leads to recruitment of pro-inflammatory macrophages and increased secretion of pro-inflammatory cytokines such as TNF-α, IL-6, and IL-1β (Spranger et al., 2003). These cytokines initiate insulin resistance, thereby increasing lipolysis and reducing glucose uptake. The release of cytokines and FFA into the blood stream affects peripheral tissues, including skeletal muscle and liver. In muscle, insulin resistance impairs GLUT4 translocation and reduces glucose uptake, thus increasing plasma glucose levels.

In mouse liver, genetic ablation of the insulin receptor (LIRKO mouse) yields hyperglycemia, glucose intolerance, and insulin resistance (Michael et al., 2000). Furthermore, high-dose hyperinsulinemic-euglycemic clamp studies in LIRKO mice reveal compromised HGP suppression despite maintaining insulin's ability to suppress FFAs (Fisher and Kahn, 2003). As previously discussed,

hepatic lipid storage increases during obesity. The FFAs entering the liver are esterified and stored as triglycerides. However, a subset of lipids become diacylglycerols (DAG), which activate atypical protein kinase C isoforms (PKC) (Samuel et al., 2007). PKCs are implemented in direct inhibition of insulin signaling through serine phosphorylation in response to nutrient overload (Perry et al., 2014). In addition to PKC, the MAPK, JNK, is activated during obesity-induced stress and directly inhibits insulin signaling through serine phosphorylation of IRS1/2 (Nakatani et al., 2004; Ozcan et al., 2004). The inhibition of hepatic insulin signaling leads to unrestricted glucose production accelerating the elevated plasma glycaemia associated with insulin resistance.

Hepatic oxidative stress: A major player in obesity-induced hepatic stress is oxidative stress caused by the by-products of β-oxidation and inflammation. Physiologically, the liver has an incredible capacity for lipid turnover during fed-fasting cycles (turnover equals ~80 and 10%/h in mice and humans, respectively) (Otero et al., 2014). The mitochondria utilizes β-oxidation to generate reducing equivalents (NADH and $FADH_2$) for the electron transport chain for oxidative phosphorylation and subsequent ATP generation (Serviddio et al., 2011). Under physiological conditions, liver oxidative phosphorylation generates reactive oxygen species (ROS) albeit in relatively small quantities compared to skeletal muscle (St-Pierre et al., 2002). Liver ROS, such as superoxides, are rapidly converted to H_2O_2 by superoxide dismutase and form adducts with lipid chains to form 4-hydroxynonenal (Esterbauer et al., 1991). Therefore, any increase in FFA concentration causes an increase in β-oxidative

and therefore ROS. In fact, studies in NAFLD patients reveal an increase in both hepatic β-oxidation and oxidative stress (Miele et al., 2003; Narasimhan et al., 2010).

Oxidative stress is often referred to as the “secondary hit” in the development of NASH (Day and James, 1998). ROS generation in NAFLD causes the activation of inflammation, DNA damage, and even cell death. Mice fed a methionine choline deficient diet (MCD, a model of NASH) develop increased oxidative stress and subsequent cytochrome 2E1 expression, which further exacerbates ROS production (Weltman et al., 1996). Although the MCD diet is not a *bona fide* model of insulin resistance (Rinella and Green, 2004), it activates inflammatory pathways through $NF_{\kappa}B$ signaling and leads to DNA damage (dela Peña et al., 2005; Gao et al., 2004). Importantly, ROS, inflammation, and DNA damage are all well-documented pathologies of NASH development in human patients (Kleiner et al., 2005; Narasimhan et al., 2010; Tanaka et al., 2013). Further still, apoptosis is present in patients with NASH and correlates with the severity of the disease (Feldstein et al., 2003; Wieckowska et al., 2006).

Hepatic ER stress: Forty percent of hepatic transcripts encode secreted proteins (Uhlén et al., 2015). In fact, albumin is secreted at a rate of 18 g/d, or about 1% of total liver weight is secreted as albumin each day (Molina and DiMaio, 2012). Therefore, the liver must maintain a massive capacity to synthesize, properly fold, and secrete proteins. The endoplasmic reticulum (ER) is the site of major protein folding and quality control for the tertiary structures of

membrane bound and secreted proteins (Mori, 2000). Several mechanisms have evolved to ensure proper ER function, mostly notably the unfolded protein response (UPR).

The canonical UPR: The ER environment is highly enriched in Ca^{2+}, chaperone proteins (Bip/GRP78, and GRP94), and isomerase, all of which are conducive towards proper protein folding (Fu et al., 2012; Mori, 2000). Upon sensing unfolded or misfolded proteins, the ER activates the UPR through three different ER membrane bound signaling arms: IRE1α/β, PERK, and ATF6. Upon sensing unfolded proteins, the chaperone Bip is released from both IRE1α/β and PERK. These kinases are phosphorylated leading to complex downstream signaling pathways. For example, activated IRE1α/β causes splicing of XBP1 mRNA allowing for translation into XBP1s transcription factor leading to expression of DnaJ/Hsp-like chaperone genes (Lee et al., 2003). In addition, IRE1α/β and PERK kinase activity phosphorylate JNK and IKK leading to inflammatory responses (Hu et al., 2006; Urano et al., 2000). More importantly, both JNK and IKK have been implicated in IRS1/2 serine phosphorylation linking ER stress to insulin resistance (Hirosumi et al., 2002; Gao et al., 2002). In addition, active PERK phosphorylates and inactivates the eukaryotic initiation factor 2 alpha (eif2α) leading to global translation blockade with the exception of genes involved in ER stress repair (Harding et al., 1999). Together IRE1α/β and PERK activate repair programs and inhibit global protein synthesis until misfolding or stress can be remedied. The third arm of the UPR pathway ATF6 is a transcription factor rendered inactive in the ER membrane. Upon stress, ATF6

is reduced and translocated to the Golgi where it is cleaved and further translocated to the nucleus where it becomes transcriptionally active for both chaperone and inflammatory mediators (Shen et al., 2002). ATF6 can also interact with XBP1s, and together regulate the transcriptional response of the UPR (Wu et al., 2007). The UPR is not only intended to alleviate ER stress caused by misfolded proteins but has recently been implicated in metabolic regulation.

UPR and hepatic metabolism: The UPR evolved to alleviated ER stress, however, the hepatic UPR also regulates metabolism, specifically through substrate control. Notably, ER stress is activated during physiological cycles of feeding and fasting and genetic and diet-induced obesity mouse models (Oyadomari et al., 2008; Ozcan et al., 2004). More importantly, ER stress is detected in human liver samples from NAFLD and NASH patients (Puri et al., 2008). As previously stated, chronic UPR activation increases insulin resistance through serine phosphorylation of IRS1/2 and activation of inflammatory mediators, which exacerbate insulin resistance leading to changes in hepatic metabolism (Ozcan et al., 2004). Importantly, hepatic ER stress is well established in both diet and genetic models of obesity (Ozcan et al., 2004). Additionally, ER stress induces both G6Pase and HGP *in vivo* and *in vitro* (Gonzales et al., 2008; Wang et al., 2006a). The change in HGP and G6Pase expression can be alleviated by overexpression of the ER chaperone protein ORP150 in *db/db* mice (Nakatani et al., 2005). Recently, ATF6α has been reported to suppress G6Pase gene expression resulting in lower HGP; however,

during sustained obesity-induced ER stress, ATF6α expression is lost (Seo et al., 2010). Interestingly, the CREB coactivator, CRTC2 (mTORC2) has been shown to bind ATF6α thereby inhibiting HGP restrainment (Wang et al., 2009). This interaction is of note because CRTC2 is activated during fasting and increases gluconeogenic genes including *PEPCK* and *G6Pase* (Cornu et al., 2013). In addition to ATF6, PERK and IRE1α/β affect hepatic metabolism. For instance, mice with an active mutation in eIF2α, part of the PERK pathway, are extremely hypoglycemic and have impaired expression of gluconeogenic genes (Scheuner et al., 2001). Moreover, XBP1s haploinsufficient mice fed a HFD exhibit weight gain, fasting hyperglycemia, and impaired glucose and insulin tolerance (Ozcan et al., 2004).

Lipid metabolism is also affected by the UPR pathways. In fact, hepatic XBP1 disruption lowers the expression of the lipogenic genes *DGAT2*, *ACC2*, and *SCD1* (Lee et al., 2008). Disruption of eIF2α phosphorylation prevents activation of PPARγ and FAS-mediated lipogenesis in response to a HFD (Oyadomari et al., 2008). Furthermore, overexpression of the ER chaperone Bip in genetically obese mouse models lowers SREBP-1c activation and improves glucose and lipid homeostasis (Kammoun et al., 2009). The alterations in both gluconeogenesis and lipogenesis coincide with the ER's central role in hepatic metabolic regulation.

The ER is the site of G6Pase system and therefore, the major site for regulation of HGP. During ER stress, the ER membrane must expand to harbor misfolded proteins and the chaperones, foldases, and degradation transporters

responsible for recovery. Thus, lipogenesis itself may accommodate the membrane expansion required to mount an appropriate recovery response to ER stress.

ER stress-mediated cell death: The UPR is designed to alleviate intracellular stress; however, chronic ER stress can precipitate the induction of apoptosis through several ER stress pathways. For example, IRE1α activates JNK, which phosphorylates and inactivates pro-survival factor Bcl2 and activates pro-apoptotic Bim leading to intrinsic apoptosis (Lei and Davis, 2003). Much of the cell death associated with ER stress is attributed to C/EBP-homologous protein (CHOP) through ATF4 expression. Indeed, diets high in fats or sucrose lead to increased CHOP and Bip expression and increased cell death, as indicated by cleaved caspase 3 activity (Wang et al., 2006b). Chop knockdown in liver cell lines reduces palmitate-induced caspase 3 activity (Pfaffenbach et al., 2010). Alternatively, CHOP deficient mice have improved liver injury following bile duct ligation though inhibition of pro-apoptotic BAX and reduced DNA damage (Tamaki et al., 2008). Though CHOP-deficient mice have similar liver injury in response to MCD diet, a model of NASH (Pfaffenbach et al., 2010). In addition to CHOP and JNK activity, ER Ca^{2+} dyshomeostasis occurs with fatty acid-induced ER stress, and likely contributes to apoptosis (Wei et al., 2009).

Mechanisms of hepatic repair: Hepatocytes maintain the capacity to proliferate following tissue injury or loss. For example, during liver resection, viral infection, or toxic stress, the remaining healthy hepatocyte population will expand to compensate for physical or functional loss. Several studies using mice

overexpressing plasminogen activator (a model of chronic liver injury) demonstrated that healthy or transplanted hepatocytes will undergo several rounds of proliferation in order to meet whole-body metabolic demand (Rhim et al., 1994, 1995; Sandgren et al., 1991). Moreover, in dogs, transplanted livers will either expand or contract to meet the metabolic demands of the recipient (Kam et al., 1987). The same is true for liver transplants in rats gradually proliferating until optimal size is reached (Francavilla et al., 1994). Stressed liver cells, however, may not possess the full ability to respond appropriately when challenged. For example, human patients with steatosis are more likely to suffer perioperative complications following liver resection than healthy patients, though these effects may be remnant of reduced hepatic secretion of clotting factors (Kooby et al., 2003). Thus, steatosis itself may limit the regenerative and repair potential of hepatocytes.

Triggers of hepatic regeneration: Following injury due to hepatotoxins or resection, inflammatory cytokines must “prime” the liver for regeneration, as first proposed by Fausto et al. The priming phase is required for full DNA replication by initiating the transition from quiescent G_0 to G_1 (Webber et al., 1994; Fausto et al., 2006). TNF-α and IL-6 are the primary cytokines responsible for inflammatory signaling through activating protein 1, STAT3, and $NF_{\kappa}B$. Inflammatory signaling is required to activate parenchymal proliferation following loss (Akerman et al., 1992; Cressman et al., 1996). In addition to cytokines, bile acids, amino acids, and inflammatory lipids, promote repair following injury.

However, mitogens and their receptors are vital to the regenerative capacity of hepatocytes and their significance will be outlined below.

Mitogens and their receptors: Mitogens include a large family of soluble proteins that act through autocrine, paracrine, and endocrine signaling. The primary mitogens involved in hepatic function (including repair, regeneration, growth, and metabolism) are insulin, HGF, TGF-α, HB-EGF, EGF, β-catenin, and many others. Insulin's role in hepatic function is primarily though metabolic regulation and was previously discussed. β-catenin signaling is implicated in repair and organogenesis but will not be outlined here. The remaining mitogens activate receptor tyrosine kinases (RTKs) and are directly involved in hepatic repair following injury and are outlined below.

Mechanical stress on hepatocytes releases several ligands associated with repair. For example, mechanical stress or tissue damage activates metallopeptidases releasing growth regulators (TGF-β) and mitogens (EGF, HB-EGF, and HGF) into the circulation or through paracrine action. These ligands act primarily through the epidermal growth factor receptor (EGFR) family. In fact, the secretion and circulating concentration of many EGFR ligands and subsequent hepatic EGFR activation increases following partial hepatectomy in mice (Berasain et al., 2005; González et al., 2010; Ito et al., 1994; Jones et al., 1995; Kiso et al., 1995; Mead and Fausto, 1989; Zerrad-Saadi et al., 2011).

Epidermal growth factor receptors and ligands: In hepatocytes, the major RTKs that governs cell proliferation and survival is the EGFR family. EGFR family members are activated by several ligands including EGF, TGFα,

amphiregulin, and HB-EGF (Berasain et al., 2005; Ito et al., 1994; Kiso et al., 1995; Natarajan et al., 2007; Paranjpe et al., 2010). There are four main EGFR family members EGFR, and ErbB 2-4. ErbB-2 and -4 have catalytically active cytosolic domains similar to EGFR, whereas ErbB-3 is catalytically inactive. Adding to the complexity, EGFR family members can form both homo- and heterodimers upon ligand activation (Bose and Zhang, 2009; Schlessinger, 2002). Studies in rat liver and rat hepatoma cells demonstrate preferential expression of EGFR and ErbB-3, with low expression levels of ErbB-2, whereas mouse liver samples contain the highest level of EGFR (Carver et al., 2002; Onuma et al., 2009). Given the expression patterns and plethora of studies revealing the importance of EGFR in hepatic regeneration, we chose to focus on EGFR.

In isolated mouse hepatocyte studies, EGFR initiates proliferation by inducing cyclins and suppressing cyclin dependent kinase inhibitors, which together promote the G_1-S phase transition (Collin de l'Hortet et al., 2012). Of note, cell cycle activation requires priming by cytokines, as previously mentioned. Conversely, inhibiting EGFR activation increases cellular caspase 3/7 activity, decreases viability, and reduces expression of pro-survival factors including Bcl-2 and Survivin (Paranjpe et al., 2010; Schiffer et al., 2005). Thus, EGFR signaling can control hepatocyte proliferation and the balance between cell survival and death through multiple mechanisms.

Under normal conditions, total hepatic mass is tightly protected; when a loss of hepatic tissue occurs, the liver (and other organs) responds by initiating

programs (e.g., EGFR signaling) aimed at increasing the numbers of hepatocytes. Studies using liver-specific EGFR ablation demonstrate EGFR is required for complete liver regeneration and activation of the stress response kinase p38 following partial hepatectomy (Natarajan et al., 2007). Additionally, shRNA-mediated knockdown of EGFR in hepatectomized rat liver reduced BrdU labeling and gene expression of several cyclins. Alternatively, these mice exhibit increased expression of pro-apoptotic genes such as BID, and Bak1, and activates caspases 3/7 while reduced expression of the pro-survival gene Survivin (Paranjpe et al., 2010).

Several signaling cascades emanating from RTKs regulate cell proliferation and survival, and these pathways may become compromised during conditions of stress (Achard and Laybutt, 2012; Hotamisligil, 2010; Wang et al., 2006b). Pathologically, hepatic EGFR signaling is decreased in mouse models of obesity, and following partial hepatectomy, the regenerative response in these mice is impaired (Collin de l'Hortet et al., 2014). Importantly, in both mice and human liver tissue, EGFR expression has been negatively correlated with steatosis. Steatosis negatively affects postsurgical outcomes in human patients following partial hepatectomy and is associated with increased hepatic apoptosis (Collin de l'Hortet et al., 2014; McCormack et al., 2007; Wieckowska et al., 2006). Unfortunately, the mechanisms for obesity-impaired regeneration and survival as well as hepatic EGFR dysfunction are not well known.

EGF regulation of metabolism: EGF is produced by the submandibularly gland and secreted into saliva and plasma. Similar to glucagon, and perhaps due

to increased catecholamines, plasma levels of EGF increase during fasting in mice (Grau et al., 1994). Importantly, microsomal studies reveal a decreased affinity of EGF for its receptor during fasting (Freidenberg et al., 1986). Early studies of EGF reveal its ability to stimulate glycogen synthesis through activation of glycogen synthase α (Bosch et al., 1986; Chan and Krebs, 1985). This dynamic regulation allows EGFR signaling to mimic insulin-mediated suppression of HGP by promoting the uptake and storage of glucose as glycogen. For example, like insulin, EGF stimulation suppresses G6Pase and PEPCK expression *in vitro* and *in vivo* and activates glycogen synthase (Fillat et al., 1993; Chan and Krebs, 1985). Moreover, adenoviral-mediated overexpression of MEK, a downstream effector of EGFR signaling, decreases G6Pase expression and fasting blood glucose in mice (Jiao et al., 2013). Furthermore, cell line studies reveal phorbol esters, which activate the MAPK cascade through phospholipase C and diacylglycerol generation, suppress G6Pase promoter activity, and this suppression is lost via treatment of MEK inhibitors (Schmoll et al., 2001). Taken together, the suppression of gluconeogenesis and activation of glycogen synthase suggest an anabolic role for EGF. These effects may be independent of hepatic EGFR expression as liver specific EGFR knockout mice display similar hepatic metabolic function on standard chow diets (Natarajan et al., 2007).

Mig6 and EGFR: Because EGFR signaling activates proliferation, migration, differentiation, and cell cycle entry, controlling stimulus duration and intensity is vital to avoid uncontrolled growth and mitigate the risk of cancer

(Fischer et al., 2003). Therefore, EGFR signaling has many negative feedback regulator mechanisms, including receptor endocytosis, phosphatases, and most importantly, inducible feedback inhibitors. Physiologically, EGFR signaling activates the transcription of several inducible feedback inhibitors, including Socs4, Socs5, Lrig1, and Mig6, which serve to shut off EGFR activation and signaling in a classical negative feedback manner (Segatto et al., 2011). Socs4, Socs5, and Mig6 are transcriptionally activated rapidly (1-4 h) following mitogenic signals (Kario et al., 2005; Fiorentino et al., 2000).

Of all the inducible EGFR negative feedback inhibitors, Mig6 is the only one known to be induced by a variety of stress stimuli including hypoxia, cytokines, and phorbol esters (Chu et al., 1988; Radaelli et al., 2003; Xu et al., 2006; Zhang and Vande Woude, 2007). Early studies reveal insulin, cAMP, and hydrocortisone induce Mig6 gene transcription (Lee et al., 1985). EGF induces Mig6 gene expression directly through EGFR mediated MAP kinase signaling, as indicated by inhibitor studies (Fiorini et al., 2002). The Mig6 gene encodes a 53 kDa protein containing 14-3-3, SH3, CRIB, PDZ, and EGFR binding domains (Makkinje et al., 2000). The expression of Mig6 correlates with the transition from G_1 to S phase in synchronized cells, indicating its importance in cell cycle control (Wick et al., 1995). Mutation and crystal structure studies established the EGFR/ErbB binding region that contributes to Mig6's inhibitory function against EGFR (Anastasi et al., 2007; Zhang et al., 2007). Thus, Mig6 is subjected to a variety of regulation allowing for the precise control of EGFR signaling during both physiological and pathophysiological conditions.

Mig6 binds to EGFR, thereby preventing its autophosphorylation, while enhancing ubiquitin-mediated degradation (Zhang et al., 2007; Frosi et al., 2010). Knockdown studies *in vitro* and gene deletion experiments *in vivo* reveal Mig6 deficiency promotes sustained EGFR signaling and enhanced ERK phosphorylation; whereas adenoviral-mediated overexpression of Mig6 has the opposite effects (Reschke et al., 2010; Colvin et al., 2013).

Control of Mig6: Mig6 has a short half-life under normal conditions (~1-2 h) (Fiorini et al., 2002). However, our group has shown protein turnover is slowed during stress conditions (here and Chen et al., 2013). Mig6 transcripts also evade transcriptional repression during ER stress conditions (Chen et al., 2013). In addition, Mig6 is subjected to posttranslational modifications. Recent studies indicate Mig6 contains several serine and tyrosine residues susceptible to phosphorylation (Liu et al., 2012; Park et al., 2015). These studies suggest Mig6 itself is subject to regulatory control, indicating the importance of EGFR feedback inhibition.

Mig6 function: As previously mentioned, Mig6 is induced by a variety of ligands, including HGF. Suppression of Mig6 via siRNA increases cell migration in mouse liver progenitor cells in a HGF/c-Met receptor dependent manor (Descot et al., 2009). Mig6 induction by EGFR activation serves to protect cells; however, Mig6 induction by cellular stressors leads to apoptosis in a variety of cell types (Chen et al., 2013, 2014; Makkinje et al., 2000; Reschke et al., 2010; Xu et al., 2005, 2006). Inversely, mic lacking Mig6 have reduced *in utero* survival and die within 6 months of age. Interestingly, these mice are subjected to hyper-

proliferation of skin, cartilage and bone (Ferby et al., 2006; Jin et al., 2007; Zhang et al., 2005). In fact, in our animal facility, out of hundreds of litters only a few pups were successfully born (Chen and Lutkewitte, personal communication). The increase in proliferative response is attributed to overactive EGFR signaling (Ferby et al., 2006). These findings reiterate the importance of Mig6 in the regulation of growth.

In liver, reducing Mig6 with either genetic ablation or siRNA-mediated suppression enhances EGFR activation and mitogen signaling (Reschke et al., 2010). Additionally, hepatocytes lacking Mig6 exhibit increased EGFR signaling *in vitro* and enhanced liver regeneration following partial hepatectomy *in vivo* (Reschke et al., 2010). Mig6 liver-specific knockout (LKO) mice present with hepatomegaly and increased serum cholesterols (HDL and LDL) (Ku et al., 2012). The changes in cholesterol have been attributed to decreases in bile acid reuptake, though the exact mechanisms need further exploration.

Given the array of pathologies associated with NAFLD and the recent links between the EGFR feedback inhibitor, Mig6, and hepatic metabolism, we sought to define a possible mechanism through which Mig6 affects NAFLD development. Because Mig6 is induced by stress, we tested the extent to which hepatic EGFR activation was decreased during pharmacological-, fatty acid-, and obesity-induced ER stress due to Mig6. We utilized both *in vitro* and *in vivo* models of substrate-induced hepatic stress and have determined several novel mechanisms through which Mig6 regulates hepatic metabolism (Figure 1).

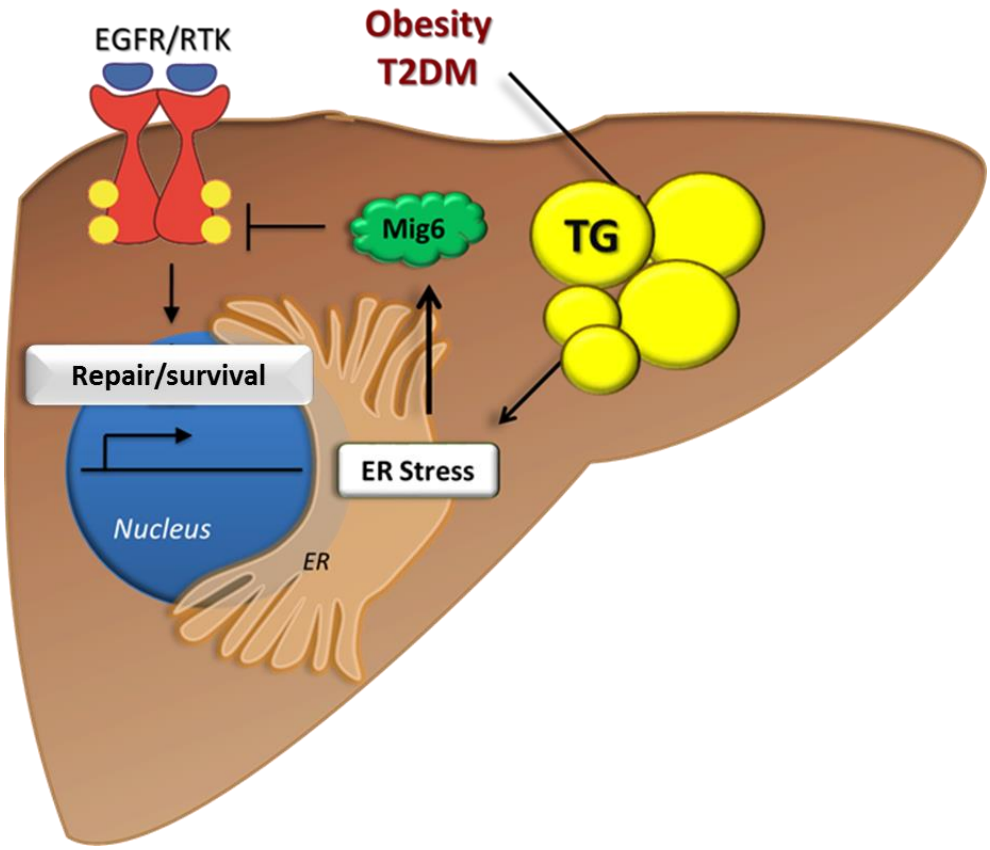

Figure 1: Proposed model for Mig6 activation and EGFR inhibition during obesity-induced stress

AIMS

Aim 1: Determine the extent to which Mig6 regulates EGFR signaling during hepatic ER stress. Given the large precedence of research outlining Mig6 as a EGFR regulator that becomes inappropriately activated during stress conditions, we **hypothesized** that fatty-acid induced ER stress activated Mig6 expression and decreased EGFR activation and cell survival.

Aim 2: Determine how Mig6 upregulation during obesity and obesity-induced ER stress alters hepatic metabolism. Several studies reveal compromised EGFR activation during obesity-induced hepatic stress. Furthermore, initial studies suggest Mig6 and EGF ligand are important regulators of hepatic metabolism and function, therefore, we **hypothesized** high fat diet-fed mice will have reduced EGF-mediated EGFR activation, and Mig6 ablation will have improved hepatic function and metabolism.

CHAPTER 2: MATERIALS AND METHODS

Animal studies

Control C57Bl/6J mice: All animals were handled and cared for according to protocols approved by the Indiana University School of Medicine Institutional Animal Care and Use Committee. Mice were weaned at three to four weeks of age depending on size, maintained on a standard 12-h light-dark cycle, and had free access to chow diet and water. BLKS *db* mice (heterozygous *db/+* and homozygous *db/db* littermates) were maintained by Dr. David Morris from the laboratory of Dr. Carmella Evans-Molina under similar conditions as C57Bl/6J mice. For initial high fat feeding studies, six-week-old male C57Bl/6J mice were fed either breeder chow (15% kcal from fat) or a high fat diet (HFD, 60% kcal from fat, no. D12492, Research Diets, New Brunswick, NJ) for 15 weeks. For fasting studies, food was removed at 9:00 a.m. for 6 or 5 h (for appropriate test). For overnight fasting and refeeding studies, mice were fasted at 5:00 p.m. through the following day or refed *ab libum* the last 6 hours.

Mig6 liver-specific knockout mice (LKO) and littermate controls: Mig6 LKO mice were generated from Mig6 homozygous flox mice ($Mig6^{fl/fl}$) obtained from Dr. George Vande Woude and crossed with mice expressing Cre recombinase under the control of the albumin promoter (B6.Cg-Tg(Alb-cre)21Mgn/J, The Jackson Laboratory, Bar Harbor, ME). DNA was extracted from tail biopsies and amplified using Extract-N-Amp® (Sigma Aldrich, St. Loius, MO), and genotypes were determined as described by Vande Woude (flox alelles) and The Jackson Laboratory (Alb-cre); examples are shown in chapter 4.

At six weeks of age, Mig6 LKO and littermate controls were fed either a low fat diet (LFD, 10% kcal from fat with matched sucrose content of HFD, no. D12492J, Research Diets) or HFD (as described above) for 16 weeks.

Metabolic studies: Blood was collected from tail veins via tail nick, and blood glucose was measured using an AlphaTRAK glucometer (Abbott Laboratories, Abbott Park, IL). Glucose tolerance tests (GTT) and modified GTT were performed on 6 h-fasted mice given an intraperitoneal (IP) bullous injection of glucose (2 g/kg bw, Sigma) and blood glucose was measured at times indicated. For modified GTT, tail blood (~100 µL) was collected into EGTA coated capillary tubes (Sarstedt, Numbrecht Germany) and plasma was separated via centrifugation at 6000 rpm for 10 min at 4°C. Plasma was diluted in plasma diluent and insulin was measured using an ultra-sensitive mouse insulin ELISA (Crystal Chem, Downers Grove, IL). Insulin tolerance tests (ITT) were performed on 5 h-fasted high fat fed mice given an IP injection of human recombinant insulin (0.75 U/kg bw in 0.01% bovine serum albumin (BSA), Novolin U100, Novo Nordisk). To avoid adverse hypoglycemia, if a blood glucose fell below 50 mg/dL, then the mouse was given an IP bolus of glucose (2g/kg bw) and further analysis was stopped. Pyruvate tolerance tests (PTT) were performed on 16 h-fasted high fat fed mice given a IP injection of sodium pyruvate (2 g/kg bw, Sigma) dissolved in phosphate-buffered saline (PBS).

Plasma metabolites: Plasma samples were collected from 16 h-fasted mice at the time of termination. Triglycerides and non-esterified free fatty acids were measured using colorimetric enzymatic assays (Wako Diagnostics,

Richmond, VA). Plasma AST, ALT, albumin, HDL, and LDL were determined by the Translation Core of the Center for Diabetes and Metabolic Diseases at Indiana University School of Medicine (IUSM). Plasma insulin was measured in 6 h- and 16-h fasted mice as described above.

Hepatic assessment

Immunohistochemistry: Following termination at 15-16 weeks of diet, livers were immediately harvested, weighed, and sections of the left lateral lobe were removed and placed in zinc formalin for 3 h, then rinsed in 70% ethanol for paraffin embedding. The remaining liver was minced and flash frozen in liquid nitrogen. Paraffin embedding, sectioning (5 µM), and hematoxylin and eosin staining was performed by the IUSM Histology Core. Microscopic examination was performed by a board-certified veterinary pathologist (Dr. Abigail Cox Durkes, MS, DVM, Diplomate ACVP, Department of Comparative Pathobiology, Purdue University College of Veterinary Medicine). The interpretation was based on standard histopathological morphology and NAFLD activity scores (NAS, (Kleiner et al., 2005)). The pathologist was blinded to the treatment groups. To determine the NAS, a semi-quantitative method was used that included percentage of hepatic steatosis, hepatic inflammation, and the presence of balloon cells indicating hepatocellular injury. A histo-morphological scale is provided in Table 1.

Table 1: Histological scoring parameters of H&E liver sections

Item	Definition	Score
Steatosis	<5% 5%-33% >33%-66% >66%	0 1 2 3
Lobular inflammation	No foci <2 foci per 200X field 2-4 foci per 200x field >4 foci per 200x field	0 1 2 3
Liver cell injury (ballooning: cellular enlargement 1.5-2 times the normal hepatocyte diameter, with rarefied cytoplasm)	None Few balloon cells (rare but definite) Many cells/prominent ballooning	0 1 2

Notes: Ballooning is difficult to assess in mice because their hepatocytes are normally variably sized. A score of 1.5 indicates that there were prominent but focal aggregates of balloon cells, not diffuse which would warrant a 2. A score of 2.5 in steatosis indicates that are areas within the section that are a 3 but also areas that are a 2.

Immunofluorescence: Paraffin-embedded liver sections were de-waxed in xylenes and rehydrated by ethanol gradient (100, 90, 80, 70% for 60 seconds each). Slides were rinsed in ddiH_2O and boiled in antigen unmasking solution (Vector Labs, Burlingame, CA) in a microwave over for 13.5 min at 1000 watts. Slides were allowed to cool before blocking in blocking solution (Vector Labs) for 30 min at RT. Primary rabbit anti-phospho-histone H3 (PHH3) antibody (Millipore, Billerica, MA) was diluted in antibody diluent (1:200, Vector Labs) and incubated overnight at 4°C. Slides were incubated in secondary Alexa Flura 555 for 1 h prior to DAPI staining (5 min in DAPI buffer (PBS with 0.3 M NaCl and 0.03 M Na^+ Citrate) and mounting. Slides were allowed to cure and imaged using a Zeiss LSM710 Confocal Microscope. Quantification of $PHH3^+$ cells and nuclei were performed on three random 3x3 40X tiles scans using ImageJ software (National Institutes of Health).

Beta cell area: Paraffin-embedded pancreata were dewaxed and prepared as before with the exception of incubation in anti-rabbit primary insulin antibody overnight at $4^{\circ}C$. Sections were washed and incubated in peroxidase conjugated anti-rabbit IgG for 30 min. Following a wash cycle sections were developed with peroxidase substrate for 2 min. The slides were then counter-stained with Hematoxylin for 10 s before dehydration and mounting. Area was quantified using Axion software and determined as area of total pancreas divided by insulin positive area.

Oil Red-O: For frozen sections, livers from the same left lateral lobe as above were incubated in 4% paraformaldehyde for 3 h, washed in PBS, and

dehydrated in 30% sucrose overnight at 4°C. The following day tissue was rinsed in 50% optimal cutting temperature resin (OCT)/sucrose for 30 min prior to transfer to 100% OCT and frozen at -80°C until sectioned (8 µm) using a cryostat. Frozen sections were thawed, dried, and stained for Oil-Red-O (Sigma) as previously described (Mehlem et al., 2013). Briefly, sections were fixed in paraformaldehyde (PFA) for 20 min, rinsed in ddiH_2O and incubated in freshly prepared Oil-Red-O for 5 min. Slides were rinsed in ddiH_2O for 30 min, and immediately mounted using water soluble mounting media. Ten random 40 X bright field images per section were used for quantification using ImageJ software.

Insulin signaling: For insulin signaling studies, mice were fasted overnight and IP injected with either vehicle (PBS with 0.01% BSA) or insulin (10 min, 5 U/kg bw) prior to harvest. Frozen liver samples were placed in lysis buffer (100 mg/mL, describe below) containing 2% SDS and homogenized (PolyTron PT2100, Kinematica AG, Luzern, Switzerland). Samples were rotated for 30 min at 4°C prior to centrifugation. The aqueous layer was removed, and samples were centrifuged again prior to western analysis.

Hepatic triglyceride content: Frozen tissue (100 mg) was homogenized in PBS (1 mL) and mixed with a 2:1 mixture of chloroform and methanol ($CHCl_3$). Samples were vortexed and mixed on a rocker for 30 min at 4ºC. Aqueous and lipid layers were separated by centrifugation (3000 rpm) for 10 min at 4ºC. The lower $CHCl_3$ layer was collected and the chloroform was evaporated overnight in a fume hood. Lipids were resuspended in isopropanol plus 1% triton-100 by

vortexing and heating at 65ºC. Triglycerides were determined using a colorimetric enzymatic assay (WAKO).

Real-time quantitative PCR and RNA sequencing: Frozen tissue was lysed in Qiazol® (≤10 mg/mL, Qiagen, Valencia, CA) and homogenized (Polytron PT2100). Samples were allowed to rest before extraction by vortexing in 2:1 chloroform: methanol. Samples were centrifuged and RNA was extracted from the aqueous layer using an RNeasy Mini Prep kit (Qiagen). Genomic DNA was removed via on column DNA digest (Qiagen).

For RT-qPCR, complementary DNA was generated using high capacity cDNA kit (Applied Biosystems, Foster City, CA). Quantitative PCR was performed using Taqman Master Mix and Taqman probes as listed in Table 2. RNA content was normalized to GAPDH and expression levels were quantified using 2-ΔΔCT method from at least three independent experiments performed in triplicate. Complete RNA sequencing studies were performed by the IUSM Center for Medical Genomics. Briefly, RNA quality was determined using a bioanalyzer (Agilent Technologies, Santa Clara, CA) and sequencing was carried out using an Ion Torrent Sequencer (Thermo Fisher).

Table 2: List of Taqman Probes for qPCR

Gene	Product number	Species
MIG6	Hs0021960_ml	Human
CHOP	Hs00358796_gl	Human
BIP/HSP5A	Hs00607129_gh	Human
SOCS4	Hs00328404_s1	Human
SOCS5	Hs00751962_s1	Human
LRIG1	Hs00394267_m1	Human
GAPDH	Hs02758991_g1	Human
mig6	Rn01520745_m1	Rat
chop	Rn01458526_m1	Rat
bip/hsp5a	Rn01435769_g1	Rat
socs4	Rn01414734_m1	Rat
socs5	Rn01769079_m1	Rat
lrig1	Rn01421201_m1	Rat
gapdh	4352338E	Rat
egfr	Mm00433023_m1	Mouse
mig6	Mm00505292_m1	Mouse
gapdh	4351309	Mouse
pepck	Mm00440636_m1	Mouse

Table 3: List of primers for SYBR green qPCR

Gene	5'-3'	Species
g6pase	Fw-CCATGCAAAGGACTAGGAACAA Rev-TACCAGGGCCGATGTCAAC	Mouse
glucokinase	Fw-CCCTGAGTGGCTTACAGTTC Rev-ACGGATGTGAGTGTTGAAGC	Mouse

Cell culture

Cell lines: Cell lines were purchased directly from ATCC (Manassas, VA). HepG2 human, male, hepatocellular carcinoma cells (HB-8065, ATCC) were cultured in DMEM containing 25 mM glucose supplemented with 10% fetal bovine serum (FBS; Sigma Aldrich, St. Louis, MO), 1 mM sodium pyruvate, and penicillin-streptomycin (100 U/mL). H4IIE rat hepatoma (CRL-1548, ATCC) were cultured similar to HepG2 cells with the exception of the DMEM contained 5.5 mM glucose. Cell lines were regularly passaged and seeded at appropriate confluence for studies.

Primary hepatocytes: Primary hepatocytes were isolated from Sprague Dawley rats at Triangle Research Labs (Durham, NC) and shipped the following day; upon arrival, shipping media was replaced with DMEM containing 25 mM glucose and supplemented as above (both dexamethasone and insulin are known to induce Mig6 gene expression and were therefore omitted during palmitate treatments (Chu et al., 1988; Colvin et al., 2013)).

Ligand stimulation and drug treatments: Sixteen hours prior to ligand stimulation and during stress treatments, FBS-containing media was replaced with media containing 0.1% bovine serum albumin (BSA, Sigma Aldrich). Cells at 70-80% confluency were treated with thapsigargin (Sigma Aldrich), tunicamycin (Sigma Aldrich), or vehicle (DMSO) as indicated. Cells were treated at dose and time indicated with palmitate or vehicle (BSA) using sodium palmitate (Sigma Aldrich) dissolved in 70% ethanol and conjugated at 7:1 ratio to BSA. Hydrogen peroxide (Sigma Aldrich) treatments were performed with freshly diluted H_2O_2 in

serum free media for times and doses indicated. Cells were stimulated with 50 ng/mL recombinant rat EGF in 0.01% BSA (R&D systems, Minneapolis, MN) for times indicated.

Western blot analysis and antibodies: HepG2, H4IIE, and primary rat hepatocytes were washed twice with ice cold PBS and lysed in IGEPAL lysis buffer (10% IGEPAL, 10% glycerol, 1 mM NaCl, 1 mM HEPES, and *O*-octyl glucoside, phosphatase and protease inhibitor tablets (Roche, Mannheim, Germany). Samples were vortexed and centrifuged at >20,000 x *g* for 10 min at 4°C. SDS (2%) was added to lysates from cells treated with palmitate, then sonicated and spun at room temperature. The middle aqueous layer was removed and re-centrifuged. Protein content was determined by bicinchoninic acid assay (ThermoFisher) and read on a spectrometer (SpectrMax M5, Molecular Devices, Sunnyvale, CA). Protein (30-40 μg) was reduced in LDS loading buffer plus reducing agent (Invitrogen) and boiled at 100°C for 6 min. Samples were loaded onto 10% Bolt Bis-Tris gels (Invitrogen) and separated at 140 volts for 50 min. Proteins were transferred to an Immunobilon-FL Transfer Membrane (Millipore, Bedford, MA) at 110 volts for 50 min in ice cold transfer buffer. Membranes were blocked in Li-Cor Odyssey blocking buffer for 1 h at room temperature and incubated with primary antibody overnight. Membranes were then washed 3 times in TBS and incubated with IRDye 800 or 700 flurophore-labeled secondary antibodies for 1 h. Antibodies were diluted in either 1% w/v polyvinylpyrrolidone or signal enhancer (Nacalai, San Diego, CA) and are listed in Table 4. Blots were washed in TBS-1% Tween and protein bands were

visualized on the Odyssey System (LI-COR) and quantified using ImageJ software. Boxes around the representative images indicate antibodies probed on the same membrane.

Table 4: List of antibodies used

Antibody	Manufacturer	Product	Dilution

		Number	
Mig6	Santa Cruz Biotechnology	137154	1:500
P-eif2α	Cell signaling	3398	1:1000
eif2α	Cell signaling	5324	1:1000
P-ERK 1/2	Cell signaling	9101S	1:1000
ERK 1/2	Cell signaling	4696S	1:1000
P-EGFR	Cell signaling	3777S	1:1000
EGFR	Cell signaling	4267S	1:1000
Caspase 3	Cell signaling	9662	1:1000
JNK	Cell signaling	9252S	1:1000
P-JNK	Cell signaling	9251S	1:1000
Actin	MP biomedical	691002	1:10000
GAPDH	Abcam	9484	1:2000
γ-tubulin	Sigma Aldrich (mouse)	T6557	1:1000
EGFR	Sigma Aldrich (mouse)	E3138	1:1000
FLAG	Sigma Aldrich (mouse)	F3165	1:1000
Insulin	Santa Cruz Biotechnology	Sc9168	1:500
Phosphohistone H3	Millipore	06-570	1:200
G6Pase	Santa Cruz Biotechnology	Sc2584	1:500
P-AKT	Cell signaling	4058S	1:1000
AKT	Cell signaling	2920S	1:1000
p-foxo1	Cell signaling	9461S	1:1000
Foxo1	Abcam	ab131206	1:2000

Reverse transcription and quantitative PCR: For RNA isolations, cells were lysed in RLT buffer containing 1% β-mercaptoethanol. Genomic DNA was removed via gDNA column (Qiagen, Valencia, CA), and RNA was isolated with

an RNeasy mini prep kit (Qiagen). Complementary DNA was generated using high capacity cDNA kit (Applied Biosystems, Foster City, CA). Quantitative PCR was performed using Taqman Master Mix and Taqman probes as listed in Table 2. Gene expression was also carried out using SYBR Green Taqman gene expression system with primer sets listed in Table 3. RNA content was normalized to GAPDH or actin and expression levels were quantified using $2^{-\Delta\Delta CT}$ method from at least three independent experiments performed in triplicate.

Mig6 overexpression and siRNA transfection: For gene overexpression studies, cells were transduced with adenoviral vectors driving the expression of green florescence protein (GFP) or Mig6 under the control of the cytomegalovirus (CMV) promoter for 24 h as previously described (Xu et al., 2005). Media was replaced with complete media the follow day and ligand stimulation was conducted 48 h after transduction. For RNA interference studies, cells were seeded at 50% confluency and forward transfected with siRNAs (30 pmol) using Lipofectamine RNAiMAX (Invitrogen, Carlsbad, CA) according to manufacturer's guidelines. Sequences for RNAi were purchased as duplexes from Invitrogen and are as follows: Mig6-1 forward 5'-CGAUAAUAGAACUAGUGACtt-3' reverse 5'-GUCACUAGUUCUAUUAUGtt-3', Mig6-2 forward 5'-GCUAUGUGUCUGACCAAAAtt-3' reverse 5'-UUUUGGUCAGACAUAGCtg-3', and the control *GL-2* siRNA forward 5'-CGUACGCGGAAUACUUCGAtt-3' reverse 5'-UCGAAGUAUUCCGCGUACGtt-3' as previously described (Reschke et al., 2010). The following day the media was replaced with complete media. Ligand and drug treatments were conducted as previously described.

Caspase 3/7 activity assay: HepG2 cells were transfected as before and the following day trypsinized and plated at 40,000 cells per well in black-walled 96-well plates. The following day media was removed and replaced with serum free media containing 0.1% BSA and treated with vehicle (BSA) or palmitate for 8 h. Following palmitate treatment, caspase 3/7 activity was measured using ApoLive-Glo Multiplex Assay (Promega, Madison, WI). Briefly, cells were incubated with Caspase-Glo 3/7 reagent for 30 min and luminescence was measured using a SpectrMax M5 (Molecular Devices, Sunnyvale, CA). Relative luminescence units were normalized to siCon untreated cells and are given as fold increase in caspase 3/7 activity.

Statistical analysis: Experiments were performed at least three independent times. Significance was determined by one- or two-tailed Student's *t*-test or one- or two-way ANOVA with Bonferroni multiple comparison tests where appropriate. Differences were considered significant when $P < 0.05$. Data are reported as means ± SEM.

CHAPTER 3: RESULTS

Mig6 decreases hepatic EGFR activation and survival during saturated fatty acid-induced endoplasmic reticulum stress.

Synopsis: Hyperlipidemia associated with obesity and T2DM promotes excess hepatic lipid storage (steatosis) and ER stress, thereby reducing hepatic cell proliferation and survival. An important receptor tyrosine kinase controlling liver proliferation and survival is EGFR. EGFR expression and activation are

decreased during steatosis in humans and several animal models of obesity. Therefore, restoring EGFR activation in obesity-induced ER stress and diabetes could restore the liver's capacity for survival and regeneration. As an inducible feedback inhibitor of EGFR activity, mitogen-inducible gene 6 (Mig6) is a novel target for enhancing EGFR signaling during diet-induced obesity (DIO) and T2D. Thus, we hypothesized hepatic ER stress induces Mig6 expression and decreases EGFR activation. We discovered that both pharmacological- and fatty acid-driven ER stress increased Mig6 expression and decreased EGF-mediated EGFR activation in primary rat hepatocytes and cell lines. Furthermore, siRNA-mediated Mig6 knockdown restored EGFR signaling and reduced caspase 3/7 activation during ER stress. Therefore, we conclude Mig6 is increased during ER stress in DIO, thereby reducing EGFR activation and enhancing cell death. The implications are the induction of Mig6 during DIO and diabetes may decrease hepatocyte survival, thus hindering cellular repair and regenerative mechanisms.

Introduction: ER stress contributes to the pathogenesis of obesity and diabetes (Oyadomari et al., 2008; Ozcan et al., 2004; Puri et al., 2008). A major contributor to ER stress in hepatocytes is increased saturated FFA delivered to the liver during chronic over nutrition (Pfaffenbach et al., 2010). The induction of chronic ER stress in hepatocytes is associated with increased lipogenesis, insulin resistance, and chronic inflammation (Hirosumi et al., 2002; Gao et al., 2004; Oyadomari et al., 2008). These pathologies are associated with increased NAFLD progression in liver. In fact, severe hepatic ER stress may cause progression towards NASH and eventual liver failure. Therefore, improving

cellular survival pathways would likely improve the overall pathogenesis of NAFLD.

The insulin receptor is a RTK critical to maintaining hepatic metabolism and its activity is decreased during NAFLD (Ozcan et al., 2004). In addition to the insulin receptor, EGFR is a master regulatory of both survival and metabolism. As previously mentioned, EGFR signaling is pro-growth, and pro-survival through the induction of pro-survival factors including bcl-2 and survivin and the inhibition of cellular caspase 3/7 activity (Paranjpe et al., 2010; Schiffer et al., 2005). Notably, chemical chaperons, which alleviate fatty acid induced ER stress improve cell survival. However, the exact mechanisms of how ER stress response impacts survival signaling remain unknown. In β-cells, ER stress induces the EGFR inhibitor, Mig6, and exacerbates cell death during chemical stress and Mig6 ablation improves survival. In liver, Mig6 knockdown, enhances EGFR signaling and cell cycle progression (Reschke et al., 2010). As the liver progresses from simple steatosis towards NASH, the regeneration capacity in conjunction with EGFR activation and expression are decreased (Collin de l'Hortet et al., 2014).

Therefore, we sought to determine the relative contributions of Mig6 during fatty-acid induced hepatic ER stress. Here we utilized several cellular modes of ER stress to show reduced EGFR activation under ER stress. Furthermore, ER stress induced Mig6 expression and enhance protein stability. Mig6 ablation using siRNAs restored EGFR signaling and reduced caspase 3/7 activity following palmitate treatment. These data suggest that Mig6 plays an

inhibitory role during ER stress and could possible serve as a target for improving cellular survival during fatty-acid induced cell stress.

Results

Palmitate and ER stress decrease EGFR activation and activates Mig6 expression: We have previously determined that cellular stress induces Mig6, which impairs EGFR signaling and promotes apoptosis in pancreatic β-cells (Chen et al., 2013). To determine if EGFR is also inhibited by fatty acid-induced ER stress, primary hepatocytes were treated with the saturated fatty acid palmitate prior to EGF stimulation. Indeed, palmitate treatment decreased EGF-mediated EGFR activation and prevented the induction of downstream ERK phosphorylation (Figure 2A-C). This signaling inhibition occurred in the context of increased intrinsic cell death as measured by caspase 3/7 activity (Figure 2D).

The magnitude and duration of EGFR signaling can be modulated by several inducible feedback inhibitors, including *Socs4, Socs5, Lrig1*, and *Mig6*. Thus, inhibitor expression levels were assessed in palmitate-treated H4IIE cells. Under these ER stress conditions with elevated levels of *Bip* and *Chop*, only *Mig6* gene expression was significantly increased whereas the other inhibitors were not induced (Figure 3).

Diet-induced obesity triggers a variety of pathological responses in the liver including inflammation, insulin resistance, steatosis, and ER stress (Hotamisligil, 2010b; Ozcan et al., 2004). Because we have previously established that Mig6 is upregulated during ER stress in non-hepatic tissues (Chen et al., 2013), we sought to directly measure the effects of chemically-

induced ER stress on EGFR inhibitors in hepatocytes, with the rationale being that ER stress in response to palmitate treatment promotes Mig6 induction. H4IIE cells were treated with the ER stress inducer thapsigargin, which inhibits the sarcoendoplasmic reticulum calcium transport ATPase, and ER stress was confirmed by elevated *Bip* and *Chop* expression (Figure 4A,B). Like palmitate exposure, thapsigargin treatment increased *Mig6* gene expression in both dose-responsive and time-dependent manners (Figure 4C). Further, ER stress, as indicated by elevated *Bip* expression, increases *Mig6* transcript and protein levels in human HepG2 cells (Figure 5). Importantly, no changes were observed in *Socs4*, *Socs5*, and *Lrig1* gene expression in H4IIE during thapsigargin treatment compared with DMSO, and only *Socs4* gene expression was increased during thapsigargin treatment in HepG2 cells (Figure 6). Thus, Mig6 alone appears to be the primary form of negative feedback inhibition of EGFR in hepatocytes during ER stress.

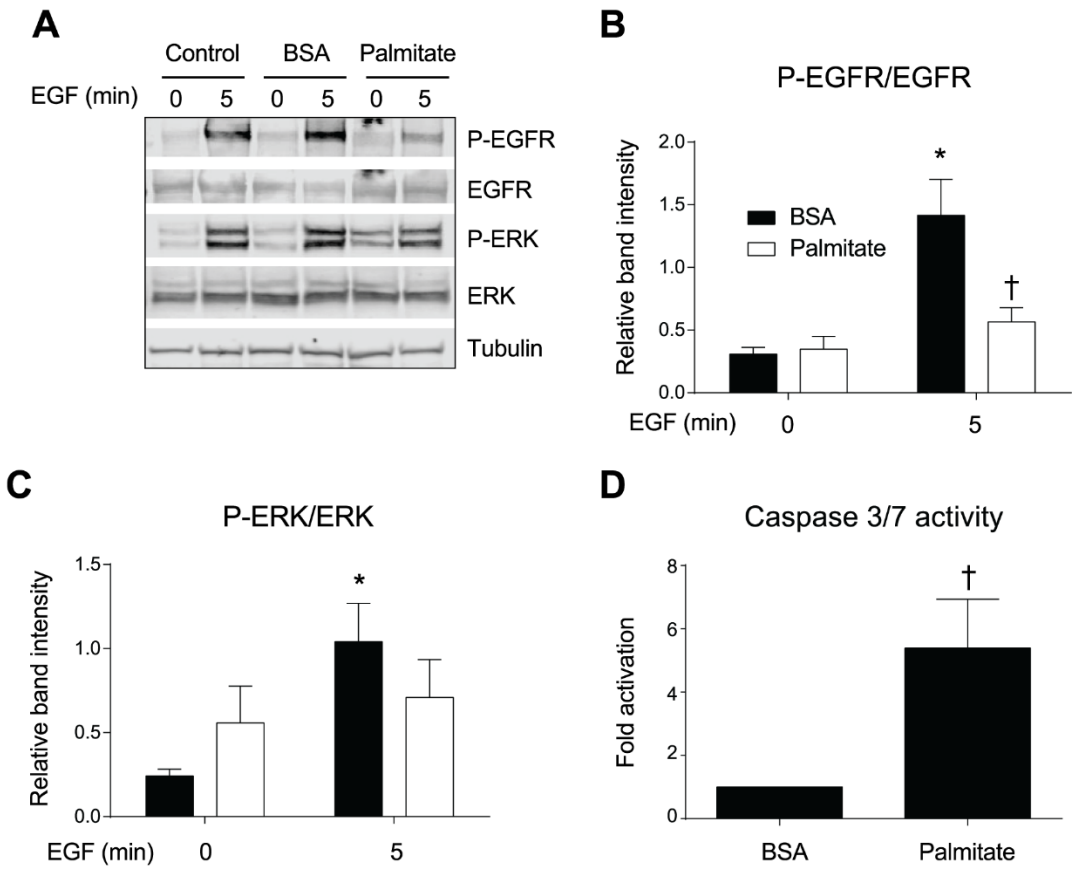

Figure 2: Palmitate decreases EGFR activation in primary hepatocytes and activates caspase 3/7.

Primary rat hepatocytes were treated with BSA or palmitate (750 μM) for 48 h. Twenty-four h prior to rrEGF (50ng/mL) media was replaced with serum free media. EGFR and ERK activation were assessed by Western blot. Shown is a representative blot (A). P-EGFR and P-ERK were normalized to EGFR and ERK, respectively (B,C). Caspase 3/7 activity was measured by luminescence following palmitate treatment for 48 h (D). Data are reported as means ± SEM; n = 3-4. *, $p < 0.05$ vs. untreated cells; †, $p < 0.05$ vs. BSA treated cells.

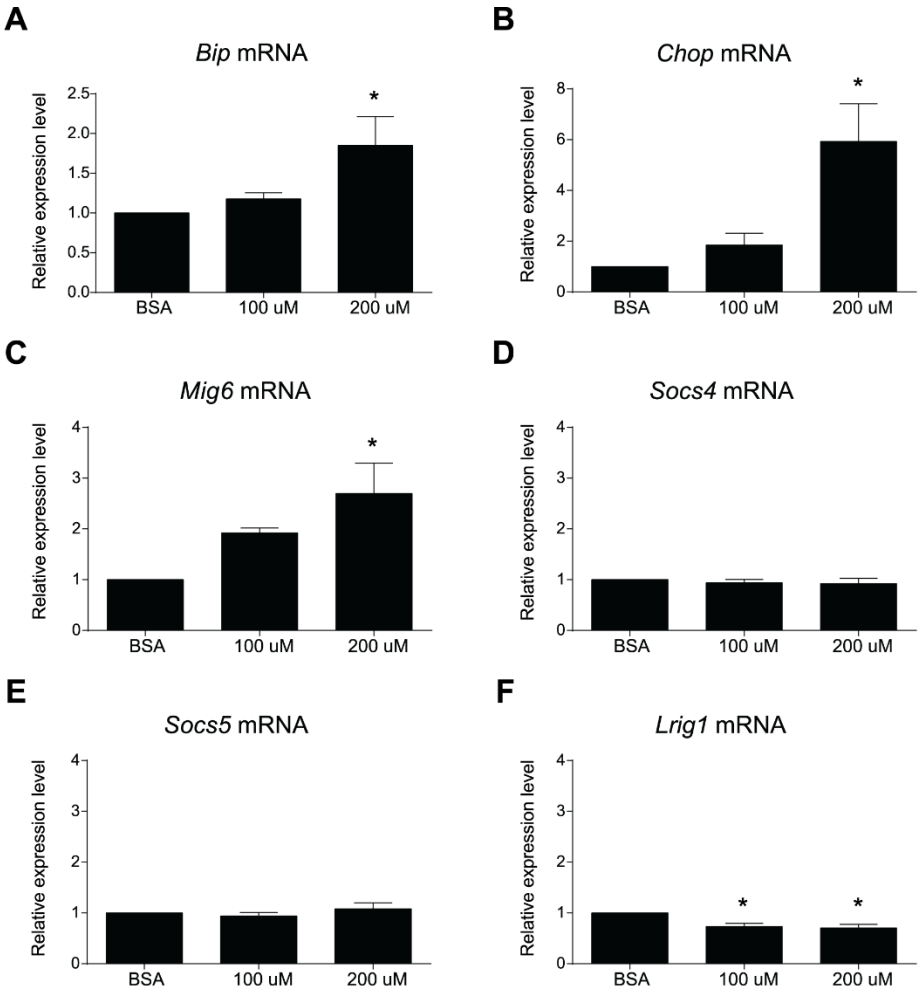

Figure 3: Palmitate-induced ER stress increases Mig6 expression in H4IIE cells.

H4IIE cells were treated with vehicle (BSA) or palmitate for 8 h at doses indicated in serum free media. mRNA expression was determined by qPCR. ER stress was confirmed by *Bip* and *Chop* mRNA expression (A,B). *Mig6, Lrig1, Socs4*, and *Socs5* mRNA were also determined (C-F). Data are reported as means ± SEM; n = 4. *, $p < 0.05$ vs. DMSO.

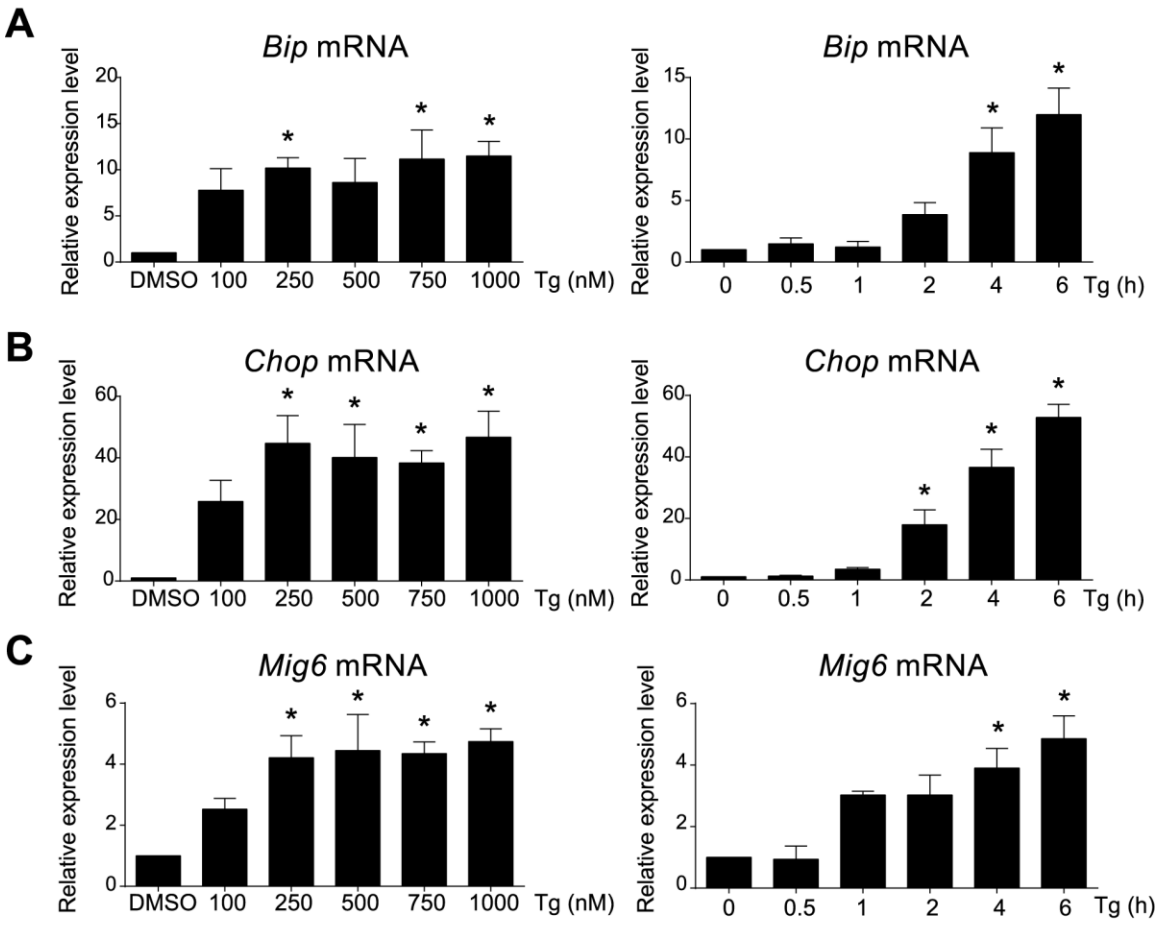

Figure 4: ER stress induces Mig6 in rat H4IIE cells.

H4IIE cells were treated with vehicle (DMSO) or 1.0 µM thapsigargin (Tg) for 6 h or dose (nM) and time (h) indicated. *Mig6*, *Chop* and *Bip* mRNA (A-C) expression were assessed by qPCR. Data are reported as means ± SEM; n = 4. *, $p < 0.05$ vs. DMSO.

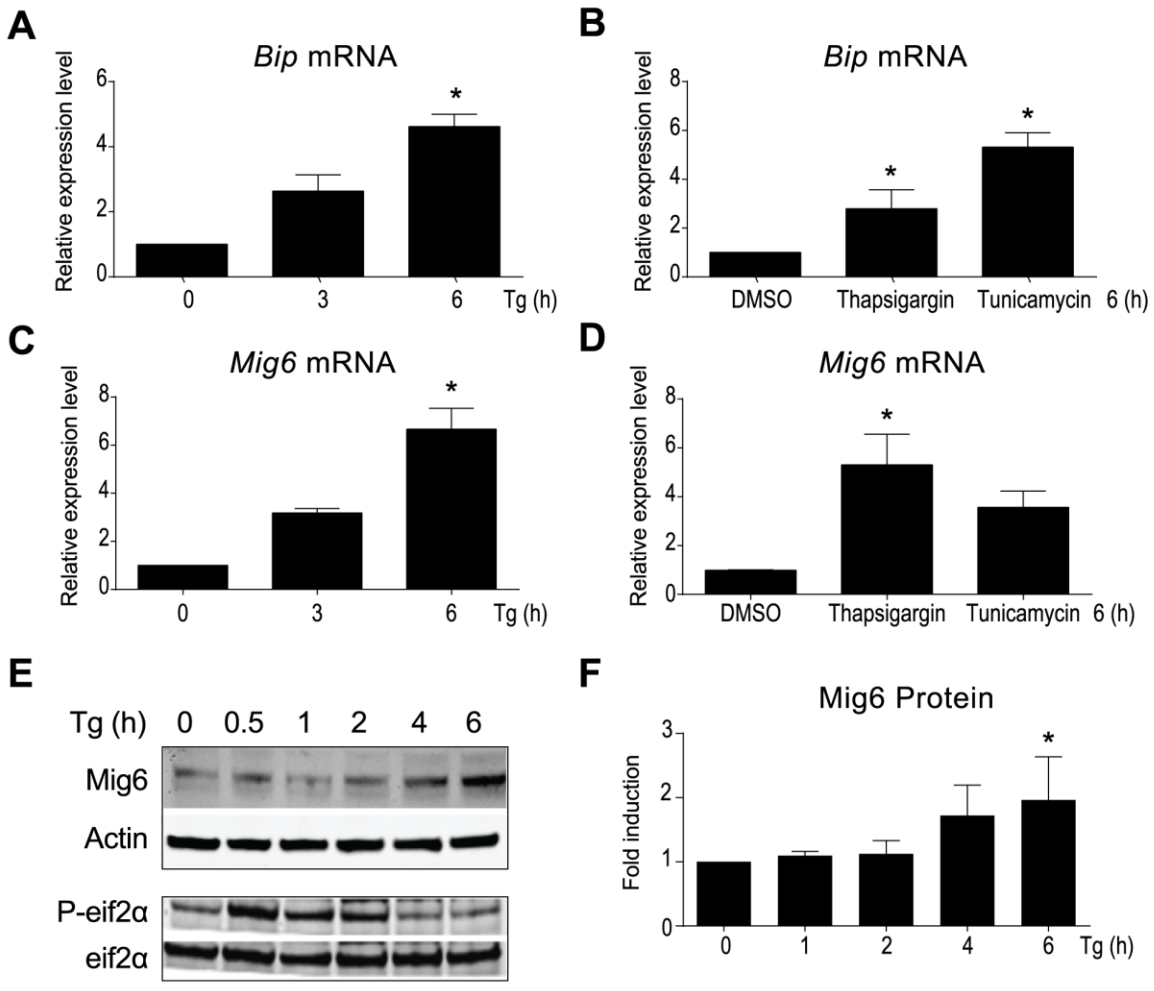

Figure 5: ER stress induces Mig6 in HepG2 cells.

HepG2 cells were treated with vehicle (DMSO), 1.0 µM thapsigargin (Tg), or 1.0 µM tunicamycin for hours (h) indicated. *Bip* and *Mig6* mRNA (A-D) expression were assessed by qPCR. Mig6, P-eif2α, and eif2α protein expression were determined by Western blot. Shown is a representative blot (E). Mig6 was normalized to actin (F). Data are reported as means ± SEM; n = 4. *, $p < 0.05$ vs. DMSO.

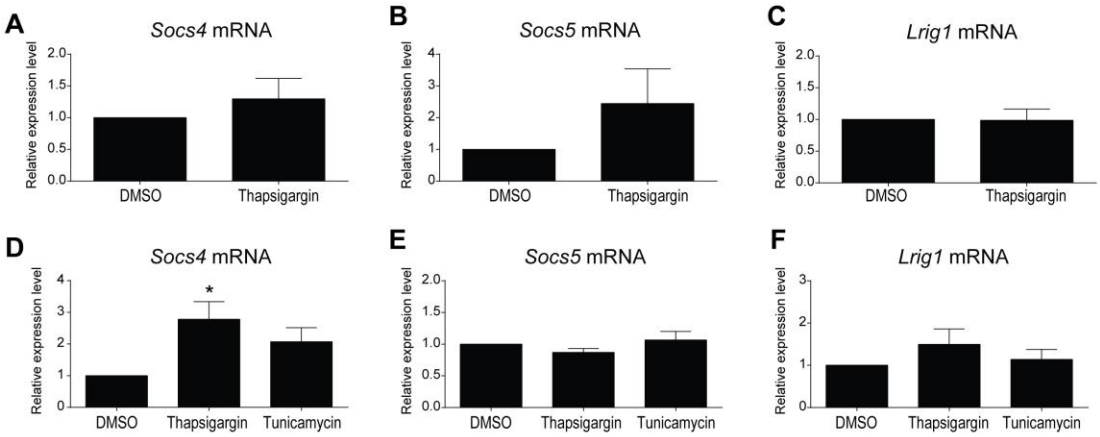

Figure 6: ER stress does not activate EGFR inhibitors in cell lines.

H4IIE cells were treated with vehicle (DMSO) or thapsigargin (1 μM) and tunicamycin (1 μM) for 6 h in serum free media. *Lrig1, Socs4,* and *Socs5* mRNA was assessed by qPCR in H4IIE cells (A-C) and HepG2 cells (D-F). Data are reported as means ± SEM; n = 4. *, $p < 0.05$ vs. DMSO.

ER stress decreases EGFR activation and stabilizes Mig6 expression: In agreement with a previous report (Xu et al., 2005) , adenoviral-mediated flag-tagged Mig6 overexpression is sufficient to decrease EGF-mediated EGFR activation as measured by phosphorylation of $EGFR^{Y1068}$ at 5 min compared with controls (Figure 7A,B). Additionally, Mig6 overexpression reduced phosphorylation of the downstream kinase ERK1/2 (Figure 7A,C). Interestingly, under these conditions in both human and rat cell lines, EGF does not induce AKT^{T308} phosphorylation (Lutkewitte, personal note). Given that maximal activation of the EGFR signaling cascade occurred at 5 min post-EGF stimulation, this time point was used in subsequent *in vitro* studies.

As Mig6 is induced during ER stress and Mig6 overexpression decreases EGFR activity, we hypothesized that EGFR activity is decreased during chemically-induced ER stress. Again, we used thapsigargin to induce hepatic ER stress in HepG2 cells (Figure 8). During this stress condition, EGF-mediated EGFR activation is markedly attenuated and apoptosis is activated, as indicated by the presence of activated, cleaved caspase 3 on the immunoblot (Figure 8A-C). Under similar ER stress conditions, we used the flag-tagged Mig6 adenovirus to show mig6 stability was markedly increased indicating Mig6 is stabilized during ER stress conditions (Figure 8D-E).

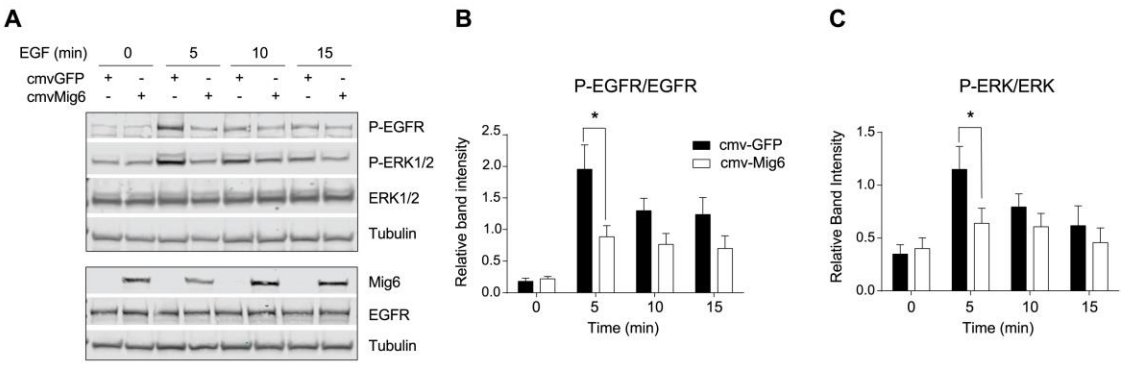

Figure 7: Mig6 overexpression reduces EGF-stimulated EGFR and ERK phosphorylation.

HepG2 cells were transduced with control GFP- or Mig6-overexpressing adenoviruses. After 24 h, media was replaced with serum free media, and the following day cells were treated with vehicle or rrEGF (50 ng/mL) for times indicated. Shown is representative Western blot (A). p-EGFR and EGFR were normalized to tubulin, and P-ERK was normalized to ERK protein, then quantified (B,C). Data are expressed as means ± SEM; n = 4. *, $p < 0.05$ vs. cmv-GFP.

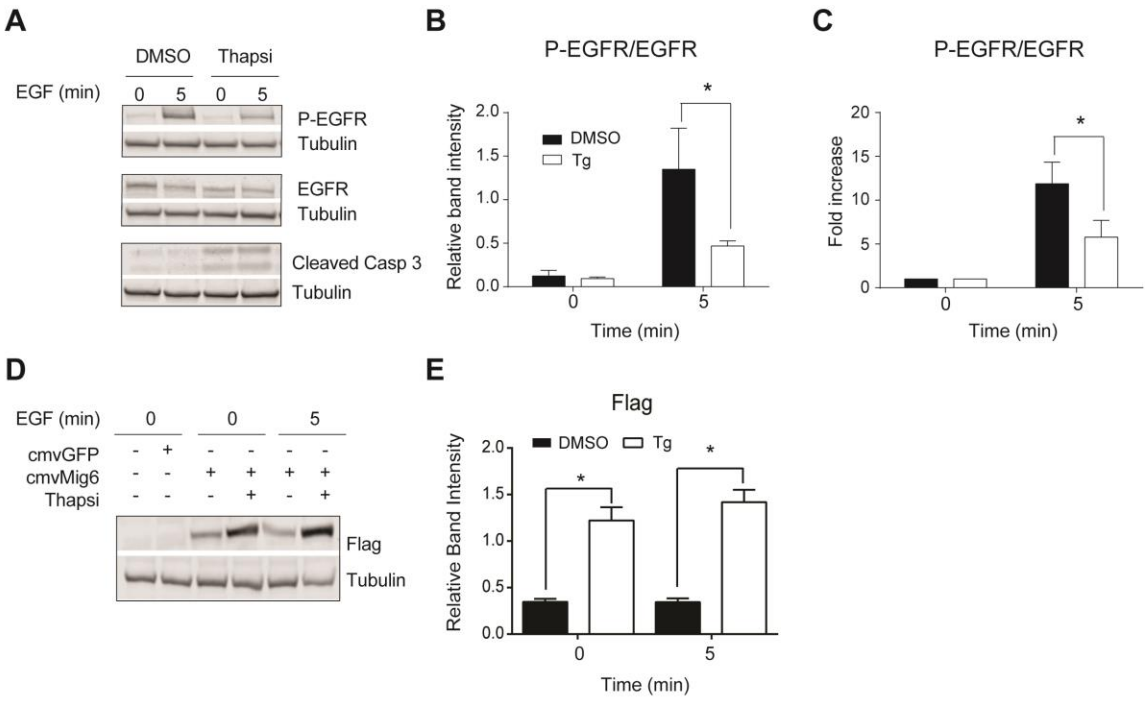

Figure 8: Thapsigargin decreases EGFR activation, induces caspase 3 activation, and stabilizes Mig6 protein expression.

HepG2 cells were treated with vehicle (DMSO) or thapsigargin (1 μM) for 24 h in serum free media prior to rrEGF (50ng/mL) stimulation as indicated (A-C). HepG2 cells were transduced with control GFP- or Mig6-overexpressing adenoviruses. After 24 h media was replaced with serum free media and treated as above (D,E). EGFR activation, caspase 3 cleavage, and flag expression were assessed by Western blot. Shown are representative blots (A&D). P-EGFR and EGFR were normalized to tubulin then quantified (B, C). Flag-tagged Mig6 expression was normalized to tubulin and quantified (E). Data are reported as means ± SEM; n = 3 (A-C) and n =4 (D,E) *, $p < 0.05$ vs. DMSO.

Mig6 knockdown enhances EGFR activation and reduces caspase 3/7 activity during ER stress: To establish that the suppression of EGFR activation during ER stress is mediated by Mig6, HepG2 cells were pre-transfected with siRNAs directed against Mig6 (siMig6) or a scrambled control siRNA (siCon) and then exposed to thapsigargin (or vehicle) prior to ligand stimulation (Figure 9). Compared to siCon-transfected cells, siMig6-transfected cells have reduced Mig6 expression and increased EGFR phosphorylation during both control (i.e., vehicle-treated) and ER stress conditions (Figure 9A,B). This observation confirms Mig6 directly inhibits EGFR activation during ER stress. To determine the functional significance of decreased EGFR signaling during ER stress, HepG2 cells were treated with palmitate following siRNA-mediated suppression of Mig6. Palmitate induced both ER stress and Mig6 transcript expression (Figure 10A,B). Mig6 suppression reduced caspase 3/7 activity during palmitate treatment compared to siControl-transfected cells (Figure 10C). These data indicate Mig6 knockdown restores EGFR signaling leading to reduced caspase 3/7 activation and enhanced survival in HepG2 cells during ER stress.

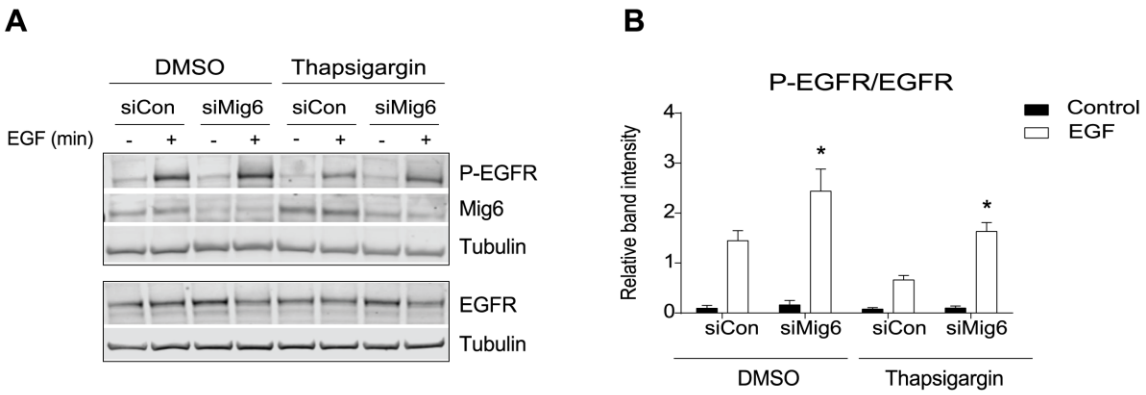

Figure 9: Mig6 ablation rescues EGFR activation during ER stress.

HepG2 cells were pretreated with siRNAs directed against control (siCon), or Mig6 (siMig6) for 48 h prior to ligand stimulation. Media was replaced with serum free media and either vehicle (DMSO) or thapsigargin (1.0 μM) 16 h prior to EGF stimulation (50ng/mL for 5 min). EGFR activation and Mig6 expression were determined by Western blot. A representative blot is shown (A). P-EGFR was normalized to total EGFR (B). Data are reported as means ± SEM; n = 3. * $p < 0.05$ vs. siControl.

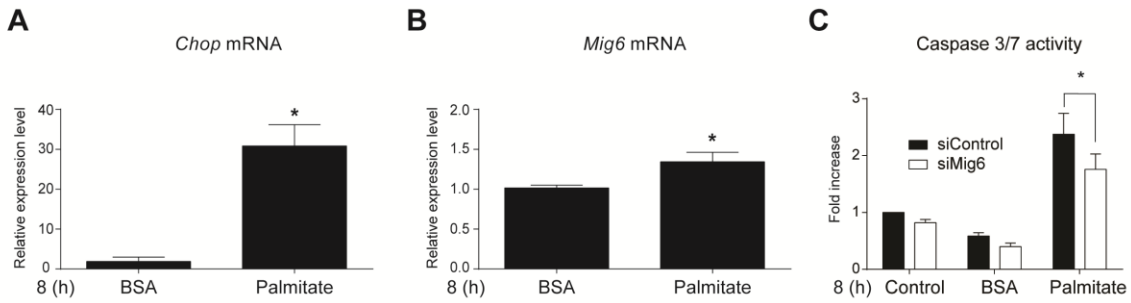

Figure 10: Mig6 knockdown during palmitate-induced ER stress decreases caspase 3/7 activity in HepG2 cells.

HepG2 cells were incubated in serum free media containing either BSA or palmitate (750 uM) for 8 h. For caspase 3/7 activity cells were treated with nothing or oligos directed against control or Mig6 for 48 h. Following transfection, media was replaced and cells were treated as before. Caspase 3/7 activity was measured using chemiluminescence. *Chop* and *Mig6* mRNA were measured by qPCR (A,B) and caspase 3/7 activity is expressed as fold increased luminescence from control non-treated cells (C). Data are reported as means ± SEM; n=3 $p < 0.05$ vs. palmitate treated siControl.

Discussion: Hyperlipidemia from over-nutrition and obesity increases hepatic lipid uptake and deposition (i.e., steatosis). Clinically, steatosis is often considered benign, requiring a "second hit" to initiate the necroinflammation and steatohepatitis-like lesions responsible for reduced patient survival during the transition from simple steatosis to non-alcoholic steatohepatitis (NASH) and cirrhosis (Adams et al., 2005; Teli et al., 1995). Hepatic necroinflammation and steatohepatitis provoke oxidative stress-induced DNA damage and caspase activation (Feldstein et al., 2003; Wieckowska et al., 2006). In response to these insults, hepatocytes and local immune cell populations trigger potent activators of hepatic DNA damage repair and synthesis, including EGFR, c-Met/HGF receptor, and TGF-β receptor and their ligands. These mitogens and their cognate receptors have been extensively investigated in healthy livers (Fausto et al., 2006b; Michalopoulos, 2007, 2010). However, the molecular mechanisms responsible for their inhibition during obesity- and ER stress, which compromises cell survival, still warrant further exploration.

One possible explanation for compromised hepatic survival in obesity could be stress-mediated feedback inhibition of RTKs. Because obesity and impaired insulin signaling cause hepatic ER stress, we also employed ER stressors to inhibit EGFR signaling and induce Mig6 expression in hepatocytes. The increased Mig6 expression was necessary for inhibiting EGFR activation, as evidenced by rescued EGFR activation following Mig6 suppression during stress conditions. We speculate Mig6 protein stability may be enhanced during stress based on our *in vitro* studies (Figure 8). Similar to diet-induced EGFR

inactivation, previous studies have revealed hepatic steatosis decreased EGFR expression and activation in *ob/ob* (i.e., leptin-deficient) mice (Collin de l'Hortet et al., 2014; Gonzalez et al., 2010). Although the exact mechanisms remain elusive, EGFR expression can be restored with growth hormone administration in *ob/ob* mice (Collin de l'Hortet et al., 2014). Moreover, leptin administration to *ob/ob* mice fails to rescue the regeneration response following partial hepatectomy, suggesting that fatty-liver pathologies might dampen the regenerative response through EGFR inactivation (Leclercq et al., 2006). More importantly, these studies did not explore the potential contribution from endogenous feedback inhibitors such as Mig6.

EGFR activation is tightly controlled by both receptor-mediated endocytosis and ligand-activated feedback inhibition (Segatto et al., 2011). Though several endogenous inhibitors exist, few have been examined during cellular stress conditions such as ER stress. Here, we demonstrate the largely exclusive upregulation of Mig6 during ER stress in liver. Additionally, there was a small but significant decrease in lrig1 mRNA expression during thapsigargin-induced ER stress in rat hepatoma cells. Unlike lrig1, socs4, and socs5, Mig6 inhibits both receptor activation and enhances receptor degradation (Segatto et al., 2011). Therefore, expression of EGFR and its ligands alone may not be capable of enhancing proliferation and survival during the mitogenic phase of regeneration if its activation is impaired by Mig6 (Ying et al., 2010; Zhang et al., 2007). During feedback inhibition, Mig6 binds to the catalytic domain of EGFR through its ERB binding domain, acting as a docking site for endocytic proteins

(Ying et al., 2010; Zhang et al., 2007). ER stress may potentially facilitate this binding interaction. However, increased binding of Mig6 to EGFR during stress remains to be demonstrated.

Obesity-induced ER stress causes decreased regeneration following partial hepatectomy (Wang et al., 2006b). Conversely, administration of the chemical chaperone tauroursodeoxycholic acid alleviates ER stress and restores hepatic regeneration in rats (Mosbah et al., 2010). Given that ER stress induces Mig6 and Mig6 halts cell cycle progression from G1 to S phase, Mig6 could potentially inhibit proliferation during ER stress. For example, proliferation requires massive ER expansion and protein translation. If sufficient stress on the ER persists, intrinsic mitogen inhibitors may become activated to halt proliferation until stress is resolved or the cell undergoes regulated apoptosis. Mig6 expression enhances apoptosis in several cell types (Makkinje et al., 2000; Xu et al., 2005; Chen et al., 2013). Importantly, active proliferation is observed in both non-fulminant and fulminant hepatitis, indicating proliferative response *alone* is not sufficient to prevent cell death (Kawakita et al., 1992; Wolf and Michalopoulos, 1992). Here, we have demonstrated Mig6 knockdown reduces apoptosis through decreased caspase 3/7 activity. Importantly, Mig6 is sufficiently upregulated and Mig6 mRNA and protein stability are enhanced during ER stress (here and Chen et al., 2013). It will be important to ultimately elucidate the extent to which Mig6 mediates the impaired hepatic regeneration during obesity and if this occurs through enhanced cell death, decreased proliferation, or both.

Mig6 could potentially halt the proliferative response of a steatotic liver following a hepatectomy. Mig6 ablation permits enhanced hepatic regeneration through heightened EGFR activation and signaling (Reschke et al., 2010). Additionally, under normal conditions, liver-specific deletion of Mig6 leads to hepatomegaly, without any reports of hepatic dysfunction or hepatocellular carcinoma development, suggesting Mig6 restricts liver proliferation (Ku et al., 2012). Physiologically, EGFR controls the initial stages of regeneration when hepatocytes are in the first round of the cell cycle. EGFR activation leads to downstream kinase cascades including ERK1/2 activation and subsequent induction of cyclins, allowing the transition between G1 and S phase of the cell cycle (Collin de l'Hortet et al., 2012; Natarajan et al., 2007). Thus, Mig6 inhibits the G_1 to S phase transition (Colvin et al., 2013). Although the regenerative response is subjected to several mitogen receptors, deletion of individual receptors, or their ligands, only delays or impairs regeneration without complete abrogation. Challenged by obesity-induced ER stress the liver loses the ability to fully regenerate following partial hepatectomy suggesting further mechanisms remain.

Here, we describe a mechanism where EGFR is inhibited during ER stress, and we speculate that other pro-survival signaling axes like HGF/c-met may also be compromised during ER stress. We believe unrestrained EGFR signaling in the context of impaired repair and proliferation (e.g., impaired regeneration during diet-induced obesity) may accelerate growth and recovery of otherwise impaired tissue. Future studies using mice lacking Mig6 in the liver

may provide insight into the complete impact of EGFR signaling inhibition during regeneration, survival, and repair.

CHAPTER 4: RESULTS

EGFR activation is decreased and mig6 protein expression is increased during obesity in mice.

Synopsis: Several available animal models exist for the study of NAFLD in rodents. Here we utilized samples from 60% HFD fed mice to demonstrate the induction of Mig6 during obesity-induced prediabetes (Figure 11). In addition to diet-induced models, liver samples from *db/db* mice were used to assess the expression of Mig6 during a condition of reduced EGFR expression and signaling. Surprisingly, EGFR expression and activation were decreased and *Mig6* gene expression was decreased in *db/db* liver samples compared to their control littermates. Next, we determined that hepatic EGFR activation and downstream signaling could be acutely activated *in vivo* and that this signaling axis may be compromised during diet-induced obesity in mice. Lastly, utilizing Mig6 liver-specific knockout mice we determined Mig6 function during NAFLD. Mig6 LKO mice develop hepatomegaly and improved ERK activation in the presence and absence of ligand. Furthermore, during HFD, Mig6 LKO mice display improved glucose tolerance compared to littermate controls. These findings indicated Mig6 may regulated hepatic metabolism during metabolic stress.

Introduction: Several models of obesity-induced NAFLD are well defined in mice. Much earlier work utilized leptin deficient models (*ob/ob* and *db/db*) that develop gross hepatic steatosis and frank diabetes (Anstee and Goldin, 2006). In addition, many other genetic mouse models develop NAFLD, including mice

lacking *ppara*, *mtp*, and *cd36* as well as *pepck/nsrebp-1a* double knockouts (Anstee and Goldin, 2006). However, many of these models do not develop NASH without a secondary insult. Perhaps the most utilized mouse model of NAFLD to NASH progression is the methionine choline deficient (MCD) diet. The MCD diet causes impairments in β-oxidation leading to ROS production, mitochondrial DNA damage, and apoptotic cell death (Gao et al., 2004). However, this diet induces weight loss, low plasma TG, and most critically, near normal insulin tolerance with dissimilar lipid distribution patterns than human patient samples (Rinella and Green, 2004).

Most importantly though, ER stress activation, oxidative stress, and inflammation are all noted in the progression of NAFLD to NASH. Therefore, we sought to test several models that activate stress and NAFLD in mice. As previously mentioned, the pro-growth, pro-survival EGFR signaling pathway is decreased in genetic models of obesity. In addition to the survival functions of EGFR, a novel role in metabolism is recently (re)emerging. EGF function as a metabolic regulator were first described in regulation of fasting by Grau et al. in 1995. Recently, EGFR inhibition is associated with improvements in glucose tolerance and insulin action in HFD fed mice (Prada et al., 2009). Conflicting studies have shown EGFR activation suppresses G6Pase gene and protein expression (Onuma et al., 2009). EGFR signals primarily through the MAPK pathway, and the role of MAPK signaling in metabolic regulation are well defined. There are four main signaling pathways: ERK1/2, ERK5, p38, and JNK. The role of JNK in metabolic regulation is well defined and described above. The p38

kinases have also been well defined in feeding/fasting regulation through transcriptional control of PGC-1α (Cao et al., 2005). However, the role of ERK1/2 in metabolic regulation is still poorly understood. Canonical ERK1/2 signaling regulates protein synthesis and DNA replication machinery. The ERK isoforms are activated by similar stimuli, however ERK2 knockout mice die *in utero* whereas ERK1 mice are viable, suggesting different functions. ERK1 knockout mice are protected from diet-induced obesity and have increased insulin sensitivity (Bost et al., 2005). These mice have reduced adipogenesis with increased energy expenditure. However, the hepatic role of ERK activity remains unclear. Recent groups have reported chemical inhibition of ERK activity improves insulin resistance in *ob/ob* mice (Banks et al., 2015). However, the role of chronic ERK activity in hepatic metabolism still remains elusive. For example, hepatic ERK1/2 activity is induced in both *ob/ob* and diet-induced mouse models (Jiao et al., 2013). Furthermore, hepatic ERK1/2 activity is dynamically regulated during fasting conditions and may regulate genes involved in both hepatic lipogenesis and gluconeogenesis (Gehart et al., 2010). Others have suggested ERK1/2 may exert this activity through the ability to phosphorylate FOXO1 transcription factors (Asada et al., 2007). Interestingly, a study using a recombinant adenovirus expressing a constitutively active form of ERK demonstrated improved glucose tolerance through the activation of beta cell expansion through a pancreatic-liver-neuronal network (Imai et al., 2008).

Undoubtedly, EGFR signaling and ERK1/2 activity affect hepatic metabolism. However, these studies completely ignore the endogenous feedback

inhibitors that regulate the EGFR signaling duration and intensity. Recently, hepatic Mig6 expression was implicated in cholesterol metabolism through modifications in bile acid synthesis. However, the role of Mig6 in hepatic glucose metabolism as well as cellular repair during obesity-induced stress remains undefined. Therefore, we sought to determine the most appropriate *in vivo* model to examine the effects of hepatic Mig6 knockout during obesity-induced stress conditions. The initial studies are outlined in the next chapter.

Results

Mig6 protein expression is elevated during obesity: Because diet-induced obesity drives hepatic ER stress, we sought to determine the impact of diet-induced obesity on hepatic Mig6 expression. Male C57Bl/6J mice were fed diets containing either 15 or 60% kcals from fat for 15 weeks. As expected, HFD-fed mice had increased body weight and pre-diabetic hyperglycemia and hyperinsulinemia compared to LFD-fed controls (Figure 11A-C). Importantly, hepatic Mig6 protein expression but not mRNA expression was increased in HFD-fed animals compared to LFD-fed controls (Figure 11D-F).

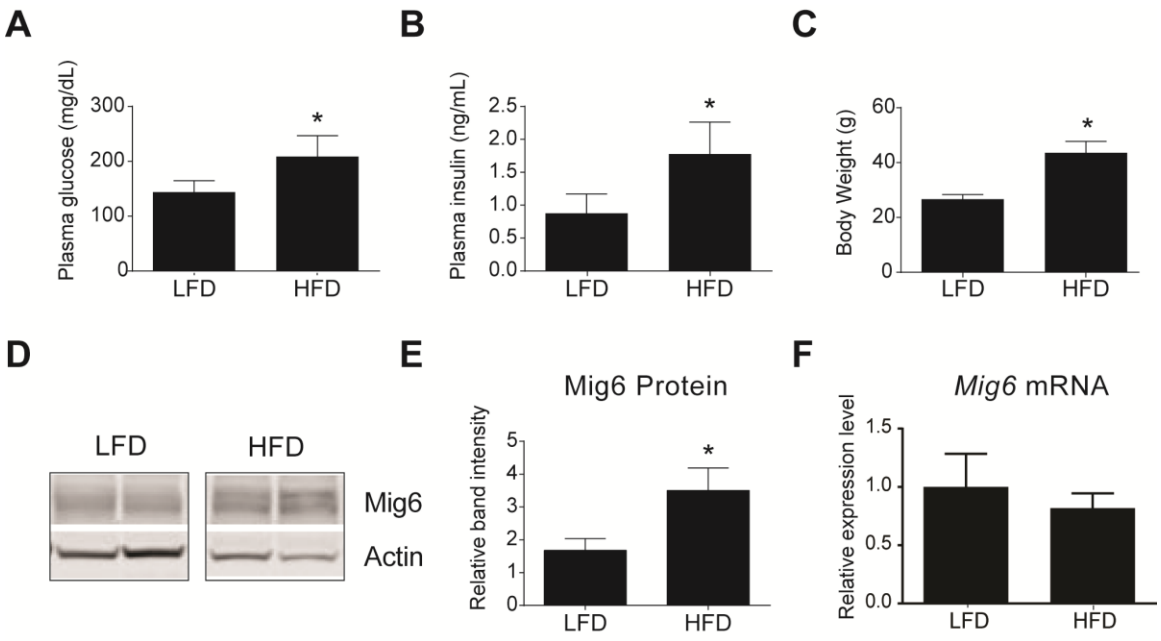

Figure 11: Mig6 is increased in diet-induced obesity and prediabetes.

Eight-week-old male C57Bl/6 mice (n=4) were fed a LFD (15% calories from fat) vs. HFD (60% calories from fat) for 15 weeks. HFD mice develop higher blood glucose (A), plasma insulin levels (B), and body weight (C) compared to LFD mice. Representative Western blots of liver tissue for Mig6 protein (D) and quantifications normalized to actin (E). *Mig6* mRNA was measured by qPCR (F). Data are reported as means ± SEM; n = 4. *, $p < 0.05$ vs. LFD.

Metabolic regulation of EGFR signaling: As previously discussed, diet-induced obesity and hepatic ER stress increase Mig6 protein expression and decrease EGFR activation (Figures 1-4, 7-11). In addition to HFD studies, genetic mouse models of obesity exhibit reduced EGFR expression and impairment of regeneration (Collin de l'Hortet et al., 2014). Though the investigators utilized growth hormone therapy to restore this impairment, they failed to examine the potential impact made by the actions of endogenous inhibitors of EGFR. Therefore, we analyzed samples from leptin signaling deficient mice for Mig6 expression. *db/db* mice were obese and hyperglycemic compared to littermate *db/+* controls (Figure 12- A,B). As expected, EGFR mRNA and EGFR activation as measured by phosphorylation of Y1068 were decreased compared to littermate controls (Figure12 C-F). Surprisingly, *Mig6* mRNA expression was decreased in *db/db* livers (Figure 12-D), perhaps due to the cumulative effects of suppressed EGFR signaling (a major stimulus for Mig6 expression). Mig6 expression is induced by EGFR signaling, yet intact EGFR signaling may not be required for Mig6 induction and to avoid confounding results, we chose not to use leptin-deficient mouse models in future studies.

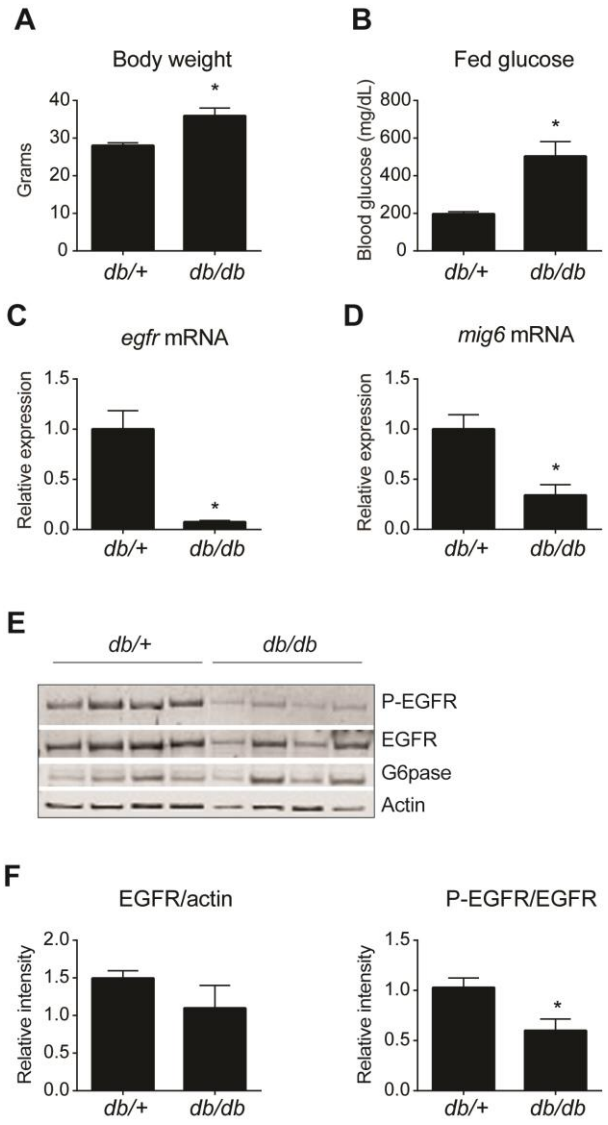

Figure 12: Mig6 and EGFR expression and activation are decreased in leptin deficient mice.

Eight-week-old *db/db* and *db/+* mice were euthanized, and body weight and fed blood glucose were measured (A&B). Livers were extracted and gene expression of EGFR and Mig6 was analyzed by qPCR (C&D). Representative Western blot shows protein expression (E) and quantification (F). Data are expressed as means ± SEM; n = 4, *, $p < 0.05$ vs *db*/+.

Obesity *per se* induced Mig6 expression, whereas genetic models of obesity reduce EGFR expression and activation. Therefore, we speculated that ligand-activated EGFR activity would be decreased in diet-induced obesity. To this end, C57Bl/6J mice were injected intraperitoneally with saline or recombinant rat EGF and after 10 min the activation of EGFR signaling was assed via Western blotting (Figure 13). These results indicate acute EGF ligand stimulation will activate EGFR *in vivo* in a dose dependent manor. To determine the extent of which obesity decreases acute EGFR activation *in vivo,* C57Bl/6 male mice were fed either a HFD or LFD control diet for 12 weeks. As designed, HFD fed mice develop obesity, fasting hyperglycemia, and glucose intolerance compared to controls (Figure 14). Following IP injection of EGF ligand, HFD fed mice had paradoxically similar EGFR activation, but reduced downstream ERK activation compared to LFD controls (Figure 15).

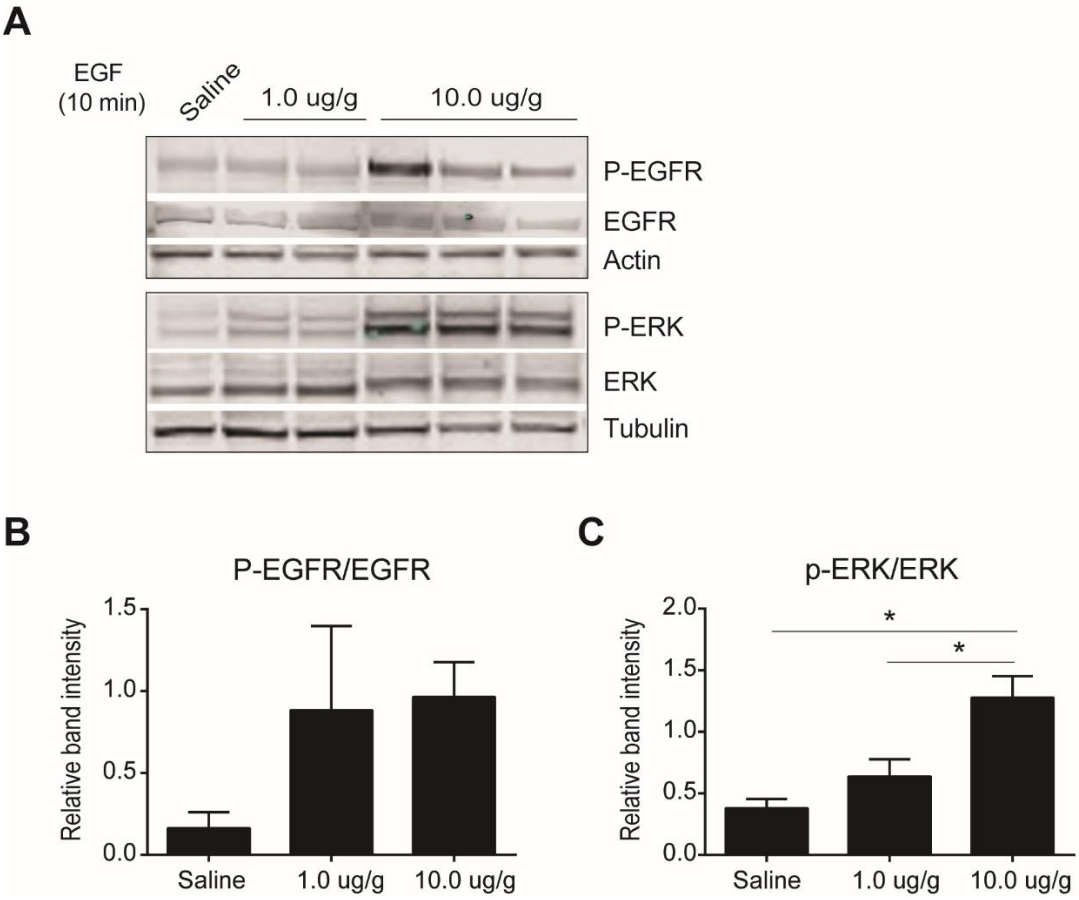

Figure 13: IP EGF injection activates EGFR in C57Bl/6 mice.

Eight- to ten-week-old mice were fasted overnight (16 h) and administered saline or recombinant rat EGF ligand at dose and time indicated. EGFR signaling was assessed via Western blot (A) and quantified (B&C). Data are expressed as means ± SEM; n = 2-3. *, $p < 0.05$.

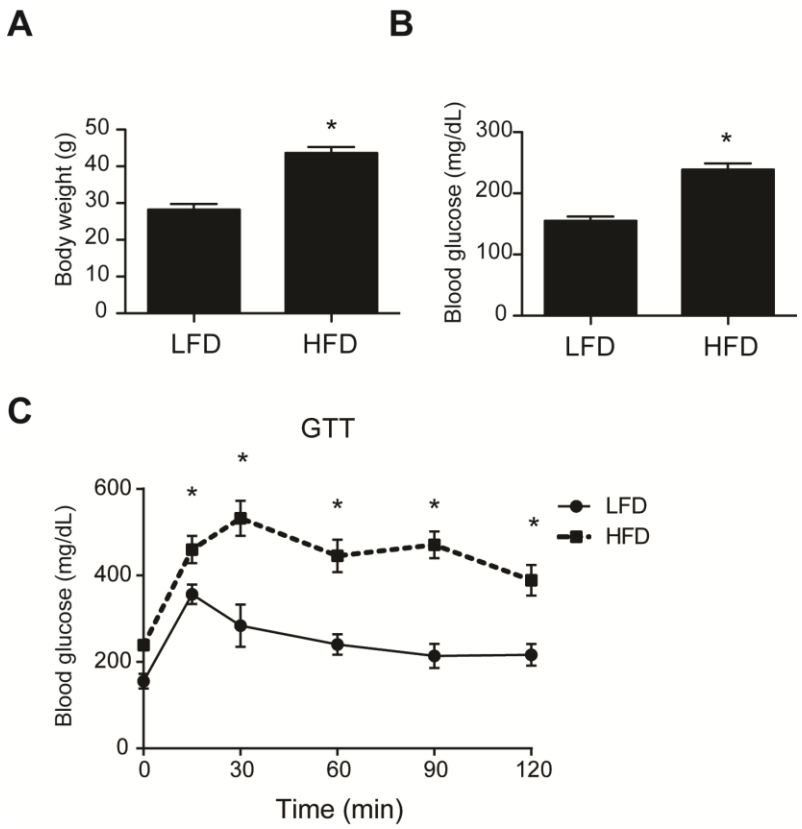

Figure 14: Male C57Bl/6 mice are obese and hyperglycemic following HFD challenge.

Six-week-old male mice were fed either a HFD (60% kcal from fat) or LFD (10% kcal from fat, matched sucrose) for 12 weeks. Body weight (A) and fasting glucose (B) were measured. Glucose tolerance tests were performed following a 6-h fast; glucose (2g/kg bw) was administered via an IP injection, and blood glucose was measured at times indicated (C). Data are expressed as means ± SEM; n = 6. *, $p < 0.05$.

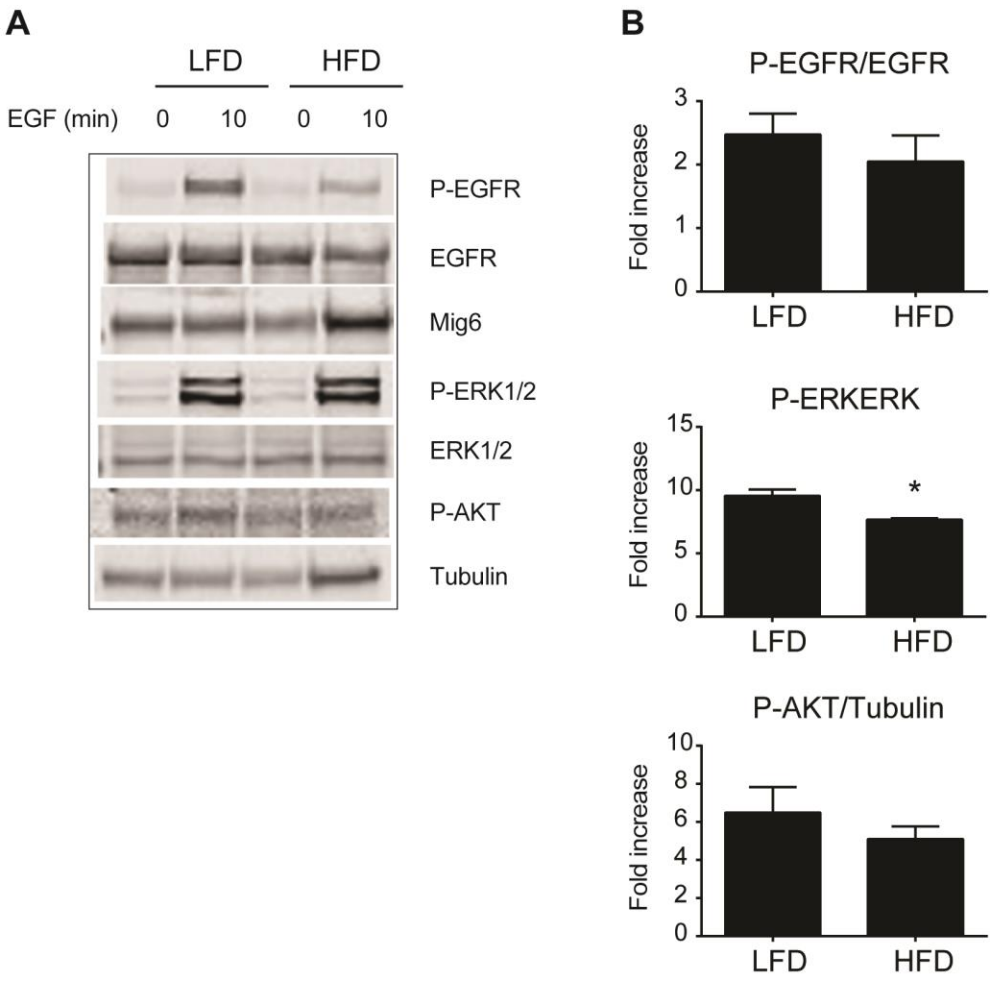

Figure 15: EGF mediated ERK activation is decreased in C57Bl/6 mice fed a HFD.

Mice were fed either a HFD (60% kcal from fat) or LFD (10% kcal from fat, matched sucrose) for 12 weeks, then fasted overnight (16 h) and administered saline or recombinant rat EGF ligand (10 ng/g bw) for times indicated. EGFR signaling was assessed via Western blot (A) and quantified (B&C). Data are expressed as means ± SEM; n = 3. *, $p < 0.05$ vs LFD.

Generation of Mig6 liver-specific knockout (LKO) mice: EGFR and Mig6 are dynamically regulated during feeding and fasting, and acute activation of downstream EGFR signaling (i.e., ERK) is decreased during obesity (Figures 11-15). In addition, obesity-induced ER stress activates Mig6 and decreases EGFR phosphorylation, while inducing pro-apoptotic pathways. Therefore, we generated Mig6 LKO mice to better define the consequences of Mig6 ablation during high fat diet challenge. We utilized mice with a homozygous floxed Mig6 gene (Jin et al., 2007) crossed with mice expressing Cre recombinase under the control of the albumin promoter driven (Postic et al., 1999) to reduce hepatic Mig6 mRNA and protein expression in male mouse livers (Figure 16, (Ku et al., 2012)).

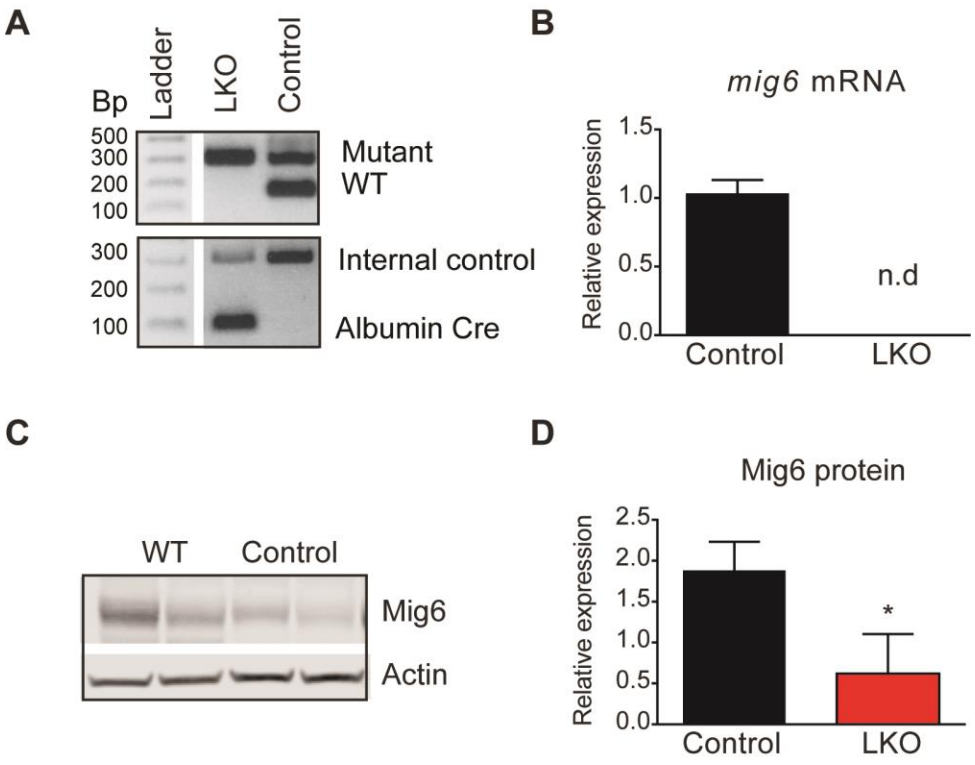

Figure 16: Mig6 LKO mice have reduced Mig6 mRNA and protein expression in liver.

Eight-week-old Mig6 LKO and littermate controls were euthanized, and livers were analyzed for Mig6 expression. Representative agarose gel images of mutant and WT alleles are shown (A). Mig6 mRNA was assessed via qPCR (B). Western blots were used to determine Mig6 protein content (C) and normalized to actin (D). Data are expressed as means ± SEM; n = 4. *, $p < 0.05$ vs littermate controls.

Characterization of Mig6 LKO mice: Eight week old male Mig6 LKO mice have similar body weight and overnight fasting glucose compared to littermate controls (Figure 17-A,B). Interestingly, Mig6 LKO mice present with hepatomegaly compared to controls (Figure 17-C,D). Notably, at eight weeks of age glucose and insulin tolerance were similar between Mig6 LKO and control male and female mice fed a chow diet (Figure 18). Therefore, we used male mice throughout the remaining studies. Although initial metabolic studies indicate normal glycemic control in Mig6 LKO mice, further analysis of hepatic tissue reveals discrepancies between groups. Importantly, *g6pase* mRNA expression is decreased in Mig6 LKO mice compared to controls at 20 weeks of age (Figure 19-A). Because *g6pase* expression is regulated by insulin signaling (Nordlie and Foster, 2010), fasting mice were injected with a bolus of insulin, and hepatic signaling pathways were analyzed (Figure 19-B). As demonstrated in Figure 19, phosphorylation of ERK is markedly upregulated in Mig6 LKO livers regardless of insulin stimulation. Importantly, AKT phosphorylation and downstream FOXO1 phosphorylation are increased in Mig6 LKO livers compared to controls (Figure 19-B). Even at 20 weeks of age, glucose tolerance tests indicate comparable glucose metabolism between groups, however, because the MIg6 LKO mice have larger livers (Figure 17-C,D), the total glycogen content is higher compared to littermates (Figure 19-C,D).

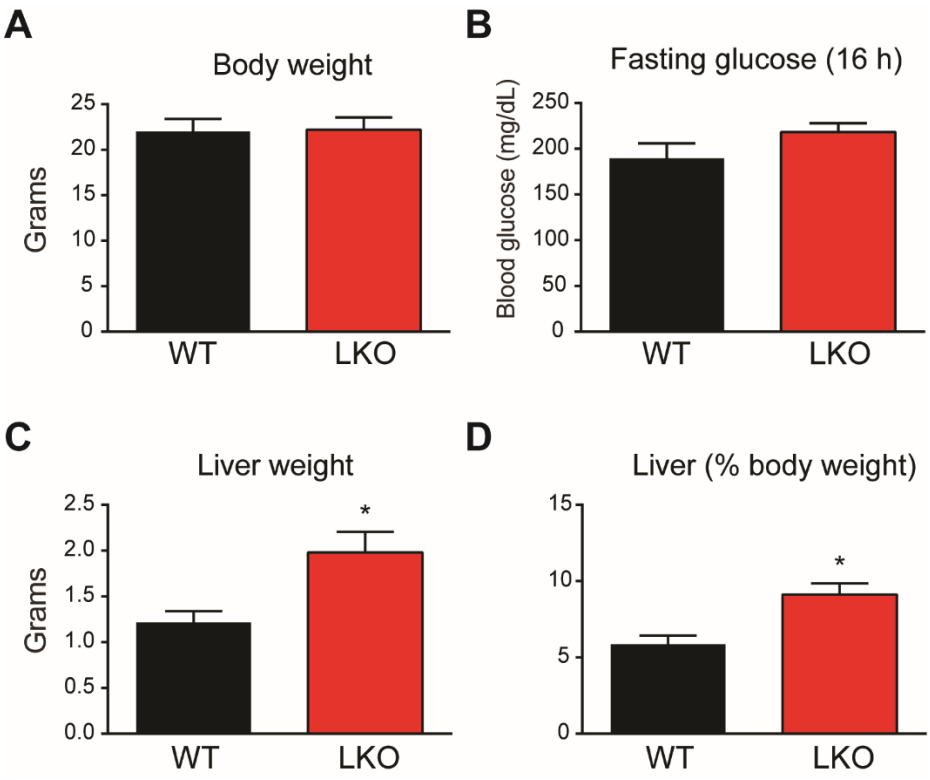

Figure 17: Mig6 LKO mice have hepatomegaly.

Eight-week-old male mice Mig6 LKO and control littermates were fasted overnight. Body weight (A) and blood glucose (B) were measured. Livers were immediately extracted and weighed (C&D). Data are expressed as means ± SEM; body and liver weight n=5, fasting glucose n = 8-9. *, $p < 0.05$ vs littermate controls.

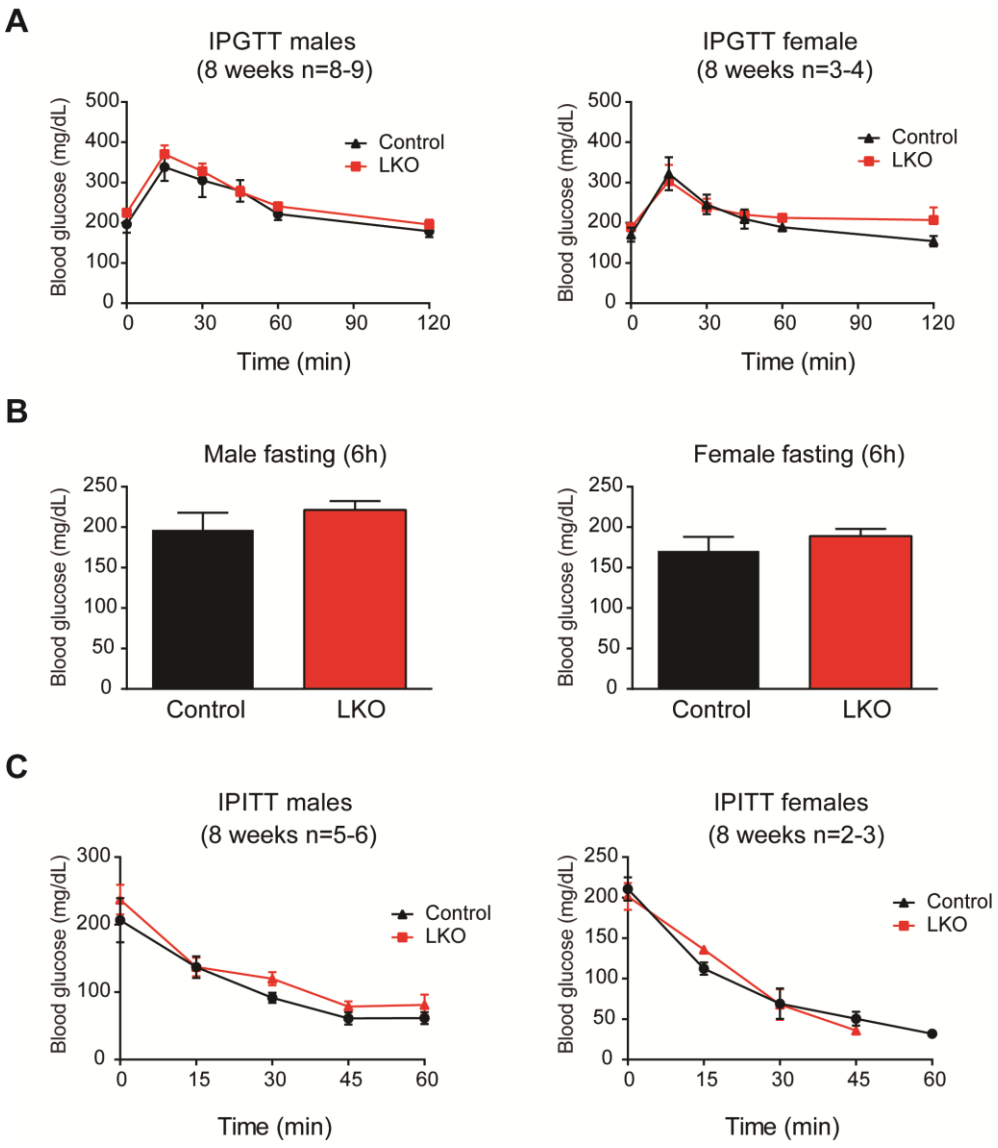

Figure 18: Mig6 LKO mice have normal metabolism.

Eight-week-old male and female mice were fasted 6 hours prior to GTT. Glucose (2g/kg bw) was administered via an IP injection, and blood glucose was measured at times indicated (A&B). Following a 5-h fast mice were administered an IP bolus of recombinant human insulin (0.75U/kg), and blood glucose was measured at times indicated (C). Data are expressed as means ± SEM; n = as indicated. *, $p < 0.05$ vs control.

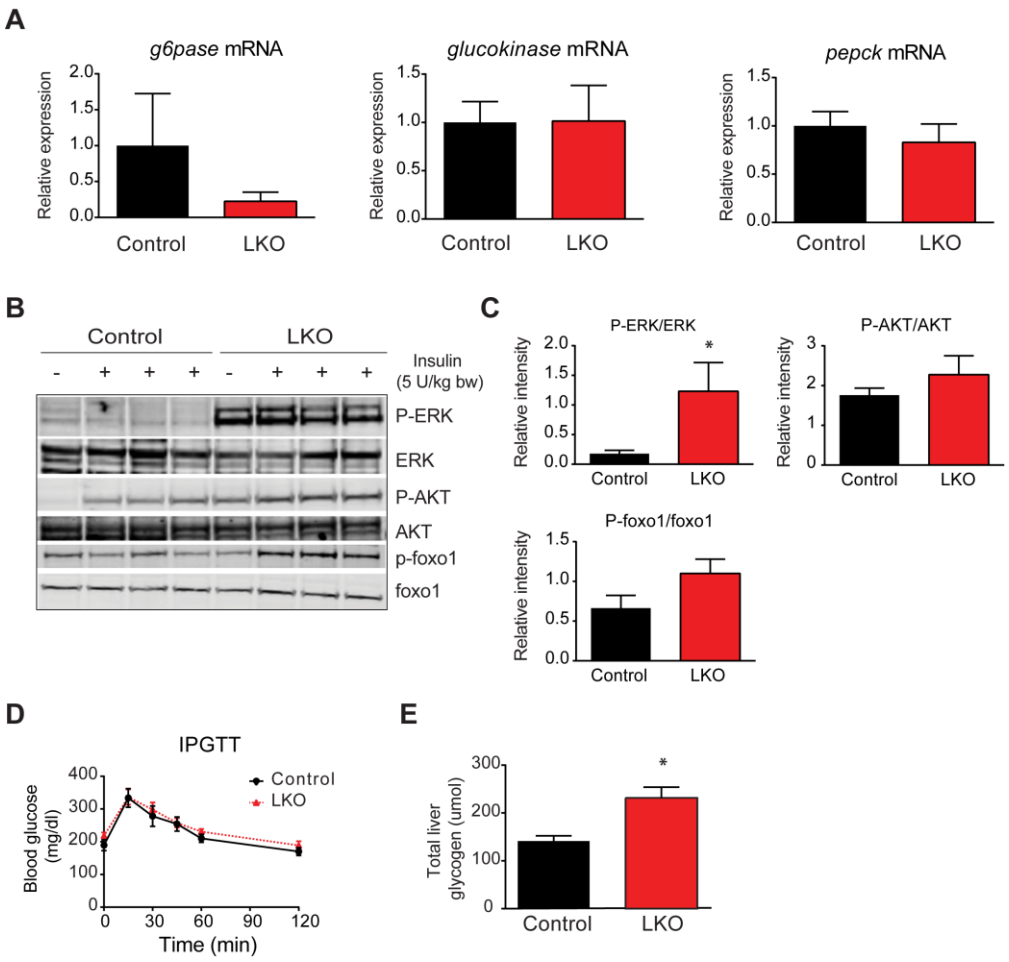

Figure 19: Mig6 LKO livers have normal insulin sensitivity with increased total glycogen content.

After 16 weeks on the diets, male Mig6 LKO and littermate controls were fasted overnight, and the livers removed for analysis. *g6pase*, *glucokinase* and *pepck* mRNA was assessed via qPCR (A). Western blots were used to determine hepatic insulin sensitivity following an IP insulin bolus (5 U/kg bw) (B) and quantified (C). Mice were fasted 6 hours prior to an IP glucose bolus (2 g/kg bw), and blood glucose was monitored at times indicated (D). Total glycogen was extracted from flash frozen livers and enzymatically quantified (E). Data are expressed as means ± SEM; n = 3-4. *, $p < 0.05$ vs littermate controls.

Mig6 LKO mice have improved glucose tolerance during a HFD challenge: Mig6 LKO mice have hepatomegaly and similar hepatic insulin sensitivity compared to controls. Previous studies have reported Mig6 LKO mice have decreased liver *g6pase* and increased *glucokinase* gene expression (Ku et al., 2012). Because g6pase and glucokinase are important regulators of hepatic glucose metabolism during obesity, and EGFR and Mig6 expression are dynamically regulated during obese mouse models, we fed six-week-old male Mig6 LKO and littermate control mice either a HFD or LFD for 16 weeks. Glucose tolerance tests performed every four weeks and indicate a trend towards improved glucose tolerance among the HFD fed Mig6 LKO and littermate control mice, reaching significance by 12 weeks (Figure 20-A-D).

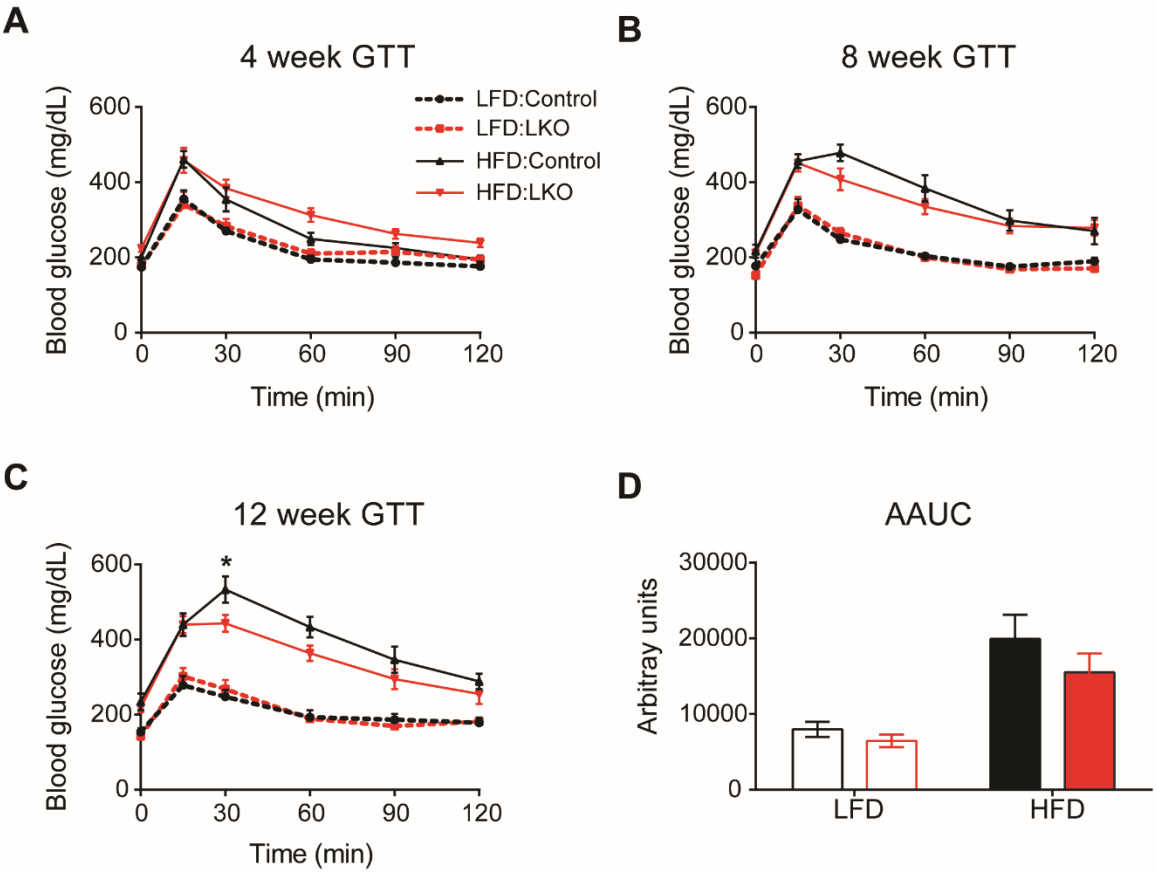

Figure 20: Mig6 LKO mice have improved glucose tolerance on a HFD.

Six-week-old male mice were fed either a HFD (60% kcal from fat) or LFD (10% kcal from fat, matched sucrose) for 12 weeks. Following a 6-hour fast, glucose (2g/kg bw) was administered via an IP injection, and blood glucose was measured at times indicated (A-C). Adjusted area-under-the-glucose-curve (AAUC) was calculated after 12 weeks of diet feeding (D). Data are expressed as means ± SEM; n = 6-10. *, $p < 0.05$ vs littermate controls.

Discussion: Obesity increases adipose tissue lipolysis and hepatic lipid deposition in several mouse models. The effects of various diets and genetic backgrounds on NAFLD has been extensively investigated and reviewed (Anstee and Goldin, 2006; Petro et al., 2004; Rossmeisl et al., 2003; Surwit et al., 1995)(Surwit, Anstee, Gajada, Petro, Rossmeisl). Here we examined two widely acceptable models of NAFLD in mice, the leptin receptor mutant *db/db* mice, which are severely steatotic and insulin resistant, and HFD-induced obesity (60% kcal from fat). First, we discovered that Mig6 gene expression is decreased and EGFR expression and activation are nearly absent in the *db/db* mice (Figure 12). This result was disappointing but not completely unexpected, as Mig6 regulates EGFR activation and not transcription by evidence of normal EGFR expression following Mig6 overexpression studies (Figure 5). Furthermore, leptin signaling activates the STAT family of transcription factors, which have highly enriched binding sites in the EGFR promoter. Therefore, due to the potential of aberrant transcriptional control of EGFR due to the absence of leptin signaling, we chose to exclude this mouse model from the remainder of our studies.

Utilizing HFD fed mice that develop hyperinsulinemia, hyperglycemia, and obesity, we discovered Mig6 protein but not mRNA expression is increased in the liver. The lack of Mig6 gene induction may indicate an increased stability of Mig6 protein under stress conditions, as occurs under ER stress *in vitro* (Figure 8), or perhaps enhanced translation. In line with the latter hypothesis, other members of our group have demonstrated Mig6 escapes the normal translational blockade following stress activation of p-eIF2α, indicating that Mig6 transcripts are

preferentially alternatively translated to inhibit EGFR during stress conditions (Chen et al., 2013). These data warrant further study on the mechanisms regulating Mig6 during obesity.

We have also determined that acute IP injection of EGF ligand will activate EGFR signaling *in* vivo and that this signaling pathway may be decreased in the setting of obesity-induced glucose intolerance. To further explore how this pathway is regulated, we generated Mig6 LKO mice. As predicted, Mig6 liver ablation induces hepatomegaly and increases hepatic ERK1/2 signaling (Figure 17,19). Surprisingly, Mig6 ablation improved diet-induced glucose intolerance in mice. Here, we have determined a diet-induced mouse model in which to study the hepatic consequences of Mig6 ablation during obesity. Initial metabolic studies reveal similarities between genders and genotypes on chow (breeder chow) diets. However, upon examination of hepatic signaling networks, marked differences were observed in hepatic ERK1/2 signaling and possible improvements in hepatic insulin signaling when comparing Mig6 LKO mice to littermate controls (Figure 19). The possibility of improved insulin sensitivity, as evidenced by insulin-mediated AKT and FOXO1 phosphorylation studies as well as the significant improvement in glucose tolerance after 12 weeks of HFD, leads us to suggest Mig6 may modulate insulin sensitivity in liver.

Mig6 has recently been implicated in hepatic metabolism through bile acid regulation and cholesterol synthesis (Ku et al., 2012). In addition to EGFR signal regulation, Mig6 is a known HGF signaling regulator. The HGF/c-met receptor has recently been proposed to bind the insulin receptor and act as a regulator of

hepatic glucose metabolism (Fafalios et al., 2011). Could Mig6 act through this signaling mechanism to regulated glucose metabolism? Or are the effects of Mig6 ablation through improvements in hepatic repair mechanisms solely through enhanced EGFR activity. The latter is certainly a plausible explanation given the increase in downstream ERK1/2 activation seen in Mig6 LKO mice. The next chapter will explore the mechanism of Mig6 regulation in liver during the context of NAFLD.

CHAPTER 5: RESULTS

Liver-specific mig6 ablation improves glucose tolerance in HFD fed mice.

Synopsis: Because HFD induces Mig6 protein expression and Mig6 ablation improves glucose tolerance during a HFD, we utilized this model to study the effects of Mig6 ablation during obesity-induced hepatic stress. Here we show Mig6 ablation improves glucose tolerance on HFD independent of whole body insulin sensitivity or beta cell function. Furthermore, Mig6 LKO mice have similar basal proliferation compared to littermate controls. The increase in liver weight is not due to increased lipid deposition as determined by similar Oil-Red-O staining and triglyceride content per mg tissue contrary to previous reports (Ku et al., 2012). This observation is divergent to histological findings indicating a slight improvement in cell death, as indicated by reduced cellular ballooning. The Mig6 LKO mice have higher plasma cholesterol with increased plasma triglycerides on HFD compared to littermate controls. Insulin-mediated AKT activation is similar among all groups, though the difference in insulin-regulated gene expression and improved glucose tolerance suggest improvements in hepatic insulin signaling. Taken together these results suggest Mig6 regulates hepatic metabolism, yet the precise molecular mechanisms remain elusive.

Introduction: Hepatic control of glucose production is highly dependent upon both substrate and hormone concentrations. During a glucose challenge, insulin must activate glucose uptake in skeletal muscle and adipose while initiating storage in hepatic tissue. Hepatic nsulin sensitivity is highly dependent

upon cellular stress levels. Indeed, ER stress conditions reduced hepatic insulin sensitivity lowering metabolic control (Ozcan et al., 2004).

Previous groups have established that in addition to the insulin receptor, EGFR may directly regulate hepatic metabolism by controlling the expression of genes involved in gluconeogenesis. Specifically, EGFR signaling suppresses the gluconeogenic genes *g6pase* and *pepck*. (Fillat et al., 1993; Chan and Krebs, 1985). Similarly, hepatic EGFR expression is altered during cycles of feeding and fasting, possibly aiding in the control of gluconeogenesis (Freidenberg et al., 1986). In addition to the control of metabolism, EGFR functions as an initiator of repair mechanisms ensuring hepatocyte survival during stress conditions (Figure 10). As discussed in previous chapters, hepatic EGFR activity is decreased during ER stress and this activity can be restored by Mig6 ablation. Therefore, we sought to determine the extent to which Mig6 ablation would improve hepatic metabolism either indirectly through increased survival mechanisms or directly through EGFR signaling suppression of gluconeogenic genes.

Results: Fasting glucose (6 h) and body weights were similar between groups throughout 16 weeks of diet (Figure 21-A,B). Notably, glucose tolerance after 16 weeks of diet was significantly improved in the Mig6 LKO mice compared to littermate controls (Figure 21-C,D). The improvement in glucose tolerance were not due to changes in whole-body insulin sensitivity nor gluconeogenesis as measured by insulin and pyruvate tolerance tests, respectively (Figure 22-A,B).

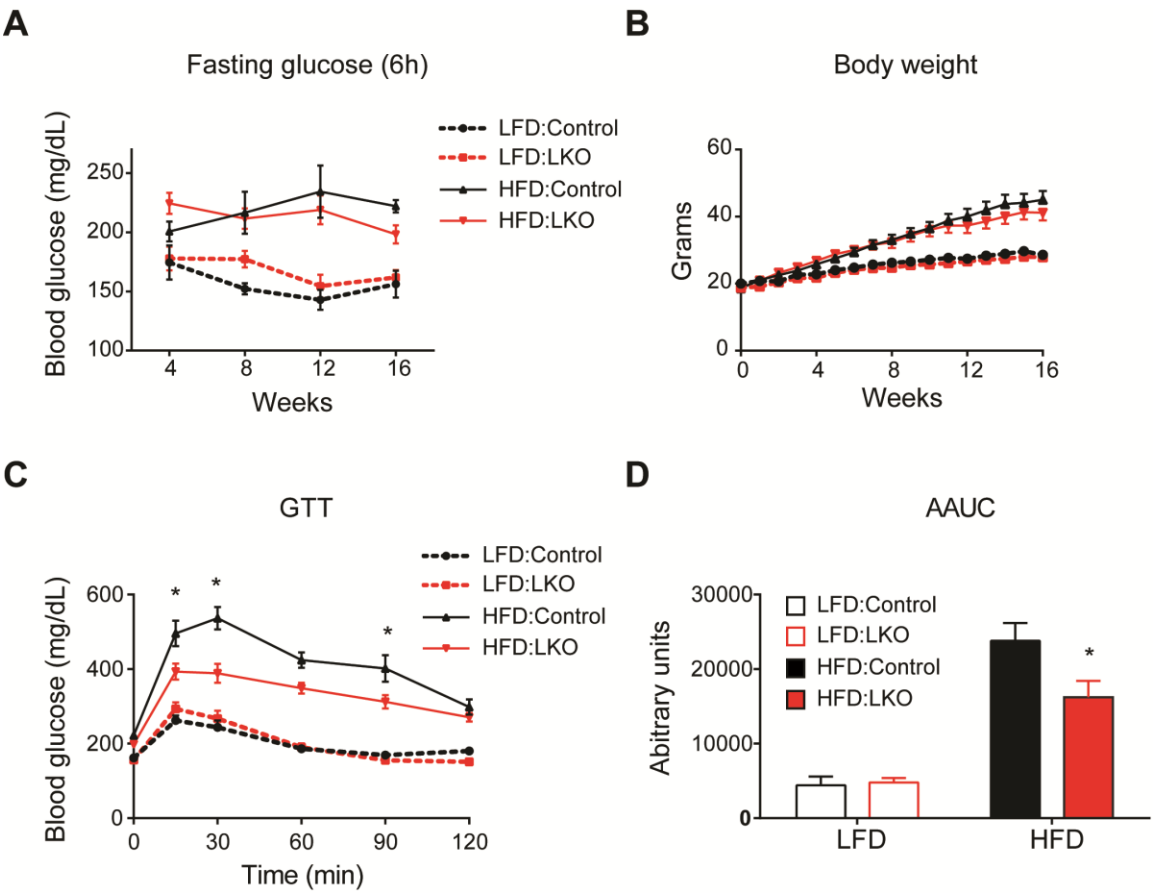

Figure 21: Mig6 LKO mice have improved glucose tolerance with similar fasting glucose and body weights.

Six-week-old male mice were fed either a HFD (60% kcal from fat) or LFD (10% kcal from fat, matched sucrose) for 16 weeks. Fasting glucose (A) and body weight (B) were monitored during the diet treatment period. Following a 6-h fast, glucose (2g/kg bw) was administered via an IP injection, and blood glucose was measured at times indicated (A-C). Adjusted area-under-the-glucose-curve (AAUC) was calculated after 16 weeks of diet (D). Data are expressed as means ± SEM; n = 7-10. *, $p < 0.05$ vs littermate controls.

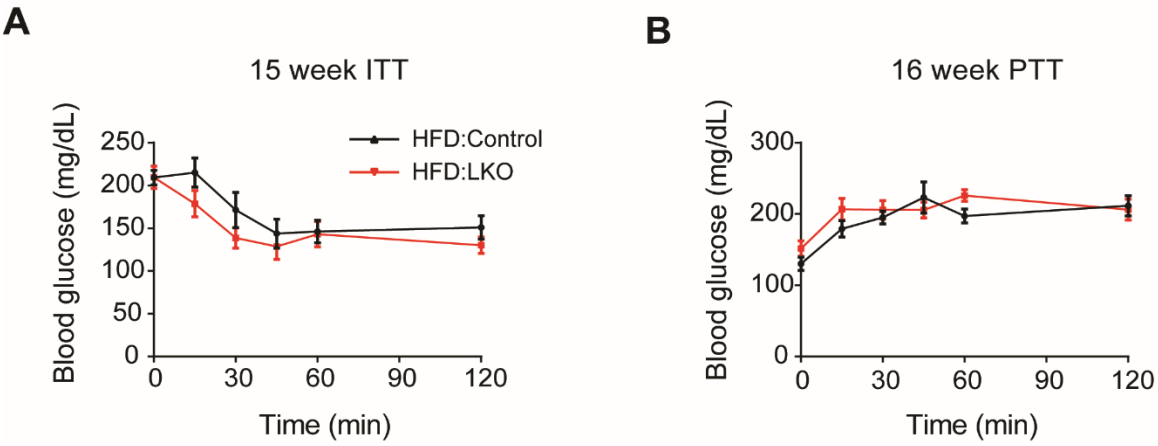

Figure 22: HFD fed Mig6 LKO have similar insulin and pyruvate tolerance compared to controls.

After 15-16 weeks of diet, mice were fasted (5 h) and insulin (0.75 U/Kg bw) was administered via an IP injection, and blood glucose was measured at times indicated (A). Following an overnight fast (16 h) mice were administered an IP bolus of sodium pyruvate (2 g/kg bw), and blood glucose was measured at times indicated (B). Data are expressed as means ± SEM; n = 6-9. *, $p < 0.05$ vs control.

Previous studies have demonstrated hepatic ERK signaling can activate pancreatic beta-cell expansion, and therefore, increase the insulin secretory response in HFD fed Mig6 LKO mice compared to controls (Imai et al., 2008). To this end, beta cell mass, fasting insulin and plasma insulin in response to a glucose bolus were monitored in HFD fed mice (Figure 23). As reported in Figure 23, fasting insulin increases on HFD in both groups whereas plasma insulin in response to glucose was not different amongst HFD diet groups (Figure 23-A,B). Moreover, beta cell area was not different amongst HFD groups (Figure 23-C,D). These data indicate Mig6 LKO mice have similar beta cell area, and enhanced beta cell function is not responsible for the improvement in glucose tolerance with hepatic Mig6 ablation.

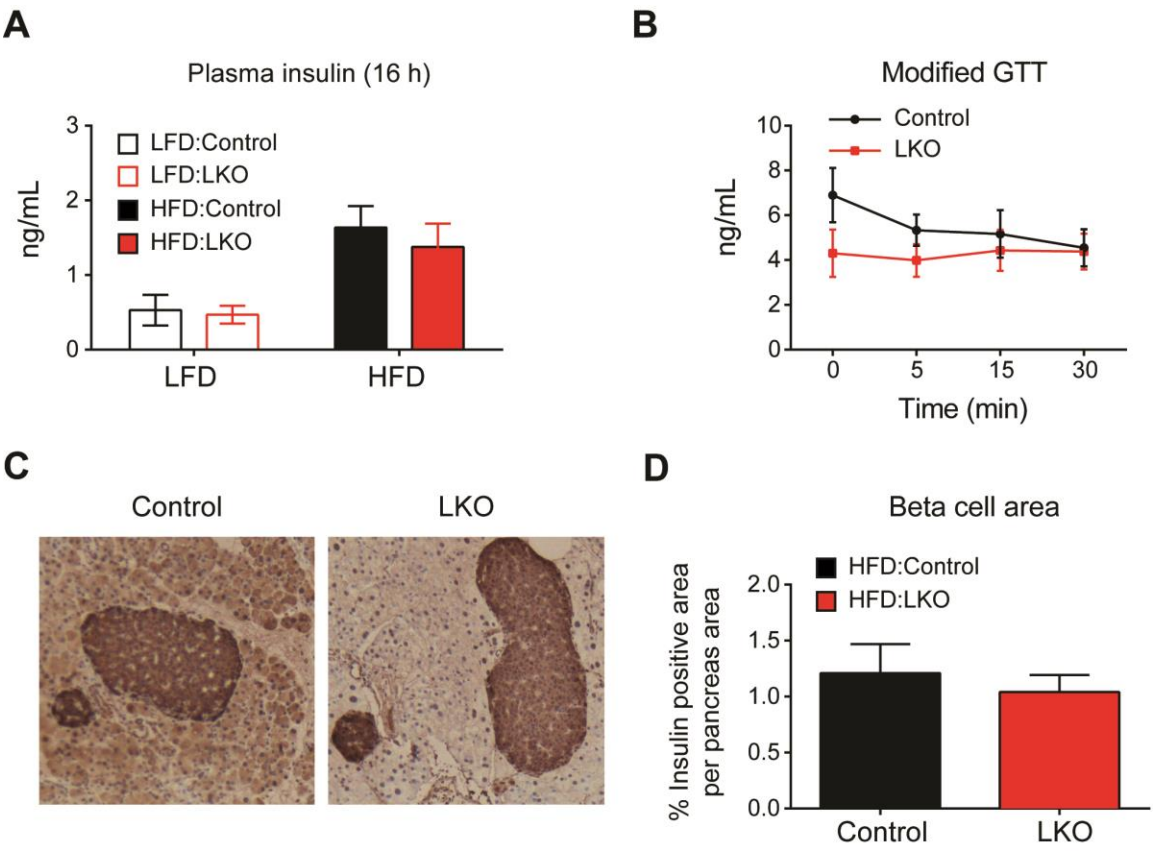

Figure 23: Mig6 LKO mice have similar plasma insulin and beta cell area compared to littermate controls.

Mice were fasted overnight and plasma insulin was determined from an ultra-sensitive mouse insulin ELISA (A). Mice were fasted (6 h) and given a bolus of glucose (2g/kg bw). Blood samples were procured at times indicated and insulin measured (B). Pancreatic tissue was fixed and paraffin embedded. Sections were stained for insulin and H&E (C). Beta cell area was quantified as insulin positive area divided by total tissue area (D). Data are expressed as means ± SEM; insulin and beta cell area n = 4-6, modified GTT n = 7-8. *, $p < 0.05$ vs control littermates.

Mig6 LKO mice have hepatomegaly and increased plasma and total liver triglycerides on HFD: Following 16 weeks on diet, mice were fasted overnight and livers removed for analysis. Livers from Mig6 LKO mice were larger in both gross and percent body weight compared to LFD and HFD controls (Figure 24-A,B). This enlargement is independent of proliferation, as indicated by phosphorylated histone H3 staining, a marker of mitosis (Figure 24-C). The HFD similarly induced hepatic hypertrophy in both genotypes, as determined by the number of nuclei per 40X field (Figure 24-D).

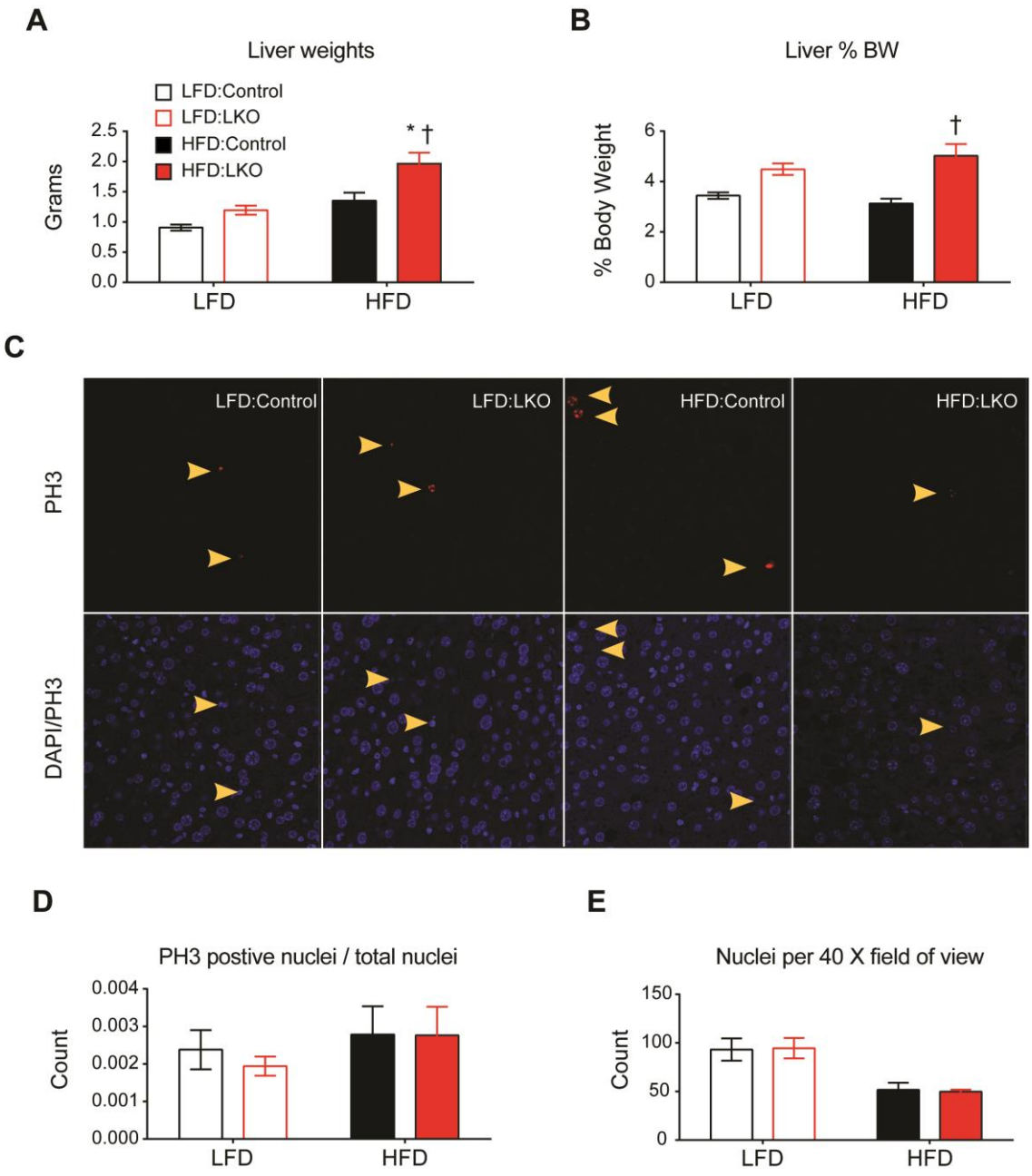
A
Liver weights
LFD:Control
LFD:LKO
HFD:Control
HFD:LKO
Grams
2.5
2.0
1.5
1.0
0.5
0.0
* †
LFD
HFD
B
Liver % BW
% Body Weight
6
4
2
0
†
LFD
HFD
C
PH3
DAPI/PH3
LFD:Control
LFD:LKO
HFD:Control
HFD:LKO
D
PH3 postive nuclei / total nuclei
Count
0.004
0.003
0.002
0.001
0.000
LFD
HFD
E
Nuclei per 40 X field of view
Count
150
100
50
0
LFD
HFD

Figure 24: Mig6 LKO mice have hepatomegaly independently of proliferation.

Following 16 weeks of diet, livers were excised and blotted to remove excess blood before being weighed (A,B). Tissue samples were fixed in zinc formalin and embedded in paraffin wax. Sections were stained for phospho-histone H3 (PH3) and counterstained with nuclei DAPI stain (C). $PH3^+$ positive and negative nuclei were counted in 27 random 40X scans and quantified using ImageJ (D,E). Arrows indicate $PH3^+$ cells. Data are expressed as means ± SEM; liver weights n = 10, PH3 n = 5-7. $p < 0.05$ vs control littermates, †, $p < 0.05$ vs LFD.

Previous studies have suggested hepatic Mig6 ablation causes increased liver triglyceride (Ku et al., 2012). In our study, however, hepatic Mig6 ablation did not increase hepatic triglyceride deposition *per se*. Biochemical extraction and Oil Red-O staining revealed similar hepatic triglycerides and neutral lipid content and distribution pattern between groups (Figure 25). However, because Mig6 LKO mice have hepatomegaly, the total liver triglyceride content was higher when compared to HFD fed littermate controls (Figure 25-B). Although hepatic triglycerides were similar between groups, serum triglycerides but not NEFAs were increased in Mig6 LKO mice compared with HFD controls (Figure 26 A,B). Additionally, plasma HDL levels but not LDL were increased in Mig6 LKO mice (Figure 26 C,D) (Ku et al., 2012).

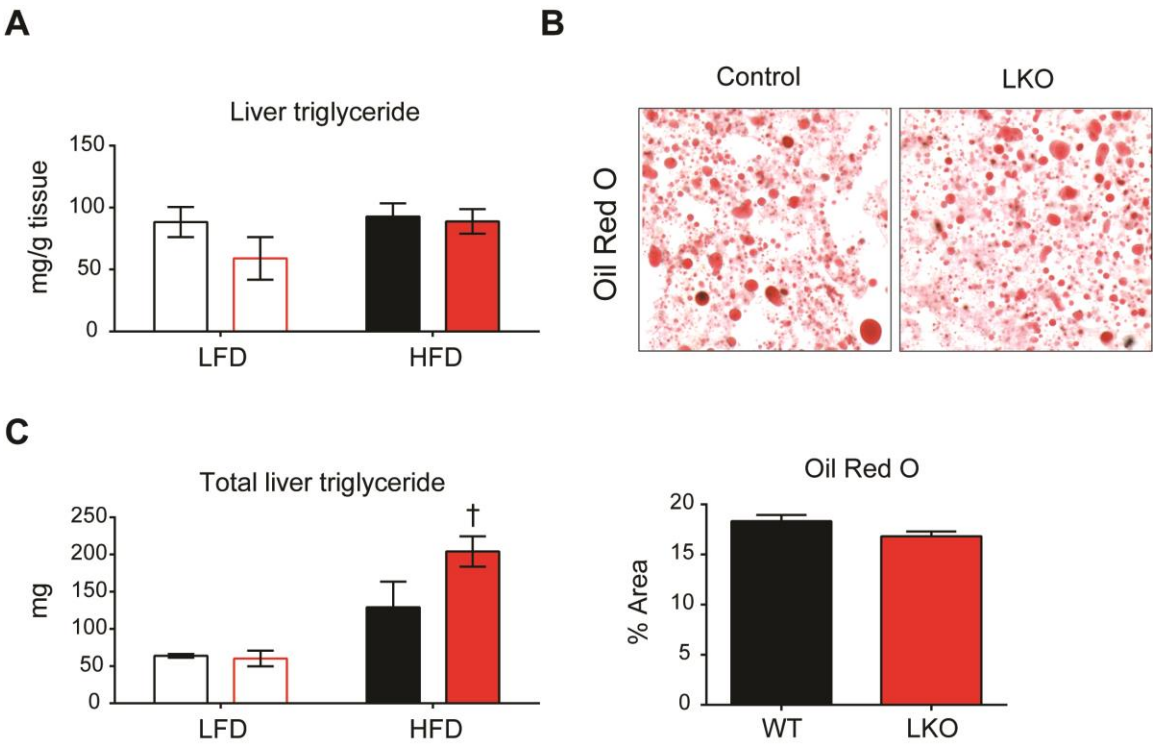

Figure 25: Mig6 LKO mice have higher total triglycerides on HFD.

At 16 weeks of HFD mice were fasted overnight and livers removed. Hepatic triglycerides were extracted by chloromethanol extraction methods and measure enzymatically (A). Tissues were fixed in paraformaldehyde, dehydrated in sucrose, and embedded in OCT. Frozen sections were stained with Oil-Red-O and images quantified using ImageJ (B). Total liver triglycerides were determined be normalization to total liver weight (C). Data are expressed as means ± SEM; n = 5-9. *, $p < 0.05$ vs LFD.

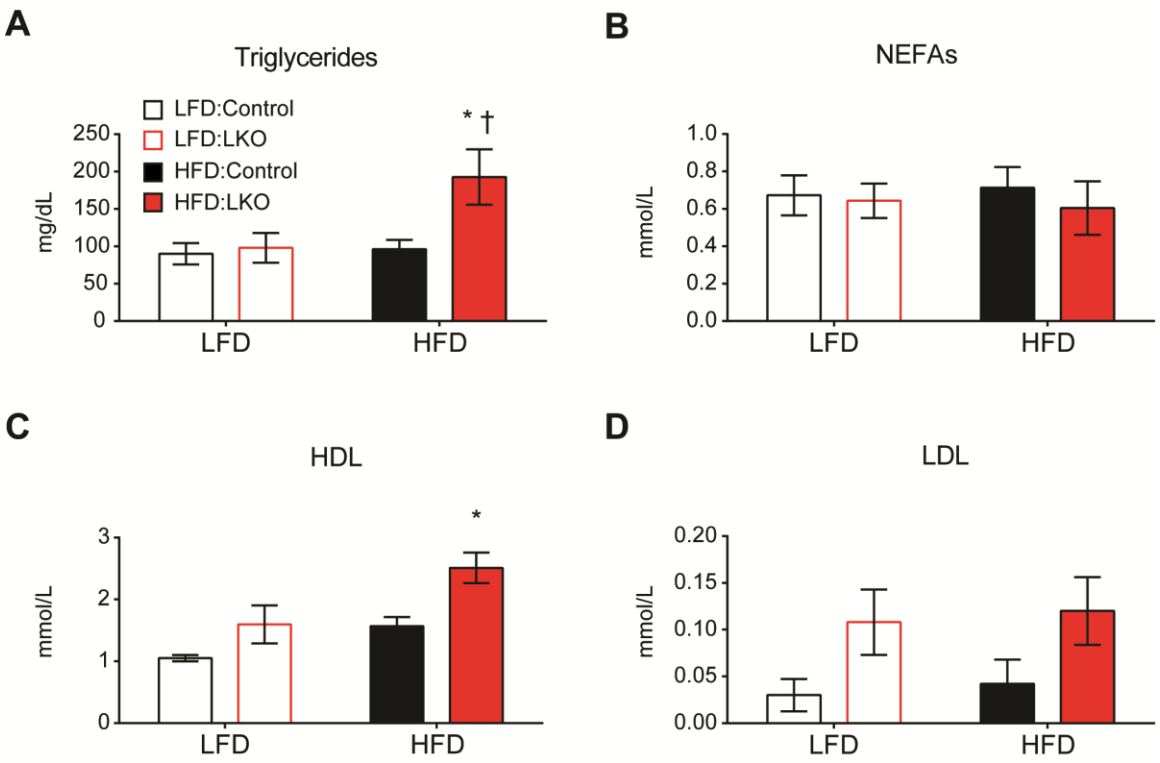

Figure 26: Mig6 LKO mice have increased plasma triglycerides and HDL cholesterol.

Mice were fed HFD for 16 weeks and fasted overnight before blood was collected via cardiac puncture. Plasma triglycerides and NEFAs were measured by a colorimetric enzymatic assay (A,B). Plasma HDL and LDL were measured by the Translational Core of the Center for Diabetes and Metabolic Diseases at Indiana University School of Medicine (C,D). Note the concentration of LDL cholesterol was at or below detection levels in our samples. Data are expressed as means ± SEM; n = 7-8 *, $p < 0.05$ vs LFD.

Mig6 LKO mice have improved cellular ballooning: Obesity-induced hepatic ER stress leads to increased cell death (Wang et al., 2006b), and Mig6 ablation reduces fatty acid-induced apoptosis in hepatic cell lines (Figure 10). More importantly NAFLD is associated with increases in hepatic cell death (Feldstein et al., 2003). In order to determine if Mig6 ablation reduces hepatic stress during NAFLD, hematoxylin- and eosin-stained liver sections were analyzed via the Kleiner method of histological scoring for NAFLD/NASH (Table 1, Kleiner et al., 2005). Section scoring revealed similar steatosis and low to undetectable levels of lobular inflammation (Figure 27-A,B). Interestingly, hepatic ballooning was increased in control livers fed a HFD compared to control LFD diet, however, no significant increase in hepatic ballooning was observed among the Mig6 LKO groups (Figure 27-B), suggesting Mig6 LKO mice were protected from liver cell damage and apoptotic death following HFD feeding. The composite total hepatic NAS score was similar between the groups, which is indicative of the mouse models. Interestingly, the reduction in ballooning dose not correlate to a decrease in plasma liver enzymes (Figure 28A-C). In fact, the Mig6 LKO mice have a subtle increase in plasma ALT, a measure of liver damage, with an increase plasma albumin, a measure of proper function (Figure 28-D). Although these measurements were significant, the ALT measurements do not always correlate with increases in hepatic pathologies (Mofrad et al., 2003), and the mild elevations in ALT found in LKO mice are markedly lower than levels found in true hepatic damage models.

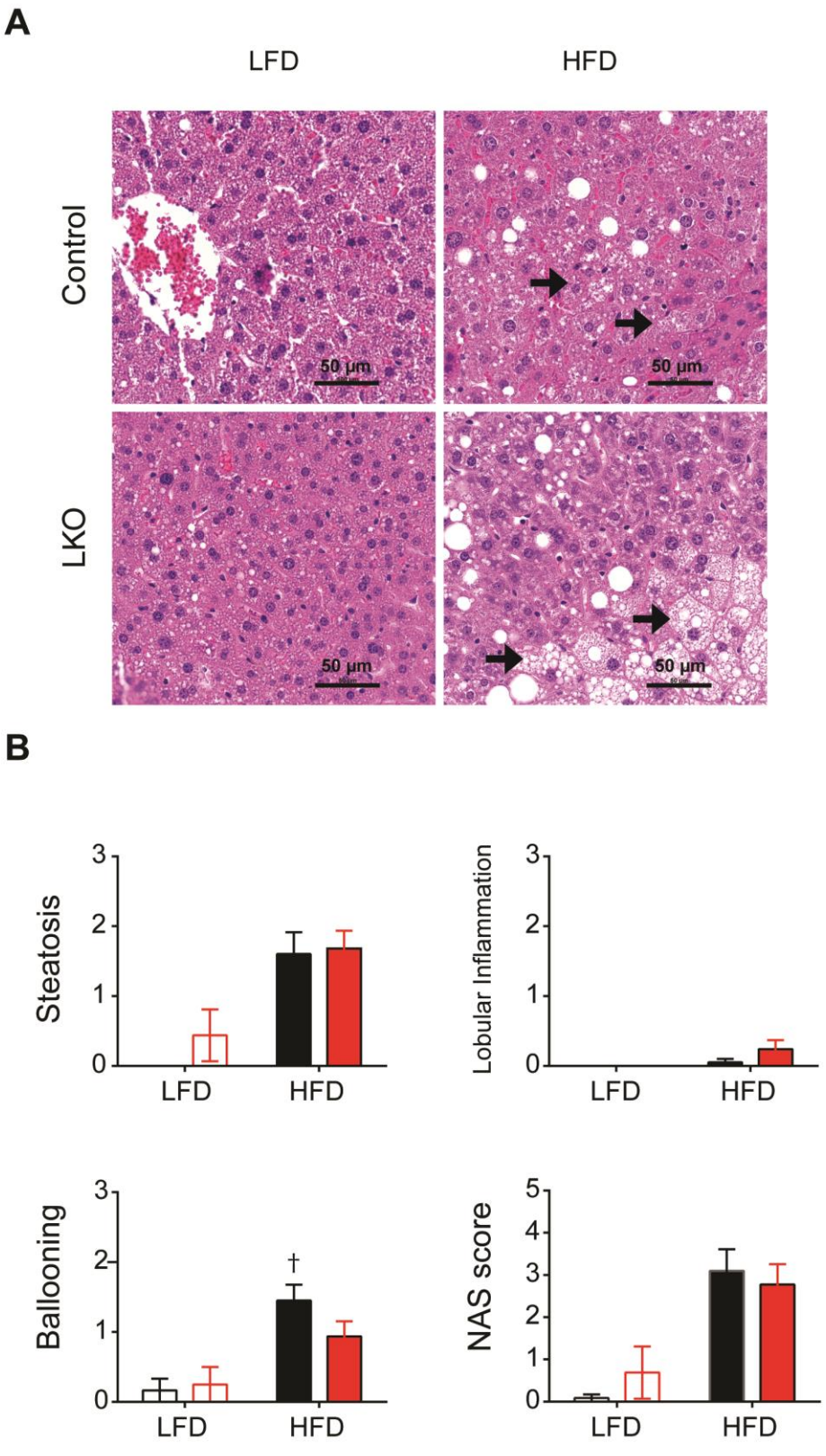
A
LFD
HFD
Control
LKO
50 µm
50 µm
50 µm
50 µm
B
Steatosis
Lobular Inflammation
Ballooning
NAS score
LFD
HFD
†

Figure 27: Mig6 ablation prevents elevated hepatic ballooning in HFD fed mice.

After 16 weeks of diet, livers samples were fixed in zinc formalin and embedded in paraffin wax. Sections (5 μm) were stained with H&E (A) scored by a board certified veterinary pathologist (B). Scoring methods are listed in Table 1. Arrows indicate hepatocellular ballooning. Data are expressed as means ± SEM; n = 6-11. †, $p < 0.05$ vs LFD.

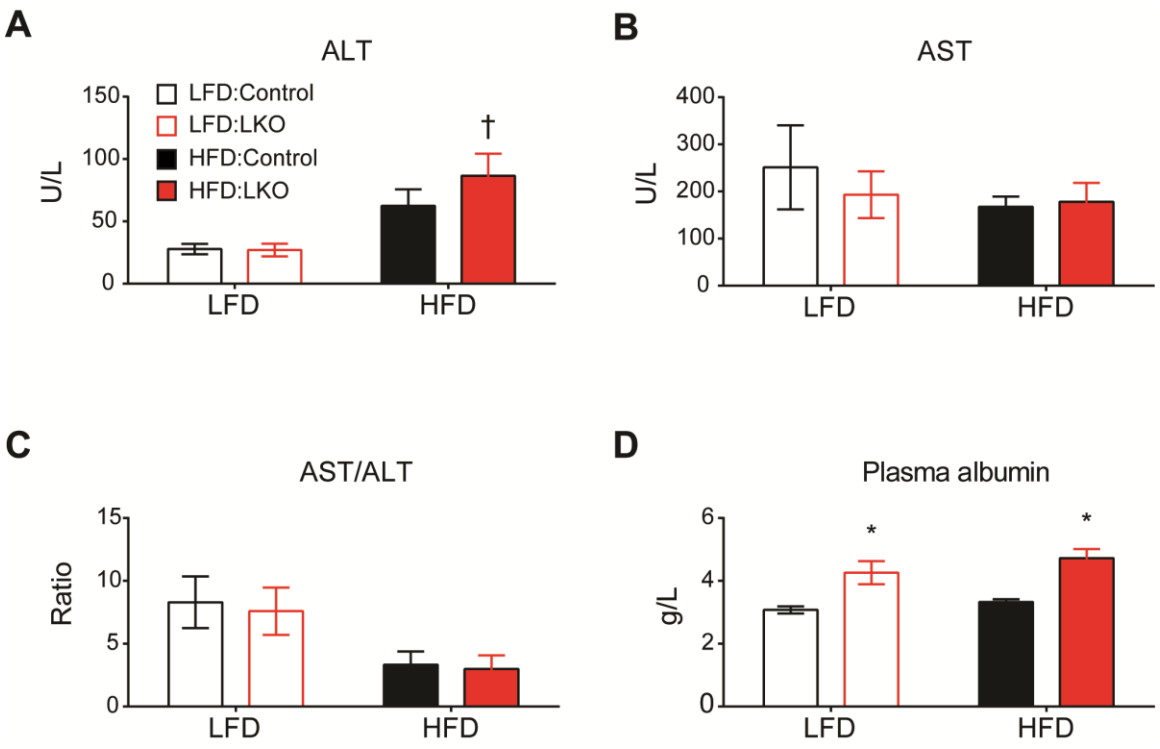

Figure 28: Plasma ALT and Albumin and elevated in Mig6 LKO mice.

Mice were fasted overnight and blood was obtained by cardiac puncture at the end of the study. ALT, AST, and plasma albumin were measured in plasma by the Translation Core of the Center for Diabetes and Metabolic Diseases at Indiana University School of Medicine (A-D). Data are expressed as means ± SEM; n = 4-6 *, $p < 0.05$ vs control, †, $p < 0.05$ vs LFD.

Hepatic ERK 1/2 activity is increased in Mig6 LKO mice fed a HFD: To determine the mechanism of increased glucose tolerance in Mig6 LKO mice fed a HFD, mice were fasted overnight and given an IP bolus injection of insulin. Hepatic insulin mediated AKT phosphorylation was decreased in both HFD fed groups moreover, Mig6 LKO mice do not have increased AKT activation compared to HFD fed controls (Figure 29-A,B). Importantly, the mitogen signaling intermediated ERK was highly phosphorylated in Mig6 LKO livers regardless of insulin stimulation (Figure 29-C). More importantly still, Mig6 LKO mice on a HFD had the highest level of ERK activation (Figure 29-C).

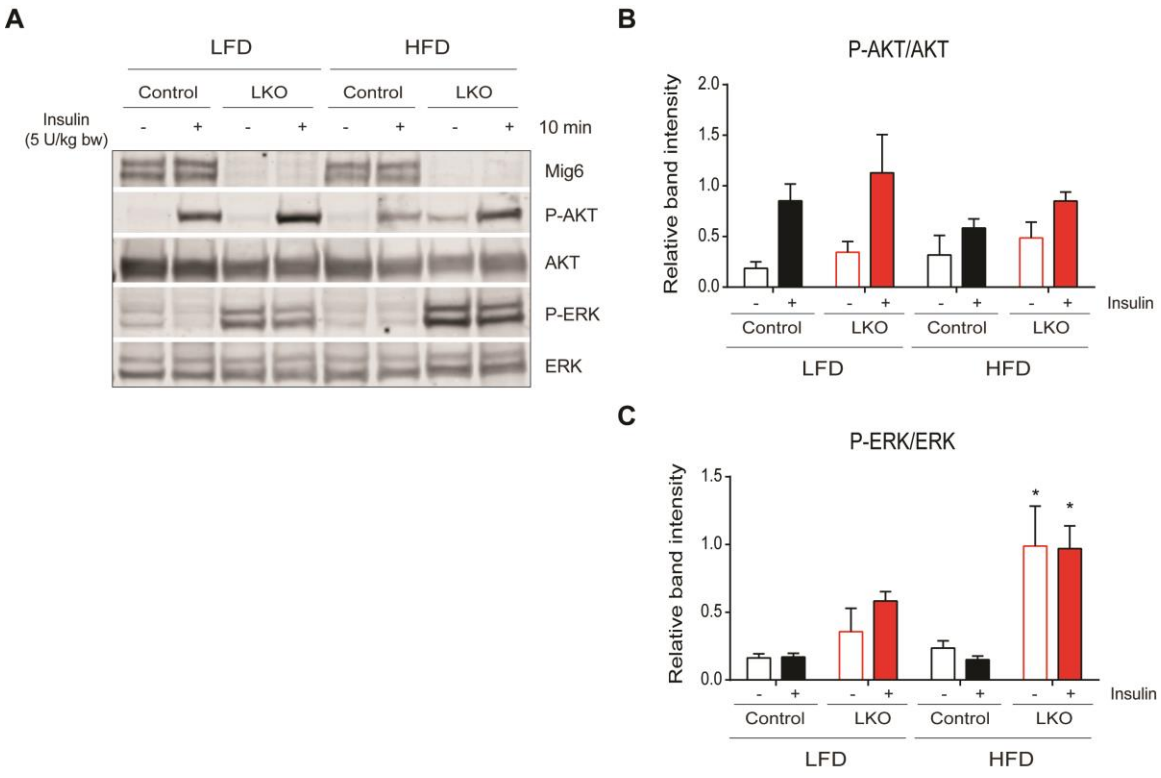

Figure 29: Mig6 LKO livers have normal insulin sensitivity following HFD. 16 weeks after diet, male Mig6 LKO and littermate controls were fasted overnight and given an IP isulin bolous (5 U/kg bw). Western blots were used to determine hepatic Mig6, AKT, and ERK expression (A). Phosphorylation of AKT and ERK were normalized to total AKT and ERK respectively (B,C). Data are expressed as means ± SEM; n =4-6 *, $p < 0.05$ vs control HFD.

In addition to protein phosphorylation, insulin regulates gluconeogenesis through regulation of gene expression and more importantly, Mig6 LKO mice have reduced expression of gluconeogenic genes on chow diet (Figure 20, Nordlie and Foster, 2010). Therefore, HFD fed livers were analyzed for glucose regulatory gene expression. Mig6 LKO mice had increased glycolytic *glucokinase*, and decreased gluconeogenic *g6pase* gene expression (Figure 30), suggesting the Mig6 LKO mice may have lower HGP than littermate controls.

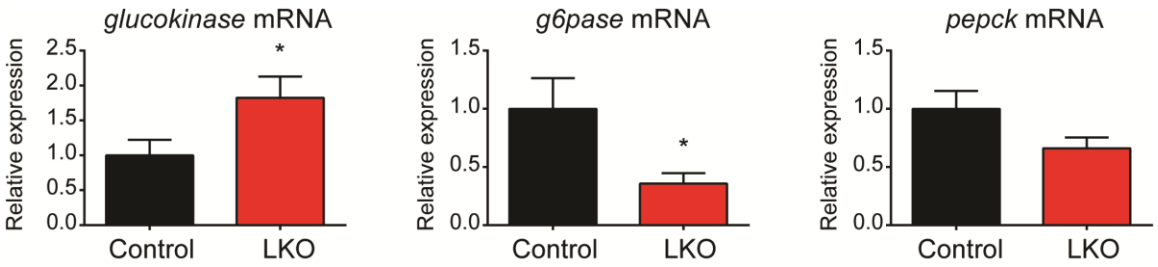

Figure 30: Mig6 LKO mice have increased glucokinase and reduced g6pase gene expression on HFD compared to littermate controls.

Following 16 weeks of HFD mice were fasted overnight and euthanized. Livers were removed and qPCR was used to analyze gene expression of *glucokinase*, *g6pase*, and *pepck*. Genes were normalized to *GAPDH* and data are expressed as means ± SEM, n=8 *, $p < 0.05$ vs control.

Discussion: The notion that Mig6 possesses an additional function as a metabolic regulator is recently emerging. Our group has previously described Mig6 as a negative regulator of functional β cell mass acting to improve glucose homeostasis through increased β cell survival (Chen et al., 2014). However, Mig6 and its known target EGFR are highly expressed in liver. In fact, EGFR is activated following stress from both injury and metabolism (i.e., prolonged fasting) (Bhushan et al., 2014; Freidenberg et al., 1986). However, few studies have described EGFR's ability to regulate hepatic metabolism and fewer still have examined Mig6's role. Other groups have recently reported that Mig6 potentially regulates hepatic cholesterol synthesis, though these studies have several methodological concerns (Ku et al., 2012). Here, we demonstrate that Mig6 LKO mice exhibit similar body weight and fasting glucose, but have enhanced glucose tolerance following the challenge of diet-induced obesity. The enhanced glucose tolerance is independent of whole-body insulin and pyruvate tolerance (a measure of gluconeogenesis) compared to littermate controls. Furthermore, the improvement of glucose tolerance was not ascribed to increased functional β cell mass. A previous report described an increase in β cell mass mediated by hepatic ERK1/2 activation (Imai et al., 2008), which was also present in our mice. Taken together, these results indicate that hepatic ablation of Mig6 leads to an inherent improvement in hepatic glucose metabolism.

Liver mass was increased in both LFD and HFD Mig6 LKO mice compared to littermate controls (Figure 24 and Ku et al., 2012). These changes

do not reflect an increased in hepatic proliferative markers or increased lipid deposition indicated by Oil Red O, triglyceride content, and gross anatomy. However, the plasma lipid profiles were markedly different among genotypes with plasma levels of TG and HDL significantly increased in the absence of Mig6. These results are contrary to the improved glucose tolerance, as increased plasma triglycerides are a hallmark of obesity-induced diabetes (Solano and Goldberg, 2006). The increase in both HDL (LDL was elevated but low in all samples) and triglycerides in the Mig6 LKO suggest inherent defects in hepatic lipoprotein uptake or hepatic lipase activity. Interestingly, human hepatic lipase overexpressing mice have decreased HDL/LDL and serum triglycerides whereas knockout mice have higher levels of plasma cholesterol and triglycerides (Dichek et al., 1998; Weinstock et al., 1995). Most importantly, hepatic lipase is transcriptionally activated by PPAR-γ, which is regulated by EGFR in several cancer models (Mansure et al., 2013; Varley et al., 2004). Nevertheless, we can only speculate on the potential link between Mig6, EGFR, and hepatic lipase at this time.

EGFR is anti-apoptotic, and NAFLD progression is correlated with increased cell death (Feldstein et al., 2003; Paranjpe et al., 2010; Schiffer et al., 2005; Wieckowska et al., 2006). Because our mice have improved ERK1/2 signaling, downstream of pro-survival, EGFR, during HFD (Figure 29), we had an independent animal pathologist score liver sections using routine NAS scoring methods (Kleiner et al., 2005). The Mig6 LKO mice displayed improved hepatic ballooning, a measure of cell death, without an improvement in hepatic enzyme

markers (Figures 27 & 28). These results were not surprising given the animal models used to induce fatty-liver fail to induce necro-inflammation and NASH. The slight increase in hepatic ALT levels is consistent with findings that patients may have increased enzymatic ALT levels during obesity although these may not correlate with severity of NAFLD (Kunde et al., 2005). In order to produce massive increases in hepatic cell death and inflammation (NASH) and activation of fibrosis a MCD diet may be required. However, as fibrosis is often regarded as a proliferative disease, Mig6 ablation may increase the severity of fibrosis and lead to cirrhosis.

Lastly, because insulin resistance and NAFLD exacerbate one another, we measured insulin sensitivity in hepatic tissue (Figure 29). We detected no significant improvements in insulin-mediated AKT phosphorylation amongst groups measured. However, we did identify profound increases in ERK1/2 activation, regardless of insulin stimulation. The Mig6 LKO mice also have improvements in transcriptional patterns of genes involved in hepatic glucose metabolism, displaying a gene expression profile reflecting a glycolytic phenotype rather than gluconeogenic. These data suggest the insulin sensitivity in these mice may be improved as *glucokinase*, *g6pase*, and *pepck* are regulated by insulin. In our mice, acute activation studies may not have the power to reach significance given the amount of groups analyzed. Another possible explanation is the emerging evidence that ERK1/2 may phosphorylate FOXO1 on several serine residues *in vivo* and *in* vitro (Asada et al., 2007). The regulatory role of FOXO1 could explain the transcription of insulin sensitive genes found in our

mice. In conclusion, the results described here suggest a novel role for Mig6 in regulating glucose metabolism during diet-induced obesity.

CHAPTER 6: DISSCUSSION AND FUTURE STUDIES

Mig6 decreases hepatic EGFR activation and survival during saturated fatty acid-induced endoplasmic reticulum stress.

Summary and perspectives: In Chapter 3, we determined Mig6 was activated during chemical- and fatty acid- induced ER stress. We also established Mig6 decreases EGFR activation and signaling during hepatic ER stress. Furthermore, under stress conditions, Mig6 protein was stabilized and Mig6 ablation could restore EGFR activity and reduced caspase 3/7 activity. These data suggest a role for Mig6 beyond the classic *in utero* development and oncogenic properties previously described. Mig6 is an early response gene, yet many studies fail to recognize the acute function of Mig6 protein, especially given the short half-life (1-2 hrs).

Furthermore, these studies link EGFR signal inhibition to hepatic ER stress. Because EGFR is a RTK that activates similar pathways as the insulin receptor, we considered the possibility of *EGFR resistance* during metabolic stress. Classically, EGFR over-activation through Mig6 absence is associated with hepatocellular carcinoma (HCC) (Reschke et al., 2010). However, during hepatic ER stress, repair mechanisms are activated to prevent the damage and restore proper cellular function prior to the onset of HCC. In fact, many NAFLD patients never develop NASH and therefore, do not progress to cirrhosis and HCC (Dixon et al., 2001).

Most importantly, we do not know the exact mechanisms of Mig6 induction during stress conditions. Although Mig6 does escape the translation blockade

during ER stress in certain cell lines, the transcription mechanisms still remain elusive (Chen et al., 2013). One possible explanation based on *in silico* analysis is through the many ER stress activated transcription factor binding sites in the Mig6 promoter, which include $NF_{\kappa}B$ and XBP-1. In this way, Mig6 transcription would increase independent of EGFR signaling, which is decreased during ER stress. Therefore, Mig6 expression could be controlled independently of EGFR activation.

Future studies: A type of stress common to NAFLD is oxidative stress. Originally, oxidative stress was referred to as the secondary hit associated with NAFLD progression towards NASH (Day and James, 1998). Another common initiator of oxidative stress is the increased oxidation of toxic by-products due to drug metabolism by CYP2E1 (Gonzalez, 2005). Clinically, acetaminophen overdose induces massive cellular loss due to oxidative stress caused by CYP2E1 activity (Manyike et al., 2000). Interestingly, EGFR activation follows APAP induced tissue loss in mouse models (Bhushan et al., 2014). We speculate that the activation of EGFR would then be regulated by concurrent induction of Mig6. Furthermore, following APAP overdose, patients either repair/regenerative damaged tissue or enter irreversible liver failure. Therefore, we wondered if severe oxidative stress would induce Mig6 gene expression. Using hydrogen peroxide (H_2O_2), a by-product created during hepatic oxidative stress, we treated HepG2 cells and induced Mig6 gene and protein expression while decreasing EGFR signaling (Y1068) and targets, cyclin D1 and birc5 (Figure 31). These data indicate Mig6 may function in a pathological role by controlling oxidative

responses. Interestingly, EGFR is thought to be inappropriately regulated by activation of pro-apoptotic tyrosine 845 phosphorylation in lung epithelial cells (Ravid et al., 2002). This group also reports an inability of EGFR to dimerize and internalize into lysosomes during oxidative stress (Filosto et al., 2011), suggesting additional roles for EGFR activation during oxidative stress response.

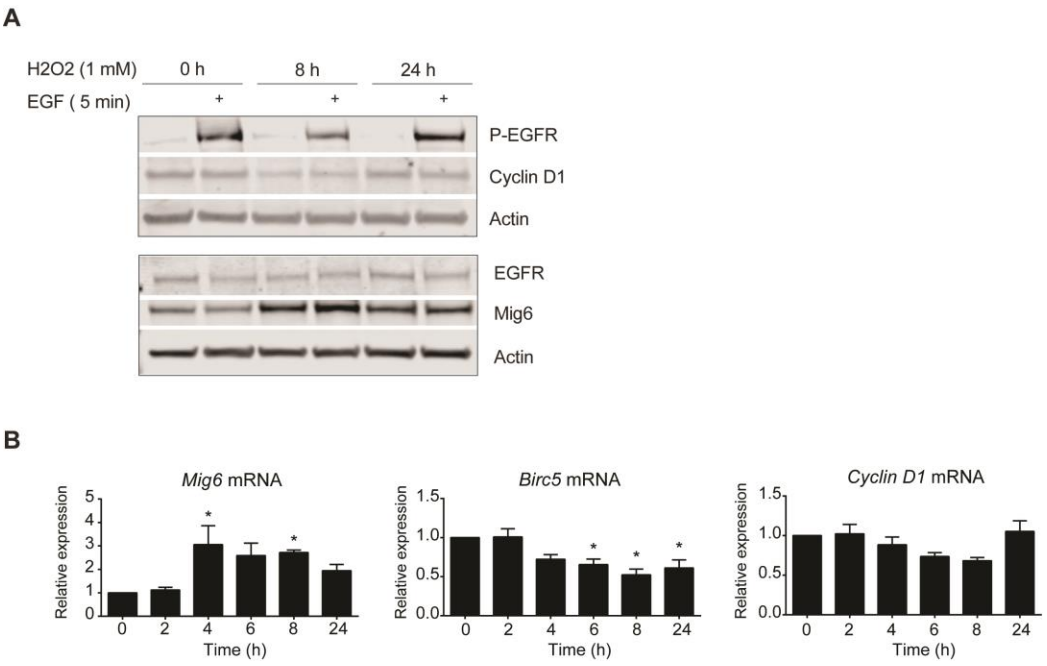

Figure 31: Oxidative stress induces Mig6 expression in HepG2 cells.

HepG2 cells were starved overnight and treated with H_2O_2 prior to ligand stimulation at dose and times indicates. Representative Western blots are shown (A). Gene expression was assessed via qPCR normalized to GAPDH and quantified (B). Data are expressed as means ± SEM; n = 4. *, $p < 0.05$ vs. untreated.

EGFR activation is decreased and Mig6 protein expression is increased during obesity in mice.

Summary and perspectives: The most appropriate model for testing the relationship between EGFR and Mig6 during obesity was the 60% HFD model. Although, we were able to demonstrate significant increases in Mig6 expression in this model, mice fail to develop hepatic pathologies similar to human NAFLD, as evidenced by low overall NAS score (Figure 27). The Mig6 LKO mice have a larger liver mass than the littermate controls, regardless of diet (Figures 17 & 24). This observation is of particular interest because liver transplants from humans and of several animal models will expand and contract to reach optimal functional size for the recipient (Francavilla et al., 1994; Kam et al., 1987). If liver mass is tightly coupled to metabolic demand, then why do the livers of the Mig6 LKO expand in both metabolically healthy and compromised individuals? Does the increase in parenchymal mass lead to improved liver function via increased storage capacity? For example, storing elevated glucose as glycogen or lipids as triglycerides, could potentially lower the available substrates or plasma glucose in this example. Further studies are need to determine the functional consequences of the increased hepatic size in this genetic model.

However, here we were able to demonstrate for the first time the inhibitory effect of obesity-induced NAFLD on EGFR signaling *in vivo*. These results help to establish endogenous feedback inhibitors such as Mig6 as possible targets for improving metabolic function during NAFLD. We also have not detected any effects of Mig6 towards the development of HCC in any of our models,

suggesting that targeting Mig6 alone would not lead to deleterious effects in liver as suggested previously (Reschke et al., 2010).

Future studies: Perhaps the most vital experiment to determine the effect of Mig6 on hepatic regeneration is the partial hepatectomy model. This model was previously used in Mig6 null mice to determine that Mig6's regulates cell cycle entry following tissue loss (Reschke et al., 2010). However, several groups have demonstrated obesity-lowers hepatic regenerative response. In this context, hepatic Mig6 ablation could potentially alleviate regenerative restraint. Furthermore, partial hepatectomy followed by a functional assay (GTT) may help answer some questions regarding liver mass and improved metabolic function.

Liver-specific Mig6 ablation improves glucose tolerance in high fat fed mice.

Summary and perspectives: The most impactful data of the project thus far is the improvement in glucose tolerance on a HFD. However slight the improvement, these data suggest a beneficial role of hepatic Mig6 ablation on whole-body physiology. The mechanisms for this beneficial outcome still remains elusive. Our data indicates a slight improvement in hepatic insulin sensitivity as indicated by gene expression studies, but a direct link is yet to be discovered. The improvement in liver health as indicated by lower levels of cellular ballooning may prove relevant in improving insulin sensitivity by mere coincidence. Indeed, mouse models of NASH development may provide additional information in this context.

The overall increase in plasma HDL/LDL and triglycerides cannot be ignored, as the liver plays a vital role in regulation of plasma lipid regulation. These results are in line with previous studies linking Mig6 to cholesterol biosynthesis (Ku et al., 2012). However, the cardiovascular effects of these changes warrant further study.

Future studies: As discussed in the introduction, EGF secretion increases during the fasting state, however, EGF/EGFR binding and phosphorylation are diminished during fasting (Freidenberg et al., 1986). This regulation has two possible but not exclusive explanations; first, because EGFR signaling suppresses *pepck* and *g6pase*, lowering its ligand affinity and activation during fasting may be required for transcription of genes necessary for HGP.

Secondly, Mig6 is upregulated during fasting and therefore, inhibits EGFR activation.

In addition to obesity, fasting is known to induce ER stress and active pro-gluconeogenic genes (Wang et al., 2009). Therefore, we sought to determine if fasting induced hepatic Mig6 protein expression. C57Bl/6J mice were fasted 24 hours or re-fed for the last 6 hours and livers examined for Mig6 expression. Indeed, Mig6 gene and protein expression are upregulated during fasting conditions similar to gluconeogenic *g6pase* mRNA expression (Figure 32). In addition, Mig6 is induced by cAMP in liver (Lee et al., 1985), a secondary signaling molecule released during the counter-regulatory response (fasting). Mig6 may be regulated by G protein coupled receptors independently of EGFR signaling. These data suggest a possible regulatory mechanism for Mig6 during fed-fasting transition. However, Mig6 ablation has no effect on fasting glucose nor gluconeogenesis (Figures 21 & 22). Although, these studies are not specific to hepatic function alone, as the kidneys and intestine retain gluconeogenic capacity during extreme fasting conditions. However incomplete, these data emphasize the need for strict adherence towards experimental conditions in mice as Mig6, a classic EGFR inhibitor, has altered expression levels during metabolic duress.

The best way to determine the contribution of Mig6 liver ablation towards whole body glucose metabolism would be through hyperinsulinemic-euglycemic clamp experiments. Using isotopic and tritiated glucose, one could determine the ability of insulin to stimulate whole-body glucose disposal, increase tissue-

specific glucose uptake, and suppress endogenous glucose production (a measure of HGP). We predict the Mig6 LKO mice would have similar whole-body disposal and tissue specific uptake of glucose, but increased insulin-mediated suppression of hepatic glucose production. These findings would help define the physiological mechanism for improved glucose tolerance.

In order to determine the molecular mechanism of improved glucose tolerance, we preformed RNA sequencing of liver samples of Mig6 LKO mice and littermate controls on both LFD and HFD (Figure 33). At present we have four unique data sets indicating separate gene expression patterns within our four groupings. A master list of differentially expressed genes revealed differences in several genes involved in glucose and lipid metabolism. However, in order to determine the functionality of the different gene sets, pathway analysis needs to be conducted.

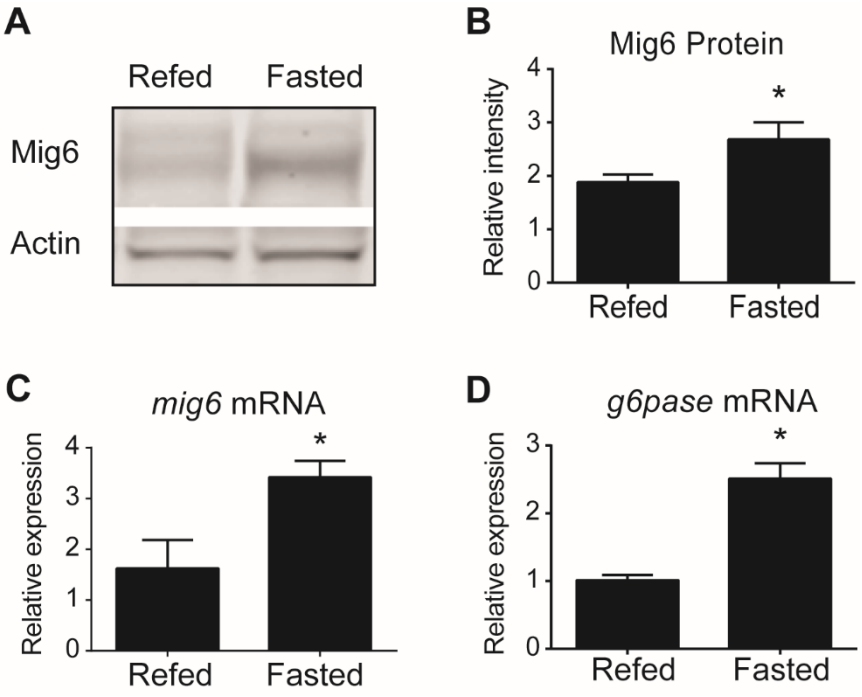

Figure 32: Fasting induces Mig6 and g6pase in male C57Bl/6 mice.

Eight week old mice were fasted (24 h) or refed (24 h fast followed by 6 h feeding ab lib). Representative Western blot of liver tissue showing Mig6 protein (A) and quantification (B). qPCR of liver tissue showing *mig6* and *g6pase* expression (C&D). Data are expressed as means ± SEM; n = 3. *, $p < 0.05$ vs. Refed.

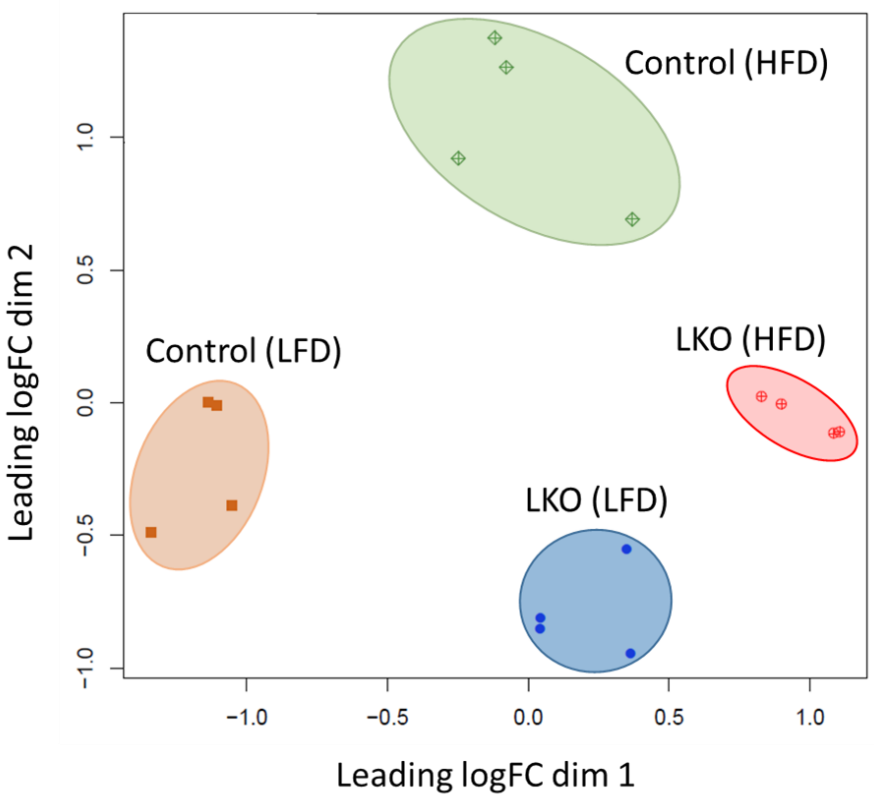

Figure 33: MDS plot showing separation among treatment groups.

Six-week-old male mice were fed either a HFD (60% kcal from fat) or LFD (10% kcal from fat, matched sucrose) for 16 weeks. Following diet livers were harvested and flash frozen. RNA was extracted and sequenced. n=4.

REFERENCES

Achard, C.S., and Laybutt, D.R. (2012). Lipid-Induced Endoplasmic Reticulum Stress in Liver Cells Results in Two Distinct Outcomes: Adaptation with Enhanced Insulin Signaling or Insulin Resistance. Endocrinology *153*, 2164–2177.

Adams, L.A., Lymp, J.F., St. Sauver, J., Sanderson, S.O., Lindor, K.D., Feldstein, A., and Angulo, P. (2005). The Natural History of Nonalcoholic Fatty Liver Disease: A Population-Based Cohort Study. Gastroenterology *129*, 113–121.

Akerman, P., Cote, P., Yang, S.Q., McClain, C., Nelson, S., Bagby, G.J., and Diehl, A.M. (1992). Antibodies to tumor necrosis factor-alpha inhibit liver regeneration after partial hepatectomy. Am. J. Physiol. - Gastrointest. Liver Physiol. *263*, G579–G585.

Anastasi, S., Baietti, M.F., Frosi, Y., Alemà, S., and Segatto, O. (2007). The evolutionarily conserved EBR module of RALT/MIG6 mediates suppression of the EGFR catalytic activity. Oncogene *26*, 7833–7846.

Anstee, Q.M., and Goldin, R.D. (2006). Mouse models in non-alcoholic fatty liver disease and steatohepatitis research. Int. J. Exp. Pathol. *87*, 1–16.

Argaud, D., Zhang, Q., Pan, W., Maitra, S., Pilkis, S.J., and Lange, A.J. (1996). Regulation of Rat Liver Glucose-6-Phosphatase Gene Expression in Different Nutritional and Hormonal States: Gene Structure and 5′-Flanking Sequence. Diabetes *45*, 1563–1571.

Asada, S., Daitoku, H., Matsuzaki, H., Saito, T., Sudo, T., Mukai, H., Iwashita, S., Kako, K., Kishi, T., Kasuya, Y., et al. (2007). Mitogen-activated protein kinases, Erk and p38, phosphorylate and regulate Foxo1. Cell. Signal. *19*, 519–527.

Banks, A.S., McAllister, F.E., Camporez, J.P.G., Zushin, P.-J.H., Jurczak, M.J., Laznik-Bogoslavski, D., Shulman, G.I., Gygi, S.P., and Spiegelman, B.M. (2015). An ERK/Cdk5 axis controls the diabetogenic actions of PPARγ. Nature *517*, 391–395.

Berasain, C., García-Trevijano, E.R., Castillo, J., Erroba, E., Lee, D.C., Prieto, J., and Avila, M.A. (2005). Amphiregulin: An early trigger of liver regeneration in mice. Gastroenterology *128*, 424–432.

Bhushan, B., Walesky, C., Manley, M., Gallagher, T., Borude, P., Edwards, G., Monga, S.P.S., and Apte, U. (2014). Pro-Regenerative Signaling after Acetaminophen-Induced Acute Liver Injury in Mice Identified Using a Novel Incremental Dose Model. Am. J. Pathol. *184*, 3013–3025.

Boney, C.M., Verma, A., Tucker, R., and Vohr, B.R. (2005). Metabolic Syndrome in Childhood: Association With Birth Weight, Maternal Obesity, and Gestational Diabetes Mellitus. Pediatrics *115*, e290–e296.

Bosch, F., Bouscarel, B., Slaton, J., Blackmore, P.F., and Exton, J.H. (1986). Epidermal growth factor mimics insulin effects in rat hepatocytes. Biochem. J. *239*, 523–530.

Bose, R., and Zhang, X. (2009). The ErbB Kinase Domain: Structural Perspectives into Kinase Activation and Inhibition. Exp. Cell Res. *315*, 649–658.

Bost, F., Aouadi, M., Caron, L., Even, P., Belmonte, N., Prot, M., Dani, C., Hofman, P., Pagès, G., Pouysségur, J., et al. (2005). The Extracellular Signal–Regulated Kinase Isoform ERK1 Is Specifically Required for In Vitro and In Vivo Adipogenesis. Diabetes *54*, 402–411.

Browning, J.D., Szczepaniak, L.S., Dobbins, R., Nuremberg, P., Horton, J.D., Cohen, J.C., Grundy, S.M., and Hobbs, H.H. (2004). Prevalence of hepatic steatosis in an urban population in the United States: impact of ethnicity. Hepatol. Baltim. Md *40*, 1387–1395.

Cao, W., Collins, Q.F., Becker, T.C., Robidoux, J., Lupo, E.G., Xiong, Y., Daniel, K.W., Floering, L., and Collins, S. (2005). p38 Mitogen-activated Protein Kinase Plays a Stimulatory Role in Hepatic Gluconeogenesis. J. Biol. Chem. *280*, 42731–42737.

Carver, R.S., Stevenson, M.C., Scheving, L.A., and Russell, W.E. (2002). Diverse expression of ErbB receptor proteins during rat liver development and regeneration. Gastroenterology *123*, 2017–2027.

Chan, C.P., and Krebs, E.G. (1985). Epidermal growth factor stimulates glycogen synthase activity in cultured cells. Proc. Natl. Acad. Sci. *82*, 4563–4567.

Chen, Y.-C., Colvin, E.S., Maier, B.F., Mirmira, R.G., and Fueger, P.T. (2013). Mitogen-inducible gene 6 triggers apoptosis and exacerbates ER stress-induced β-cell death. Mol. Endocrinol. Baltim. Md *27*, 162–171.

Chen, Y.-C., Colvin, E.S., Griffin, K.E., Maier, B.F., and Fueger, P.T. (2014). Mig6 haploinsufficiency protects mice against streptozotocin-induced diabetes. Diabetologia *57*, 2066–2075.

Chu, D.T., Davis, C.M., Chrapkiewicz, N.B., and Granner, D.K. (1988). Reciprocal regulation of gene transcription by insulin. Inhibition of the phosphoenolpyruvate carboxykinase gene and stimulation of gene 33 in a single cell type. J. Biol. Chem. *263*, 13007–13011.

Collin de l'Hortet, A., Gilgenkrantz, H., and Guidotti, J.-E. (2012). EGFR: A Master Piece in G1/S Phase Transition of Liver Regeneration. Int. J. Hepatol. *2012*, 1–9.

Collin de l'Hortet, A., Zerrad-Saadi, A., Prip-Buus, C., Fauveau, V., Helmy, N., Ziol, M., Vons, C., Billot, K., Baud, V., Gilgenkrantz, H., et al. (2014). GH Administration Rescues Fatty Liver Regeneration Impairment by Restoring GH/EGFR Pathway Deficiency. Endocrinology *155*, 2545–2554.

Colvin, E.S., Ma, H.-Y., Chen, Y.-C., Hernandez, A.M., and Fueger, P.T. (2013). Glucocorticoid-induced suppression of β-cell proliferation is mediated by Mig6. Endocrinology *154*, 1039–1046.

Coppack, S.W., Fisher, R.M., Gibbons, G.F., Humphreys, S.M., McDonough, M.J., Potts, J.L., and Frayn, K.N. (1990). Postprandial Substrate Deposition in Human Forearm and Adipose Tissues in Vivo. Clin. Sci. *79*, 339–348.

Cornu, M., Albert, V., and Hall, M.N. (2013). mTOR in aging, metabolism, and cancer. Curr. Opin. Genet. Dev. *23*, 53–62.

Cressman, D.E., Greenbaum, L.E., DeAngelis, R.A., Ciliberto, G., Furth, E.E., Poli, V., and Taub, R. (1996). Liver Failure and Defective Hepatocyte Regeneration in Interleukin-6-Deficient Mice. Science *274*, 1379–1383.

Day, C.P., and James, O.F.W. (1998). Steatohepatitis: A tale of two "hits"? Gastroenterology *114*, 842–845.

Descot, A., Hoffmann, R., Shaposhnikov, D., Reschke, M., Ullrich, A., and Posern, G. (2009). Negative regulation of the EGFR-MAPK cascade by actin-MAL-mediated Mig6/Errfi-1 induction. Mol. Cell *35*, 291–304.

De Souza, C.T., Araujo, E.P., Bordin, S., Ashimine, R., Zollner, R.L., Boschero, A.C., Saad, M.J.A., and Velloso, L.A. (2005). Consumption of a Fat-Rich Diet Activates a Proinflammatory Response and Induces Insulin Resistance in the Hypothalamus. Endocrinology *146*, 4192–4199.

Dichek, H.L., Brecht, W., Fan, J., Ji, Z.-S., McCormick, S.P.A., Akeefe, H., Conzo, L., Sanan, D.A., Weisgraber, K.H., Young, S.G., et al. (1998). Overexpression of Hepatic Lipase in Transgenic Mice Decreases Apolipoprotein B-containing and High Density Lipoproteins EVIDENCE THAT HEPATIC LIPASE ACTS AS A LIGAND FOR LIPOPROTEIN UPTAKE. J. Biol. Chem. *273*, 1896–1903.

Dixon, J.B., Bhathal, P.S., and O'Brien, P.E. (2001). Nonalcoholic Fatty Liver Disease: Predictors of Nonalcoholic Steatohepatitis and Liver Fibrosis in the Severely Obese. Gastroenterology *121*, 91–100.

Donnelly, K.L., Smith, C.I., Schwarzenberg, S.J., Jessurun, J., Boldt, M.D., and Parks, E.J. (2005). Sources of fatty acids stored in liver and secreted via lipoproteins in patients with nonalcoholic fatty liver disease. J. Clin. Invest. *115*, 1343–1351.

Dummler, B., Tschopp, O., Hynx, D., Yang, Z.-Z., Dirnhofer, S., and Hemmings, B.A. (2006). Life with a Single Isoform of Akt: Mice Lacking Akt2 and Akt3 Are Viable but Display Impaired Glucose Homeostasis and Growth Deficiencies. Mol. Cell. Biol. *26*, 8042–8051.

England, C. (2012). Your child. Your choice.

Esterbauer, H., Schaur, R.J., and Zollner, H. (1991). Chemistry and biochemistry of 4-hydroxynonenal, malonaldehyde and related aldehydes. Free Radic. Biol. Med. *11*, 81–128.

Faergeman, N.J., and Knudsen, J. (1997). Role of long-chain fatty acyl-CoA esters in the regulation of metabolism and in cell signalling. Biochem. J. *323 (Pt 1)*, 1–12.

Fafalios, A., Ma, J., Tan, X., Stoops, J., Luo, J., DeFrances, M.C., and Zarnegar, R. (2011). A Hepatocyte Growth Factor Receptor (Met)–Insulin Receptor hybrid governs hepatic glucose metabolism. Nat. Med. *17*, 1577–1584.

Falta, W., and Boller, R. (1931). Insulärer und Insulinresistenter Diabetes. Klin. Wochenschr. *10*, 438–443.

Fausto, N., Campbell, J.S., and Riehle, K.J. (2006). Liver regeneration. Hepatology *43*, S45–S53.

Feldstein, A.E., Canbay, A., Angulo, P., Taniai, M., Burgart, L.J., Lindor, K.D., and Gores, G.J. (2003). Hepatocyte apoptosis and fas expression are prominent features of human nonalcoholic steatohepatitis. Gastroenterology *125*, 437–443.

Ferby, I., Reschke, M., Kudlacek, O., Knyazev, P., Pantè, G., Amann, K., Sommergruber, W., Kraut, N., Ullrich, A., Fässler, R., et al. (2006). Mig6 is a negative regulator of EGF receptor-mediated skin morphogenesis and tumor formation. Nat. Med. *12*, 568–573.

Fillat, C., Valera, A., and Bosch, F. (1993). Epidermal growth factor inhibits phosphoenolpyruvate carboxykinase gene expression in rat hepatocytes in primary culture. FEBS Lett. *318*, 287–291.

Filosto, S., Khan, E.M., Tognon, E., Becker, C., Ashfaq, M., Ravid, T., and Goldkorn, T. (2011). EGF Receptor Exposed to Oxidative Stress Acquires Abnormal Phosphorylation and Aberrant Activated Conformation That Impairs Canonical Dimerization. PLoS ONE *6*.

Fiorentino, L., Pertica, C., Fiorini, M., Talora, C., Crescenzi, M., Castellani, L., Alemà, S., Benedetti, P., and Segatto, O. (2000). Inhibition of ErbB-2 Mitogenic and Transforming Activity by RALT, a Mitogen-Induced Signal Transducer Which Binds to the ErbB-2 Kinase Domain. Mol. Cell. Biol. *20*, 7735–7750.

Fiorini, M., Ballarò, C., Sala, G., Falcone, G., Alemà, S., and Segatto, O. (2002). Expression of RALT, a feedback inhibitor of ErbB receptors, is subjected to an integrated transcriptional and post-translational control. Oncogene *21*, 6530–6539.

Fischer, O.M., Hart, S., Gschwind, A., and Ullrich, A. (2003). EGFR signal transactivation in cancer cells. Biochem. Soc. Trans. *31*, 1203–1208.

Fisher, S.J., and Kahn, C.R. (2003). Insulin signaling is required for insulin's direct and indirect action on hepatic glucose production. J. Clin. Invest. *111*, 463–468.

Flegal KM, Carroll MD, Kit BK, and Ogden CL (2012). PRevalence of obesity and trends in the distribution of body mass index among us adults, 1999-2010. JAMA *307*, 491–497.

Francavilla, A., Zeng, Q., Polimeno, L., Carr, B.I., Sun, D., Porter, K.A., Van Thiel, D.H., and Starzl, T.E. (1994). Small-for-size Liver Transplanted into Larger Recipient: A Model of Hepatic Regeneration. Hepatol. Baltim. Md *19*, 210–216.

Freidenberg, G.R., Klein, H.H., Kladde, M.P., Cordera, R., and Olefsky, J.M. (1986). Regulation of epidermal growth factor receptor number and phosphorylation by fasting in rat liver. J. Biol. Chem. *261*, 752–757.

Frosi, Y., Anastasi, S., Ballarò, C., Varsano, G., Castellani, L., Maspero, E., Polo, S., Alemà, S., and Segatto, O. (2010). A two-tiered mechanism of EGFR inhibition by RALT/MIG6 via kinase suppression and receptor degradation. J. Cell Biol. *189*, 557–571.

Fu, S., Watkins, S.M., and Hotamisligil, G.S. (2012). The Role of Endoplasmic Reticulum in Hepatic Lipid Homeostasis and Stress Signaling. Cell Metab. *15*, 623–634.

Gao, D., Wei, C., Chen, L., Huang, J., Yang, S., and Diehl, A.M. (2004). Oxidative DNA damage and DNA repair enzyme expression are inversely related in murine models of fatty liver disease. Am. J. Physiol. - Gastrointest. Liver Physiol. *287*, G1070–G1077.

Gao, Z., Hwang, D., Bataille, F., Lefevre, M., York, D., Quon, M.J., and Ye, J. (2002). Serine Phosphorylation of Insulin Receptor Substrate 1 by Inhibitor κB Kinase Complex. J. Biol. Chem. *277*, 48115–48121.

Gehart, H., Kumpf, S., Ittner, A., and Ricci, R. (2010). MAPK signalling in cellular metabolism: stress or wellness? EMBO Rep. *11*, 834–840.

Giorgino, F., Laviola, L., and Eriksson, J.W. (2005). Regional differences of insulin action in adipose tissue: insights from in vivo and in vitro studies. Acta Physiol. Scand. *183*, 13–30.

Gonzales, J.C., Gentile, C.L., Pfaffenbach, K.T., Wei, Y., Wang, D., and Pagliassotti, M.J. (2008). Chemical induction of the unfolded protein response in the liver increases glucose production and is activated during insulin-induced hypoglycaemia in rats. Diabetologia *51*, 1920–1929.

Gonzalez, F.J. (2005). Role of cytochromes P450 in chemical toxicity and oxidative stress: studies with CYP2E1. Mutat. Res. Mol. Mech. Mutagen. *569*, 101–110.

González, L., Díaz, M.E., Miquet, J.G., Sotelo, A.I., Fernández, D., Dominici, F.P., Bartke, A., and Turyn, D. (2010). GH modulates hepatic epidermal growth factor signaling in the mouse. J. Endocrinol. *204*, 299–309.

Grau, M., Rodríguez, C., Soley, M., and Ramírez, I. (1994). Relationship between epidermal growth factor in mouse submandibular glands, plasma, and bile: effects of catecholamines and fasting. Endocrinology *135*, 1854–1862.

Gross, D.N., van den Heuvel, A.P.J., and Birnbaum, M.J. (2008). The role of FoxO in the regulation of metabolism. Oncogene *27*, 2320–2336.

Guyenet, S.J., and Schwartz, M.W. (2012). Regulation of Food Intake, Energy Balance, and Body Fat Mass: Implications for the Pathogenesis and Treatment of Obesity. J. Clin. Endocrinol. Metab. *97*, 745–755.

H, V., Dm, R., V, K., R, D., W, H., J, L., U, S., C, K., and U, J. (2005). Hepatic steatosis is associated with an increased risk of carotid atherosclerosis., Hepatic steatosis is associated with an increased risk of carotid atherosclerosis. World J. Gastroenterol. World J. Gastroenterol. WJG *11, 11*, 1848, 1848–1853.

Hales, C.N., and Barker, D.J.P. (1992). Type 2 (non-insulin-dependent) diabetes mellitus: the thrifty phenotype hypothesis. Diabetologia *35*, 595–601.

Harding, H.P., Zhang, Y., and Ron, D. (1999). Protein translation and folding are coupled by an endoplasmic-reticulum-resident kinase. Nature *397*, 271–274.

Himsworth, H.P. (1936). Originally published as Volume 1, Issue 5864DIABETES MELLITUS. The Lancet *227*, 127–130.

Hirosumi, J., Tuncman, G., Chang, L., Görgün, C.Z., Uysal, K.T., Maeda, K., Karin, M., and Hotamisligil, G.S. (2002). A central role for JNK in obesity and insulin resistance. Nature *420*, 333–336.

Hotamisligil, G.S. (2010a). Endoplasmic Reticulum Stress and the Inflammatory Basis of Metabolic Disease. Cell *140*, 900–917.

Hotamisligil, G.S. (2010b). Endoplasmic reticulum stress and the inflammatory basis of metabolic disease. Cell *140*, 900–917.

Hu, P., Han, Z., Couvillon, A.D., Kaufman, R.J., and Exton, J.H. (2006). Autocrine Tumor Necrosis Factor Alpha Links Endoplasmic Reticulum Stress to the Membrane Death Receptor Pathway through IRE1α-Mediated NF-κB Activation and Down-Regulation of TRAF2 Expression. Mol. Cell. Biol. *26*, 3071–3084.

Imai, J., Katagiri, H., Yamada, T., Ishigaki, Y., Suzuki, T., Kudo, H., Uno, K., Hasegawa, Y., Gao, J., Kaneko, K., et al. (2008). Regulation of Pancreatic β Cell Mass by Neuronal Signals from the Liver. Science *322*, 1250–1254.

Isomaa, B., Almgren, P., Tuomi, T., Forsén, B., Lahti, K., Nissén, M., Taskinen, M.-R., and Groop, L. (2001). Cardiovascular Morbidity and Mortality Associated With the Metabolic Syndrome. Diabetes Care *24*, 683–689.

Ito, N., Kawata, S., Tamura, S., Kiso, S., Tsushima, H., Damm, D., Abraham, J.A., Higashiyama, S., Taniguchi, N., and Matsuzawa, Y. (1994). Heparin-Binding EGF-like Growth-Factor Is a Potent Mitogen for Rat Hepatocytes. Biochem. Biophys. Res. Commun. *198*, 25–31.

Jebb, S.A., and Moore, M.S. (1999). Contribution of a sedentary lifestyle and inactivity to the etiology of overweight and obesity: current evidence and research issues: Med. Sci. Sports Exerc. *31*, S534.

Jéquier, E. (2002). Pathways to obesity. Int. J. Obes. Relat. Metab. Disord. *26*, S12.

Jiao, P., Feng, B., Li, Y., He, Q., and Xu, H. (2013). Hepatic ERK activity plays a role in energy metabolism. Mol. Cell. Endocrinol. *375*, 157–166.

Jin, N., Gilbert, J.L., Broaddus, R.R., Demayo, F.J., and Jeong, J.-W. (2007). Generation of a Mig-6 conditional null allele. Genes. N. Y. N 2000 *45*, 716–721.

Jones, D.E., Tran-Patterson, R., Cui, D.M., Davin, D., Estell, K.P., and Miller, D.M. (1995). Epidermal growth factor secreted from the salivary gland is necessary for liver regeneration. Am. J. Physiol. - Gastrointest. Liver Physiol. *268*, G872–G878.

Kam, I., Lynch, S., Svanas, G., Todo, S., Polimeno, L., Francavilla, A., Penkrot, R.J., Takaya, S., Ericzon, B.G., Starzl, T.E., et al. (1987). Evidence that Host Size Determines Liver Size: Studies in Dogs Receiving Orthotopic Liver Transplants. Hepatol. Baltim. Md *7*, 362–366.

Kammoun, H.L., Chabanon, H., Hainault, I., Luquet, S., Magnan, C., Koike, T., Ferré, P., and Foufelle, F. (2009). GRP78 expression inhibits insulin and ER stress-induced SREBP-1c activation and reduces hepatic steatosis in mice. J. Clin. Invest. *119*, 1201–1215.

Kario, E., Marmor, M.D., Adamsky, K., Citri, A., Amit, I., Amariglio, N., Rechavi, G., and Yarden, Y. (2005). Suppressors of Cytokine Signaling 4 and 5 Regulate Epidermal Growth Factor Receptor Signaling. J. Biol. Chem. *280*, 7038–7048.

Katz, N.R., Nauck, M.A., and Wilson, P.T. (1979). Induction of glucokinase by insulin under the permissive action of dexamethasone in primary rat hepatocyte cultures. Biochem. Biophys. Res. Commun. *88*, 23–29.

Kawakita, N., Seki, S., Sakaguchi, H., Yanai, A., Kuroki, T., Mizoguchi, Y., Kobayashi, K., and Monna, T. (1992). Analysis of proliferating hepatocytes using a monoclonal antibody against proliferating cell nuclear antigen/cyclin in embedded tissues from various liver diseases fixed in formaldehyde. Am. J. Pathol. *140*, 513–520.

Kawano, Y., and Cohen, D.E. (2013). Mechanisms of hepatic triglyceride accumulation in non-alcoholic fatty liver disease. J. Gastroenterol. *48*, 434–441.

Kiso, S., Kawata, S., Tamura, S., Higashiyama, S., Ito, N., Tsushima, H., Taniguchi, N., and Matsuzawa, Y. (1995). Role of heparin-binding epidermal growth factor–like growth factor as a hepatotrophic factor in rat liver regeneration after partial hepatectomy. Hepatology *22*, 1584–1590.

Kleiner, D.E., Brunt, E.M., Van Natta, M., Behling, C., Contos, M.J., Cummings, O.W., Ferrell, L.D., Liu, Y.-C., Torbenson, M.S., Unalp-Arida, A., et al. (2005). Design and validation of a histological scoring system for nonalcoholic fatty liver disease. Hepatol. Baltim. Md *41*, 1313–1321.

Koning, L. de, Merchant, A.T., Pogue, J., and Anand, S.S. (2007). Waist circumference and waist-to-hip ratio as predictors of cardiovascular events: meta-regression analysis of prospective studies. Eur. Heart J. *28*, 850–856.

Kooby, D.A., Fong, Y., Suriawinata, A., Gonen, M., Allen, P.J., Klimstra, D.S., DeMatteo, R.P., Angelica, M.D., Blumgart, L.H., and Jarnagin, W.R. (2003). Impact of steatosis on perioperative outcome following hepatic resection. J. Gastrointest. Surg. *7*, 1034–1044.

Ku, B.J., Kim, T.H., Lee, J.H., Buras, E.D., White, L.D., Stevens, R.D., Ilkayeva, O.R., Bain, J.R., Newgard, C.B., DeMayo, F.J., et al. (2012). Mig-6 plays a critical role in the regulation of cholesterol homeostasis and bile acid synthesis. PloS One *7*, e42915.

Kunde, S.S., Lazenby, A.J., Clements, R.H., and Abrams, G.A. (2005). Spectrum of NAFLD and diagnostic implications of the proposed new normal range for serum ALT in obese women. Hepatology *42*, 650–656.

Leclercq, I.A., Vansteenberghe, M., Lebrun, V.B., VanHul, N.K., Abarca-Quinones, J., Sempoux, C.L., Picard, C., Stärkel, P., and Horsmans, Y.L. (2006). Defective hepatic regeneration after partial hepatectomy in leptin-deficient mice is not rescued by exogenous leptin. Lab. Invest. *86*, 1161–1171.

Lee, A.-H., Iwakoshi, N.N., and Glimcher, L.H. (2003). XBP-1 regulates a subset of endoplasmic reticulum resident chaperone genes in the unfolded protein response. Mol. Cell. Biol. *23*, 7448–7459.

Lee, A.-H., Scapa, E.F., Cohen, D.E., and Glimcher, L.H. (2008). Regulation of hepatic lipogenesis by the transcription factor XBP1. Science *320*, 1492–1496.

Lee, K.L., Isham, K.R., Stringfellow, L., Rothrock, R., and Kenney, F.T. (1985). Molecular cloning of cDNAs cognate to genes sensitive to hormonal control in rat liver. J. Biol. Chem. *260*, 16433–16438.

Lei, K., and Davis, R.J. (2003). JNK phosphorylation of Bim-related members of the Bcl2 family induces Bax-dependent apoptosis. Proc. Natl. Acad. Sci. U. S. A. *100*, 2432–2437.

Lim, J.S., Mietus-Snyder, M., Valente, A., Schwarz, J.-M., and Lustig, R.H. (2010). The role of fructose in the pathogenesis of NAFLD and the metabolic syndrome. Nat. Rev. Gastroenterol. Hepatol. *7*, 251–264.

Liu, N., Matsumoto, M., Kitagawa, K., Kotake, Y., Suzuki, S., Shirasawa, S., Nakayama, K.I., Nakanishi, M., Niida, H., and Kitagawa, M. (2012). Chk1 phosphorylates the tumour suppressor Mig-6, regulating the activation of EGF signalling. EMBO J. *31*, 2365–2377.

Lu, M., Wan, M., Leavens, K.F., Chu, Q., Monks, B.R., Fernandez, S., Ahima, R.S., Ueki, K., Kahn, C.R., and Birnbaum, M.J. (2012). Insulin regulates liver metabolism in vivo in the absence of hepatic Akt and Foxo1. Nat. Med. *18*, 388–395.

Maffei, M., Halaas, J., Ravussin, E., Pratley, R.E., Lee, G.H., Zhang, Y., Fei, H., Kim, S., Lallone, R., Ranganathan, S., et al. (1995). Leptin levels in human and rodent: Measurement of plasma leptin and ob RNA in obese and weight-reduced subjects. Nat. Med. *1*, 1155–1161.

Makkinje, A., Quinn, D.A., Chen, A., Cadilla, C.L., Force, T., Bonventre, J.V., and Kyriakis, J.M. (2000a). Gene 33/Mig-6, a transcriptionally inducible adapter protein that binds GTP-Cdc42 and activates SAPK/JNK. A potential marker transcript for chronic pathologic conditions, such as diabetic nephropathy.

Possible role in the response to persistent stress. J. Biol. Chem. *275*, 17838–17847.

Mansure, J.J., Nassim, R., Chevalier, S., Szymanski, K., Rocha, J., Aldousari, S., and Kassouf, W. (2013). A Novel Mechanism of PPAR Gamma Induction via EGFR Signalling Constitutes Rational for Combination Therapy in Bladder Cancer. PLOS ONE *8*, e55997.

Manyike, P.T., Kharasch, E.D., Kalhorn, T.F., and Slattery, J.T. (2000). Contribution of CYP2E1 and CYP3A to acetaminophen reactive metabolite formation. Clin. Pharmacol. Ther. *67*, 275–282.

McCormack, L., Petrowsky, H., Jochum, W., Furrer, K., and Clavien, P.-A. (2007). Hepatic steatosis is a risk factor for postoperative complications after major hepatectomy: a matched case-control study. Ann. Surg. *245*, 923–930.

Mead, J.E., and Fausto, N. (1989). Transforming growth factor alpha may be a physiological regulator of liver regeneration by means of an autocrine mechanism. Proc. Natl. Acad. Sci. *86*, 1558–1562.

Mehlem, A., Hagberg, C.E., Muhl, L., Eriksson, U., and Falkevall, A. (2013). Imaging of neutral lipids by oil red O for analyzing the metabolic status in health and disease. Nat. Protoc. *8*, 1149–1154.

Michael, M.D., Kulkarni, R.N., Postic, C., Previs, S.F., Shulman, G.I., Magnuson, M.A., and Kahn, C.R. (2000). Loss of Insulin Signaling in Hepatocytes Leads to Severe Insulin Resistance and Progressive Hepatic Dysfunction. Mol. Cell *6*, 87–97.

Michalopoulos, G.K. (2007). Liver regeneration. J. Cell. Physiol. *213*, 286–300.

Michalopoulos, G.K. (2010). Liver Regeneration after Partial Hepatectomy. Am. J. Pathol. *176*, 2–13.

Miele, L., Grieco, A., Armuzzi, A., Candelli, M., Forgione, A., Gasbarrini, A., and Gasbarrini, G. (2003). Hepatic mitochondrial beta-oxidation in patients with nonalcoholic steatohepatitis assessed by 13C-octanoate breath test. Am. J. Gastroenterol. *98*, 2335–2336.

M J Pagliassotti, and Cherrington, and A.D. (1992). Regulation of Net Hepatic Glucose Uptake in VIVO. Annu. Rev. Physiol. *54*, 847–860.

Mofrad, P., Contos, M.J., Haque, M., Sargeant, C., Fisher, R.A., Luketic, V.A., Sterling, R.K., Shiffman, M.L., Stravitz, R.T., and Sanyal, A.J. (2003). Clinical and histologic spectrum of nonalcoholic fatty liver disease associated with normal ALT values. Hepatology *37*, 1286–1292.

Mokdad AH, Ford ES, Bowman BA, and et al (2003). PRevalence of obesity, diabetes, and obesity-related health risk factors, 2001. JAMA *289*, 76–79.

Molina, D.K., and DiMaio, V.J.M. (2012). Normal organ weights in men: part II-the brain, lungs, liver, spleen, and kidneys. Am. J. Forensic Med. Pathol. *33*, 368–372.

Mori, K. (2000). Tripartite Management of Unfolded Proteins in the Endoplasmic Reticulum. Cell *101*, 451–454.

Mosbah, I.B., Alfany-Fernández, I., Martel, C., Zaouali, M.A., Bintanel-Morcillo, M., Rimola, A., Rodés, J., Brenner, C., Roselló-Catafau, J., and Peralta, C. (2010). Endoplasmic reticulum stress inhibition protects steatotic and non-steatotic livers in partial hepatectomy under ischemia–reperfusion. Cell Death Dis. *1*, e52.

Nakatani, Y., Kaneto, H., Kawamori, D., Hatazaki, M., Miyatsuka, T., Matsuoka, T., Kajimoto, Y., Matsuhisa, M., Yamasaki, Y., and Hori, M. (2004). Modulation of the JNK Pathway in Liver Affects Insulin Resistance Status. J. Biol. Chem. *279*, 45803–45809.

Nakatani, Y., Kaneto, H., Kawamori, D., Yoshiuchi, K., Hatazaki, M., Matsuoka, T., Ozawa, K., Ogawa, S., Hori, M., Yamasaki, Y., et al. (2005). Involvement of Endoplasmic Reticulum Stress in Insulin Resistance and Diabetes. J. Biol. Chem. *280*, 847–851.

Narasimhan, S., Gokulakrishnan, K., Sampathkumar, R., Farooq, S., Ravikumar, R., Mohan, V., and Balasubramanyam, M. (2010). Oxidative stress is independently associated with non-alcoholic fatty liver disease (NAFLD) in subjects with and without type 2 diabetes. Clin. Biochem. *43*, 815–821.

Natarajan, A., Wagner, B., and Sibilia, M. (2007). The EGF receptor is required for efficient liver regeneration. Proc. Natl. Acad. Sci. *104*, 17081–17086.

Neuschwander-Tetri, B.A. (2010). Hepatic lipotoxicity and the pathogenesis of nonalcoholic steatohepatitis: The central role of nontriglyceride fatty acid metabolites. Hepatology *52*, 774–788.

Nordlie, R.C., and Foster, J.D. (2010). A retrospective review of the roles of multifunctional glucose-6-phosphatase in blood glucose homeostasis: Genesis of the tuning/retuning hypothesis. Life Sci. *87*, 339–349.

Nordlie, R.C., and Snoke, R.E. (1967). Regulation of liver microsomal inorganic pyrophosphate-glucose phosphotransferase, glucose-6-phosphatase and inorganic pyrophosphatase. Biochim. Biophys. Acta BBA - Gen. Subj. *148*, 222–232.

Obici, S., Feng, Z., Karkanias, G., Baskin, D.G., and Rossetti, L. (2002a). Decreasing hypothalamic insulin receptors causes hyperphagia and insulin resistance in rats. Nat. Neurosci. *5*, 566–572.

Obici, S., Zhang, B.B., Karkanias, G., and Rossetti, L. (2002b). Hypothalamic insulin signaling is required for inhibition of glucose production. Nat. Med. *8*, 1376–1382.

Onuma, H., Oeser, J.K., Nelson, B.A., Wang, Y., Flemming, B.P., Scheving, L.A., Russell, W.E., and O'brien, R.M. (2009). Insulin and epidermal growth factor suppress basal glucose-6-phosphatase catalytic subunit gene transcription through overlapping but distinct mechanisms. Biochem. J. *417*, 611–620.

Otero, Y.F., Stafford, J.M., and McGuinness, O.P. (2014). Pathway-selective Insulin Resistance and Metabolic Disease: The Importance of Nutrient Flux. J. Biol. Chem. *289*, 20462–20469.

Oyadomari, S., Harding, H.P., Zhang, Y., Oyadomari, M., and Ron, D. (2008). Dephosphorylation of Translation Initiation Factor 2α Enhances Glucose Tolerance and Attenuates Hepatosteatosis in Mice. Cell Metab. *7*, 520–532.

Ozcan, U., Cao, Q., Yilmaz, E., Lee, A.-H., Iwakoshi, N.N., Ozdelen, E., Tuncman, G., Görgün, C., Glimcher, L.H., and Hotamisligil, G.S. (2004). Endoplasmic reticulum stress links obesity, insulin action, and type 2 diabetes. Science *306*, 457–461.

Paranjpe, S., Bowen, W.C., Tseng, G.C., Luo, J.-H., Orr, A., and Michalopoulos, G.K. (2010). RNA Interference Against Hepatic Epidermal Growth Factor Receptor Has Suppressive Effects on Liver Regeneration in Rats. Am. J. Pathol. *176*, 2669–2681.

Park, E., Kim, N., Ficarro, S.B., Zhang, Y., Lee, B.I., Cho, A., Kim, K., Park, A.K.J., Park, W.-Y., Murray, B., et al. (2015). Structure and mechanism of activity-based inhibition of the EGF receptor by Mig6. Nat. Struct. Mol. Biol. *22*, 703–711.

dela Peña, A., Leclercq, I., Field, J., George, J., Jones, B., and Farrell, G. (2005). NF-κB Activation, Rather Than TNF, Mediates Hepatic Inflammation in a Murine Dietary Model of Steatohepatitis. Gastroenterology *129*, 1663–1674.

Perry, R.J., Samuel, V.T., Petersen, K.F., and Shulman, G.I. (2014). The role of hepatic lipids in hepatic insulin resistance and type 2 diabetes. Nature *510*, 84–91.

Petro, A.E., Cotter, J., Cooper, D.A., Peters, J.C., Surwit, S.J., and Surwit, R.S. (2004). Fat, carbohydrate, and calories in the development of diabetes and obesity in the C57BL/6J mouse. Metabolism. *53*, 454–457.

Pfaffenbach, K.T., Gentile, C.L., Nivala, A.M., Wang, D., Wei, Y., and Pagliassotti, M.J. (2010). Linking endoplasmic reticulum stress to cell death in hepatocytes: roles of C/EBP homologous protein and chemical chaperones in palmitate-mediated cell death. Am. J. Physiol. - Endocrinol. Metab. *298*, E1027–E1035.

Posey, K.A., Clegg, D.J., Printz, R.L., Byun, J., Morton, G.J., Vivekanandan-Giri, A., Pennathur, S., Baskin, D.G., Heinecke, J.W., Woods, S.C., et al. (2009). Hypothalamic proinflammatory lipid accumulation, inflammation, and insulin resistance in rats fed a high-fat diet. Am. J. Physiol. - Endocrinol. Metab. *296*, E1003–E1012.

Postic, C., Shiota, M., Niswender, K.D., Jetton, T.L., Chen, Y., Moates, J.M., Shelton, K.D., Lindner, J., Cherrington, A.D., and Magnuson, M.A. (1999). Dual roles for glucokinase in glucose homeostasis as determined by liver and pancreatic beta cell-specific gene knock-outs using Cre recombinase. J. Biol. Chem. *274*, 305–315.

Prada, P.O., Ropelle, E.R., Mourão, R.H., Souza, C.T. de, Pauli, J.R., Cintra, D.E., Schenka, A., Rocco, S.A., Rittner, R., Franchini, K.G., et al. (2009). EGFR Tyrosine Kinase Inhibitor (PD153035) Improves Glucose Tolerance and Insulin Action in High-Fat Diet–Fed Mice. Diabetes *58*, 2910–2919.

Puigserver, P., Rhee, J., Donovan, J., Walkey, C.J., Yoon, J.C., Oriente, F., Kitamura, Y., Altomonte, J., Dong, H., Accili, D., et al. (2003). Insulin-regulated hepatic gluconeogenesis through FOXO1|[ndash]|PGC-1|[alpha]| interaction. Nature *423*, 550–555.

Puri, P., Mirshahi, F., Cheung, O., Natarajan, R., Maher, J.W., Kellum, J.M., and Sanyal, A.J. (2008). Activation and Dysregulation of the Unfolded Protein Response in Nonalcoholic Fatty Liver Disease. Gastroenterology *134*, 568–576.

Radaelli, T., Varastehpour, A., Catalano, P., and Hauguel-de Mouzon, S. (2003). Gestational diabetes induces placental genes for chronic stress and inflammatory pathways. Diabetes *52*, 2951–2958.

Ravid, T., Sweeney, C., Gee, P., Carraway, K.L., and Goldkorn, T. (2002). Epidermal Growth Factor Receptor Activation under Oxidative Stress Fails to Promote c-Cbl Mediated Down-regulation. J. Biol. Chem. *277*, 31214–31219.

Reschke, M., Ferby, I., Stepniak, E., Seitzer, N., Horst, D., Wagner, E.F., and Ullrich, A. (2010). Mitogen-inducible gene-6 is a negative regulator of epidermal growth factor receptor signaling in hepatocytes and human hepatocellular carcinoma. Hepatol. Baltim. Md *51*, 1383–1390.

Rhim, J.A., Sandgren, E.P., Degen, J.L., Palmiter, R.D., and Brinster, R.L. (1994). Replacement of Diseased Mouse Liver by Hepatic Cell Transplantation. Science *263*, 1149–1152.

Rhim, J.A., Sandgren, E.P., Palmiter, R.D., and Brinster, R.L. (1995). Complete reconstitution of mouse liver with xenogeneic hepatocytes. Proc. Natl. Acad. Sci. *92*, 4942–4946.

Rinella, M., and Charlton, M. (2016). The globalization of nonalcoholic fatty liver disease: Prevalence and impact on world health. Hepatology *64*, 19–22.

Rinella, M.E., and Green, R.M. (2004). The methionine-choline deficient dietary model of steatohepatitis does not exhibit insulin resistance. J. Hepatol. *40*, 47–51.

Rossmeisl, M., Rim, J.S., Koza, R.A., and Kozak, L.P. (2003). Variation in type 2 diabetes--related traits in mouse strains susceptible to diet-induced obesity. Diabetes *52*, 1958–1966.

Samuel, V.T., Liu, Z.-X., Wang, A., Beddow, S.A., Geisler, J.G., Kahn, M., Zhang, X., Monia, B.P., Bhanot, S., and Shulman, G.I. (2007). Inhibition of protein kinase Cε prevents hepatic insulin resistance in nonalcoholic fatty liver disease. J. Clin. Invest. *117*, 739–745.

Sandgren, E.P., Palmiter, R.D., Heckel, J.L., Daugherty, C.C., Brinster, R.L., and Degen, J.L. (1991). Complete hepatic regeneration after somatic deletion of an albumin-plasminogen activator transgene. Cell *66*, 245–256.

Scheuner, D., Song, B., McEwen, E., Liu, C., Laybutt, R., Gillespie, P., Saunders, T., Bonner-Weir, S., and Kaufman, R.J. (2001). Translational Control Is Required for the Unfolded Protein Response and In Vivo Glucose Homeostasis. Mol. Cell *7*, 1165–1176.

Schiffer, E., Housset, C., Cacheux, W., Wendum, D., Desbois-Mouthon, C., Rey, C., Clergue, F., Poupon, R., Barbu, V., and Rosmorduc, O. (2005). Gefitinib, an EGFR inhibitor, prevents hepatocellular carcinoma development in the rat liver with cirrhosis. Hepatol. Baltim. Md *41*, 307–314.

Schlessinger, J. (2002). Ligand-Induced, Receptor-Mediated Dimerization and Activation of EGF Receptor. Cell *110*, 669–672.

Schmoll, D., Grempler, R., Barthel, A., Joost, H.G., and Walther, R. (2001). Phorbol ester-induced activation of mitogen-activated protein kinase/extracellular-signal-regulated kinase kinase and extracellular-signal-regulated protein kinase decreases glucose-6-phosphatase gene expression. Biochem. J. *357*, 867–873.

Scott, D.K., O'Doherty, R.M., Stafford, J.M., Newgard, C.B., and Granner, D.K. (1998). The Repression of Hormone-activated PEPCK Gene Expression by Glucose Is Insulin-independent but Requires Glucose Metabolism. J. Biol. Chem. *273*, 24145–24151.

Segatto, O., Anastasi, S., and Alemà, S. (2011). Regulation of epidermal growth factor receptor signalling by inducible feedback inhibitors. J. Cell Sci. *124*, 1785–1793.

Seo, H.-Y., Kim, M.-K., Min, A.-K., Kim, H.-S., Ryu, S.-Y., Kim, N.-K., Lee, K.M., Kim, H.-J., Choi, H.-S., Lee, K.-U., et al. (2010). Endoplasmic Reticulum Stress-Induced Activation of Activating Transcription Factor 6 Decreases cAMP-Stimulated Hepatic Gluconeogenesis via Inhibition of CREB. Endocrinology *151*, 561–568.

Serviddio, G., Bellanti, F., Vendemiale, G., and Altomare, E. (2011). Mitochondrial dysfunction in nonalcoholic steatohepatitis. Expert Rev. Gastroenterol. Hepatol. *5*, 233–244.

Shen, J., Chen, X., Hendershot, L., and Prywes, R. (2002). ER Stress Regulation of ATF6 Localization by Dissociation of BiP/GRP78 Binding and Unmasking of Golgi Localization Signals. Dev. Cell *3*, 99–111.

Smith, G.D., Swenson, D.C., Dodson, E.J., Dodson, G.G., and Reynolds, C.D. (1984). Structural stability in the 4-zinc human insulin hexamer. Proc. Natl. Acad. Sci. U. S. A. *81*, 7093–7097.

Solano, M.P., and Goldberg, R.B. (2006). Lipid Management in Type 2 Diabetes. Clin. Diabetes *24*, 27–32.

Spranger, J., Kroke, A., Möhlig, M., Hoffmann, K., Bergmann, M.M., Ristow, M., Boeing, H., and Pfeiffer, A.F.H. (2003). Inflammatory Cytokines and the Risk to Develop Type 2 Diabetes. Diabetes *52*, 812–817.

St-Pierre, J., Buckingham, J.A., Roebuck, S.J., and Brand, M.D. (2002). Topology of Superoxide Production from Different Sites in the Mitochondrial Electron Transport Chain. J. Biol. Chem. *277*, 44784–44790.

Surwit, R.S., Feinglos, M.N., Rodin, J., Sutherland, A., Petro, A.E., Opara, E.C., Kuhn, C.M., and Rebuffé-Scrive, M. (1995). Differential effects of fat and sucrose on the development of obesity and diabetes in C57BL/6J and A/J mice. Metabolism. *44*, 645–651.

Tamaki, N., Hatano, E., Taura, K., Tada, M., Kodama, Y., Nitta, T., Iwaisako, K., Seo, S., Nakajima, A., Ikai, I., et al. (2008). CHOP deficiency attenuates cholestasis-induced liver fibrosis by reduction of hepatocyte injury. Am. J. Physiol. - Gastrointest. Liver Physiol. *294*, G498–G505.

Tanaka, S., Miyanishi, K., Kobune, M., Kawano, Y., Hoki, T., Kubo, T., Hayashi, T., Sato, T., Sato, Y., Takimoto, R., et al. (2013). Increased hepatic oxidative DNA damage in patients with nonalcoholic steatohepatitis who develop hepatocellular carcinoma. J. Gastroenterol. *48*, 1249–1258.

Targher, G., Bertolini, L., Padovani, R., Rodella, S., Zoppini, G., Zenari, L., Cigolini, M., Falezza, G., and Arcaro, G. (2006). Relations Between Carotid Artery Wall Thickness and Liver Histology in Subjects With Nonalcoholic Fatty Liver Disease. Diabetes Care *29*, 1325–1330.

Teli, M.R., James, O.F.W., Burt, A.D., Bennett, M.K., and Day, C.P. (1995). The natural history of nonalcoholic fatty liver: A follow-up study. Hepatology *22*, 1714–1719.

Uhlén, M., Fagerberg, L., Hallström, B.M., Lindskog, C., Oksvold, P., Mardinoglu, A., Sivertsson, Å., Kampf, C., Sjöstedt, E., Asplund, A., et al. (2015). Tissue-based map of the human proteome. Science *347*, 1260419.

Urano, F., Wang, X., Bertolotti, A., Zhang, Y., Chung, P., Harding, H.P., and Ron, D. (2000). Coupling of stress in the ER to activation of JNK protein kinases by transmembrane protein kinase IRE1. Science *287*, 664–666.

Varley, C.L., Stahlschmidt, J., Lee, W.-C., Holder, J., Diggle, C., Selby, P.J., Trejdosiewicz, L.K., and Southgate, J. (2004). Role of PPAR γ and EGFR signalling in the urothelial terminal differentiation programme. J. Cell Sci. *117*, 2029–2036.

Vilsbøll, T., and Holst, J.J. (2004). Incretins, insulin secretion and Type 2 diabetes mellitus. Diabetologia *47*, 357–366.

Wang, D., Wei, Y., Schmoll, D., Maclean, K.N., and Pagliassotti, M.J. (2006a). Endoplasmic reticulum stress increases glucose-6-phosphatase and glucose cycling in liver cells. Endocrinology *147*, 350–358.

Wang, D., Wei, Y., and Pagliassotti, M.J. (2006b). Saturated Fatty Acids Promote Endoplasmic Reticulum Stress and Liver Injury in Rats with Hepatic Steatosis. Endocrinology *147*, 943–951.

Wang, Y., Vera, L., Fischer, W.H., and Montminy, M. (2009). The CREB coactivator CRTC2 links hepatic ER stress and fasting gluconeogenesis. Nature *460*, 534–537.

Webber, E.M., Godowski, P.J., and Fausto, N. (1994). In vivo response of hepatocytes to growth factors requires an initial priming stimulus. Hepatology *19*, 489–497.

Wei, Y., Wang, D., Gentile, C.L., and Pagliassotti, M.J. (2009). Reduced Endoplasmic Reticulum Luminal Calcium Links Saturated Fatty Acid-Mediated Endoplasmic Reticulum Stress and Cell Death in Liver Cells. Mol. Cell. Biochem. *331*, 31–40.

Weinstock, P.H., Bisgaier, C.L., Aalto-Setälä, K., Radner, H., Ramakrishnan, R., Levak-Frank, S., Essenburg, A.D., Zechner, R., and Breslow, J.L. (1995). Severe

hypertriglyceridemia, reduced high density lipoprotein, and neonatal death in lipoprotein lipase knockout mice. Mild hypertriglyceridemia with impaired very low density lipoprotein clearance in heterozygotes. J. Clin. Invest. *96*, 2555–2568.

Weltman, M., Farrell, G., and Liddle, C. (1996). Increased hepatocyte CYP2E1 expression in a rat nutritional model of hepatic steatosis with inflammation. Gastroenterology *111*, 1645–1653.

White, M.F. (2003). Insulin Signaling in Health and Disease. Science *302*, 1710–1711.

Wick, M., Bürger, C., Funk, M., and Müller, R. (1995). Identification of a Novel Mitogen-Inducible Gene (mig-6): Regulation during G1 Progression and Differentiation. Exp. Cell Res. *219*, 527–535.

Wieckowska, A., Zein, N.N., Yerian, L.M., Lopez, A.R., McCullough, A.J., and Feldstein, A.E. (2006). In vivo assessment of liver cell apoptosis as a novel biomarker of disease severity in nonalcoholic fatty liver disease. Hepatol. Baltim. Md *44*, 27–33.

Wolf, H.K., and Michalopoulos, G.K. (1992). Hepatocyte regeneration in acute fulminant and nonfulminant hepatitis: A study of proliferating cell nuclear antigen expression. Hepatology *15*, 707–713.

Wu, J., Rutkowski, D.T., Dubois, M., Swathirajan, J., Saunders, T., Wang, J., Song, B., Yau, G.D.-Y., and Kaufman, R.J. (2007). ATF6α Optimizes Long-Term Endoplasmic Reticulum Function to Protect Cells from Chronic Stress. Dev. Cell *13*, 351–364.

Xu, D., Makkinje, A., and Kyriakis, J.M. (2005a). Gene 33 Is an Endogenous Inhibitor of Epidermal Growth Factor (EGF) Receptor Signaling and Mediates Dexamethasone-induced Suppression of EGF Function. J. Biol. Chem. *280*, 2924–2933.

Xu, D., Makkinje, A., and Kyriakis, J.M. (2005). Gene 33 Is an Endogenous Inhibitor of Epidermal Growth Factor (EGF) Receptor Signaling and Mediates Dexamethasone-induced Suppression of EGF Function. J. Biol. Chem. *280*, 2924–2933.

Xu, D., Patten, R.D., Force, T., and Kyriakis, J.M. (2006). Gene 33/RALT is induced by hypoxia in cardiomyocytes, where it promotes cell death by suppressing phosphatidylinositol 3-kinase and extracellular signal-regulated kinase survival signaling. Mol. Cell. Biol. *26*, 5043–5054.

Yecies, J.L., Zhang, H.H., Menon, S., Liu, S., Yecies, D., Lipovsky, A.I., Gorgun, C., Kwiatkowski, D.J., Hotamisligil, G.S., Lee, C.-H., et al. (2011). Akt Stimulates Hepatic SREBP1c and Lipogenesis through Parallel mTORC1-Dependent and Independent Pathways. Cell Metab. *14*, 21–32.

Ying, H., Zheng, H., Scott, K., Wiedemeyer, R., Yan, H., Lim, C., Huang, J., Dhakal, S., Ivanova, E., Xiao, Y., et al. (2010). Mig-6 controls EGFR trafficking and suppresses gliomagenesis. Proc. Natl. Acad. Sci. U. S. A. *107*, 6912–6917.

Younossi, Z.M., Koenig, A.B., Abdelatif, D., Fazel, Y., Henry, L., and Wymer, M. (2016). Global epidemiology of nonalcoholic fatty liver disease—Meta-analytic assessment of prevalence, incidence, and outcomes. Hepatology *64*, 73–84.

Zerrad-Saadi, A., Lambert-Blot, M., Mitchell, C., Bretes, H., Collin de l'Hortet, A., Baud, V., Chereau, F., Sotiropoulos, A., Kopchick, J.J., Liao, L., et al. (2011). GH Receptor Plays a Major Role in Liver Regeneration through the Control of EGFR and ERK1/2 Activation. Endocrinology *152*, 2731–2741.

Zhang, Y.-W., and Vande Woude, G.F. (2007). Mig-6, signal transduction, stress response and cancer. Cell Cycle Georget. Tex *6*, 507–513.

Zhang, W., Patil, S., Chauhan, B., Guo, S., Powell, D.R., Le, J., Klotsas, A., Matika, R., Xiao, X., Franks, R., et al. (2006). FoxO1 Regulates Multiple Metabolic Pathways in the Liver EFFECTS ON GLUCONEOGENIC, GLYCOLYTIC, AND LIPOGENIC GENE EXPRESSION. J. Biol. Chem. *281*, 10105–10117.

Zhang, X., Pickin, K.A., Bose, R., Jura, N., Cole, P.A., and Kuriyan, J. (2007). Inhibition of the EGF receptor by binding of MIG6 to an activating kinase domain interface. Nature *450*, 741–744.

Zhang, Y.-W., Su, Y., Lanning, N., Swiatek, P.J., Bronson, R.T., Sigler, R., Martin, R.W., and Woude, G.F.V. (2005). Targeted disruption of Mig-6 in the mouse genome leads to early onset degenerative joint disease. Proc. Natl. Acad. Sci. U. S. A. *102*, 11740–11745.

CURRICULUM VITAE

Andrew J. Lutkewitte

Education

2011-2016 Ph.D., Cellular and Integrative Physiology
Indiana University, Indianapolis, Indiana
Thesis title, “Stress-activated Mig6 compromises hepatic metabolism during diet-induced obesity”

2007-2011 B.S., Dual majors in Biology and Chemistry
Butler University, Indianapolis, Indiana

Funding

01/2015-12/2016 American Heart Association Predoctoral Fellowship
“Control of hepatic metabolism by the dynamic expression of the EGFR inhibitor Mig6”

Academic and Professional Honors

2014 Poster Presentation Award, Indiana Physiological Society 4th Annual Meeting

2014 Graduate and Professional Student Government Educational Enhancement Grant, Indiana University School of Medicine

2015 Poster Presentation Award, First Annual Diabetes Symposium, Indiana Diabetes Research Center, Indiana University School of Medicine

2015 Gabor Kaley Professional Opportunity Award, Experimental Biology Abstract Award, American Physiology Society

2016 Oral Presentation Award, Indiana Physiological Society 6th Annual Meeting

2016 Campbell Poster Participation Award, Experimental Biology, American Physiology Society

2016 Poster Presentation Award, 9th Annual Midwestern Islet Club meeting

Experience and Career Development

2011 Intern, Research and Development, Protein Assays and Technology, Sigma Aldrich Chemical Company, St. Louis, MO.

2012-2016 Graduate student instructor, Molecular Medicine in Action, Summer High School Student and Faculty Mentoring Program

2015 Writing and Reviewing for Scientific Journals, Professional Skills Development Course, American Physiology Society, Orlando. FL.

2016 Certificate in the Business of Life Sciences, Kelly School of Business, Indiana University, Bloomington, IN.

Manuscripts

1. Chen, Y.-C., **Lutkewitte, A.J.,** Fueger, P.T. Glucolipotoxicity-induced Mig6 desensitizes EGFR signaling and promotes pancreatic beta cell death *(In preparation)*

2. **Lutkewitte, A.J.,** Chen, Y.-C., Hansen J.L., Fueger, P.T. Lipotoxic-induced Mig6 decrease EGFR activation and cell survival in hepatocytes *(In review)*

3. **Lutkewitte, A.J.,** Fong, K.M., Fueger, P.T. Liver-specific Mig6 ablation improves glucose tolerance in high fat fed mice (*In preparation)*

Meeting Abstracts

1. **Lutkewitte, A.J.,** & Fueger, P.T., An emerging link Between the negative EGFR feedback regulator, Mig6 and hepatic glucose metabolism. Poster presentation. Experimental Biology. San Diego, CA. 2014.

2. **Lutkewitte, A.J.,** & Fueger, P.T., An emerging link Between the negative EGFR feedback regulator, Mig6 and hepatic glucose metabolism. Poster presentation. Indiana Physiological Society 4th Annual Meeting. Evansville, IN. 2014.

3. Chen, Y.-C., **Lutkewitte, A.J.,** Colvin, E.S., Kono, T.M., Evans-Molina, C., Fueger, P.T. Glucolipotoxicity-induced Mig6 desensitizes EGFR signaling pathway and promotes pancreatic beta cell death. Oral Presentation. Experimental Biology. San Diego, CA.
4. **Lutkewitte, A.J.,** Chen, Y.-C., Hansen, J.L., Jeong, J.W., Fueger, P.T. Mitogen inducible gene 6 restricts epidermal growth factor receptor activation during hepatic endoplasmic reticulum stress. Poster presentation. Indiana Physiological Society 5th Annual Meeting, Indianapolis, IN. 2015.

5. **Lutkewitte, A.J.,** Chen, Y.-C., Hansen, J.L., Fueger, P.T. Diet-induced obesity and hepatic ER stress increase mig6 and dampen EGFR activity. Poster presentation. Experimental Biology. Boston, MA. 2015.

6. **Lutkewitte, A.J.,** Chen, Y.-C., Hansen, J.L., Fueger, P.T. Diet-Induced obesity increases hepatic mig6 expression and attenuates EGFR signaling. Oral presentation. Indiana Physiological Society 6th Annual Meeting. Greencastle, IN. 2016.

7. **Lutkewitte, A.J.,** Chen, Y.-C., Hansen, J.L., Fueger, P.T. Diet-Induced obesity increases hepatic mig6 expression and attenuates EGFR signaling. Poster presentation. Experimental Biology. San Diego, CA. 2016.

8. **Lutkewitte, A.J.,** Chen, Y.-C., Hansen, J.L., Fueger, P.T. Diet-Induced obesity increases hepatic mig6 expression and attenuates EGFR signaling. Poster presentation. 9th Annual Midwest Islet Club Meeting. Indianapolis, IN. 2016.